Sensor System for Autonomous Detection of Mold Spore Contamination

Poornachandra Papireddy Vinayaka

Universität Bremen 2019

Primary supervisor:	Prof. Dr.-Ing. Michael J. Vellekoop Universität Bremen Bremen, Germany
Secondary supervisor:	Prof. Dr. Bernhard Jakoby Johannes Kepler Universität Linz Linz, Austria
Date of the doctoral colloquium:	21.01.2019

Sensor System for Autonomous Detection of Mold Spore Contamination

Vom Fachbereich für Physik und Elektrotechnik
der Universität Bremen

zur Erlangung des akademischen Grades

Doktor–Ingenieur (Dr.-Ing.)

genehmigte Dissertation

von

M. Sc. Poornachandra Papireddy Vinayaka

wohnhaft in Bengaluru, Indien

To my Parents
P. Vijayasekhara Reddy and P. Jyotheeswari

&

To my lovely wife
Bujji (B. Lakshmi Lavanya)

Contents

Abstract

An autonomous sensor system for monitoring mold spore contaminations inside archives at desired time intervals is presented. Presence of airborne mold spores in the indoor environment poses severe threat to the organic material present within the archives. These mold spores are airborne, i.e., they are easily transported from one place to another through human (or animal) interventions or via air conditioning systems. At sufficient high temperature and humidity, the mold spores start to grow by decomposing books, paper, files and other organic material present within the archives. If the mold contamination is not monitored at its initial state then the damage spreads throughout the indoor, possibly leading to permanent loss of material. It could incur huge expenses to restore the infected material. Furthermore, exposure to high concentration of the spores is linked to severe respiratory illnesses in humans and animals. To avoid this potential risk a sensor system for monitoring mold spore concentrations is of great importance. Moreover, having an autonomous sensor system provides the possibility of real-time intervention (if a contamination is detected) to prevent further spread in contamination.

In this thesis, a mold sensor system with a replaceable bioreactor array for autonomous detection of the airborne spores has been investigated. The sensor system consists of a bioreactor cartridge to analyze the mold growth, an air sampling unit for distributing the mold spores (present in the air sample) into the bioreactors and a control unit to automatize the detection process.

The cartridge comprises of 16 membrane sealed bioreactors arranged in 4x4 array format for monitoring spore concentrations at regular intervals. Each bioreactor is sealed with a sacrificial silicon nitride membrane, which can be opened on demand. Sealing the bioreactor also prevents the contamination of the culture medium. Once activated, the membrane gets opened and the spores present in the air sample get in contact with the culture medium and start to germinate. The mold detection is performed by using an integrated approach of impedance and colorimetric principles. The colorimetric principle acts as a reference measurement for determining the absolute pH of the culture medium directly on-chip. If mold contamination is detected the control unit sends a warning signal to the end user. To provide the possibility of long-term monitoring, the cartridge is replaced after using all the 16 bioreactors. Major mold species involved in the contamination of archives like, *Eurotium amstelodami, Aspergillus penicilloides, Aspergillus restrictus* and *Cladosporium cladosporiodes* have been successfully detected on-chip using the sensor system.

Kurzfassung

Ein autonomes Sensorsystem mit zeitlich frei wählbaren Messintervallen zur Erkennung von Schimmelpilzkontaminationen in Archiven wird vorgestellt. Schimmelpilzsporen in Innenräumen kontaminieren organisches Material in Archiven. Diese Schimmelpilzsporen werden durch menschliche (oder tierische) Einflüsse verursacht oder auch über Klimaanlagen von einem Ort zum anderen transportiert. Bei ausreichender Temperatur und Luftfeuchtigkeit beginnen die Schimmelpilzsporen zu wachsen und beschädigen Bücher, Papier, Akten und anderes organisches Material, das in Archiven vorhanden ist. Wenn die Schimmelpilzkontamination nicht erkannt wird, breitet sich der Schaden im gesamten Innenbereich aus und beschädigt das Material dauerhaft. Dies verursacht enorme Kosten um das infizierte Material wiederherzustellen. Darüberhinaus führt das Einatmen hoher Sporenkonzentrationen zu schweren Atemwegserkrankungen bei Mensch und Tier.

Um dieses potentielle Risiko zu vermeiden, wird ein Sensorsystem zur Überwachung der Konzentration von Schimmelpilzsporen benötigt.

In dieser Arbeit wurde ein Sensorsystem mit einem austauschbaren Bioreaktor-Array für die autonome Detektion der über Luft beförderten Sporen entwickelt. Das Sensorsystem besteht aus einer Bioreaktorkartusche zur Analyse des Schimmelpilzwachstums, einer Luftprobenahmeeinheit zur Verteilung der Schimmelpilzsporen in die Bioreaktoren und einer Kontrolleinheit zur Automatisierung des Detektionsprozesses.

Die Kartusche besteht aus 16 membranabgedichteten Bioreaktoren. Jeder Bioreaktor ist mit einer Siliziumnitrid-Membran verschlossen, die bei Bedarf geöffnet werden kann. Das Abdichten des Bioreaktors verhindert eine Kontamination des Kulturmediums. Nach der Aktivierung öffnet sich die Membran und die Sporen kommen in Kontakt mit dem Kulturmedium und beginnen zu wachsen. Das Schimmelwachstum wird unter Verwendung eines integrierten Ansatzes von Impedanz- und kolorimetrischen Prinzipien überwachtet. Wird Schimmelpilzkontamination festgestellt, sendet das Steuergerät ein Warnsignal an den Benutzer. Schimmelpilzarten wie, *Eurotium amstelodami, Aspergillus penicilloides, Aspergillus restrictus* und *Cladosporium cladosporiodes* wurden mit Hilfe des Sensorsystems erfolgreich auf dem Chip analysiert.

Nomenclature

List of abbreviations

Symbol	Description
ADC	analog to digital converter
ATP	adenosine triphosphate
CAD	computer aided design
CFU	colony forming unit
CMOS	complementary metal-oxide-semiconductor
CVD	chemical vapor deposition
DDS	direct digital synthesis
DNA	deoxyribonucleic acid
DPDT	double pole double throw
DSP	digital signal processing
EIS	electrochemical impedance spectroscopy
FAD	flavin adenine dinucleotide
FMN	flavin mononucleotide
FTIR	fourier transform infrared spectroscopy
HEPA	high efficiency particulate air filtration
IC	integrated circuit
IgE	immunoglobulin E
IHL	inner Helmholtz layer
LED	light emitting diode
LPCVD	low pressure chemical vapor deposition
MEMS	microelectro mechanical systems
MOSFET	metal-oxide-semiconductor field-effect transistor

Symbol	Description
MVOC	microbial volatile organic compounds
NADH	nicotinamide adenine dinucleotide
NADPH	nicotinamide adenine dinucleotide phosphate
OHP	outer Helmholtz layer
PCB	printed circuit board
PCR	polymerase chain reaction
PDA	potato dextrose agarose
PECVD	plasma enhanced chemical vapor deposition
PES	polyethersulfone
PVD	physical vapor deposition
RH	relative humidity
UV	ultraviolet

List of symbols

Symbol	Description	Unit
A	area of electrode	m^2
C	electrical capacitance	F
C_{dl}	double layer capacitance	F
$C_{Helmholtz}$	Helmholtz capacitance	F
$C_{diffuse}$	Diffuse capacitance	F
C_{bulk}	bulk capacitance	F
C_s	parasitic capacitance	F
C_c	parasitic capacitance	F
d	distance between electrodes	m
F	Faradays constant	
f	frequency	Hz
I	electric current	A

Symbol	Description	Unit
K	Boltzmann constant	
$L_{Helmholtz}$	Helmholtz layer thickness	nm
pK_a	dissociation constant	
R	electrical resistance	Ω
R_{ct}	charge transfer resistance	Ω
R_{bulk}	bulk resistance	Ω
R_s	substrate resistance	Ω
T	absolute temperature	K
V	voltage	V
V_0	amplitude of excitation signal	V
λ_{Debye}	diffuse layer thickness	nm
ρ	electrical resistivity	Ω-m
σ	electrical conductivity	1/ (Ω-m)

1 Introduction

In recent years, evaluation of indoor air for mold spore contamination has received a major attention. The presence of mold spores within archives is a potential threat to the stored organic material. In addition, some of these mold spores when inhaled induce several toxicological effects in humans and animals. This thesis discusses possible methods, which can be applied for the detection of airborne mold spores and presents a novel sensor system for autonomous indoor monitoring of airborne mold spore contaminations.

1.1 Mold and its effects

Mold is a general terminology used for filamentous fungi, which are multicellular in nature. Recent studies suggest that there are about 5.1 million species of mold in the earth's environment, out of which merely 120000 species have been classified [1]. This shows that mold is one of the major biological species of the natural environment, which is present everywhere. Molds obtain nutrients required for their growth by decomposing the organic matter through a process termed as extracellular digestion. In this digestion process, molds secrete enzymes to breakdown the host organic material into soluble products, which are later absorbed. Molds play a significant role in decomposition of the dead organic matter and allow recycling of the nutrients required for the life in the earth's ecosystem. However, presence of the mold in indoor is considered as a potential threat because mold contamination not only destroys perishable goods, food, books, buildings, or other organic material but it is also proven to be dangerous to human and animal health [2].

Mold spreads through propagation of spores. The growth of mold facilitates the production of spores, which are transported from once place to other via air currents, insects, or by animals. Mold spores enter the indoor through air ventilators or by human interventions. These spores remain inactive until they have favorable environmental conditions to grow. The outer shell of the spore protects them from extreme heat or cold and thus keeping them inactive but alive for years. Once the environmental conditions (temperature and humidity) are favorable to the spores, they will start to germinate by degrading the host material. These spores start to grow and develop into a network of branches (termed as mycelium), which intern will produce

spores and thus the cycle repeats. If the concentration of spores is not monitored the contamination spreads throughout the indoor space, thus destroying valuable material.

For example in archives, infestation of books, documents, files or other stored organic material with mold is a major issue. One of the reasons for the mold infestation is due to improper control of the climatic conditions inside the archives. Especially for the archives that are located in basements, files, documents and books are easily prone to the mold infestation because of high humidity. If the mold growth is unnoticed in its initial state, then the contamination spreads throughout the archives resulting in the permanent damage of the materials. Also once infected with mold it either incurs huge expenses to restore the damaged files or in some cases the damage might not be repairable. Fig. 1 shows images of some of the mold contaminated files taken in an archive.

Figure 1: Pictures taken within archives in Bochum city library, Germany; a) contaminated archive; b) and c) uncontaminated archive; d) Files without mold contamination; e) mold infected files.

In addition to the material damage, persistent exposure to the mold spores results in adverse health problems for humans and animals. Particularly mold spores are responsible for respiratory illnesses and other diseases like pneumonitis, asthama, etc. [3][4][5]. Because of their lightweight and small size (1 µm to 100 µm), once they are inhaled they reach deeper parts of human respiratory system, which in some instances leads to several allergic reactions. Furthermore, growth of mold produces mycotoxins and microbial volatile organic compounds (MVOC's), which are also associated with human or animal diseases [6]. To avoid this potential risk it is necessary to monitor the concentrations of mold spores inside indoor. Determining the spore concentrations manually is time consuming and labor intensive, so a sensor system is

needed to monitor the spores regularly. Till date, there are no autonomous sensor systems available in the market for monitoring mold spore concentrations inside indoor at regular intervals.

Traditional methods employed for monitoring the spore concentrations are based on sample collection followed by an analysis in a laboratory. Different methods used for the detection of mold spores are cultivation techniques, optical analysis, spectroscopic methods, molecular methods, bioluminescence technique, gas chromatography for monitoring MVOC's emitted by mold, etc. Though immense research has been done in the mold detection methods, these methods are not automatized. An autonomous sensor system should be able to perform steps from sample collection to detection of spores automatically without any manual interventions.

In this thesis, a novel standalone sensor system has been designed with an integrated air sampling unit to automate the traditional culturing technique for measuring the mold spore concentrations at regular time intervals. Furthermore, the proposed sensor system consists of a replaceable bioreactor array, allowing the possibility for long-term monitoring of the mold spore concentrations.

1.2 Objectives of this work

Goal of this thesis is to design an autonomous sensor system for monitoring of airborne mold spore contaminations at desired time intervals. Major research objectives of the thesis are summarized below:

1. Investigation of different mold spore detection methods and their possibilities to be integrated into an autonomous sensor system.
2. Design, realization and characterization of an autonomous sensor system suitable for out-of-lab mold detection.
3. Integration of a colorimetric reference measurement, for measuring pH changes in the culture medium as the mold spores germinate.
4. Design of a replaceable membrane-sealed bioreactor cartridge for long-term monitoring of mold spores at defined time.
5. Design of an air sampling unit to distribute the incoming spores uniformly among the bioreactor cartridge.
6. Detection of major mold species responsible for the contamination of food, paper and indoor, like *Fusarium oxysporum, Aspergillus penicillioides, Aspergillus restrictus, Cladosporium Cladosporioides, Eurotium amstelodami* and *Aspergillus versicolor*.

In addition to the monitoring of airborne spores, this thesis also presents a novel concept of a sensor sticker, for monitoring the growth of mold on fruits during

transportations. Growth of mold on fruits during transportation not only damages the food but also incurs huge transportation losses for logistic firms. For studying the effect of spores on the development of mold on fruits, a sensor sticker has been designed. This sensor sticker comprises of a capacitive element and a structured cultured medium with integrated air cavities. Integrating air cavities allows investigation of mold growth in a controllable way. This sensor sticker is applied for determining different concentrations of *Fusarium Oxysporum*, a major mold species responsible for banana contamination.

1.3 Thesis outline

This thesis consists of eight chapters. It starts with a brief introduction in chapter 1, Chapter 2 explains in detail about the molds, their characteristics and how they are reproduced. This chapter also provides information regarding different mold detection techniques that are currently employed for analysis of the mold spores. Also, advantages and disadvantages of integrating these detection methods into an autonomous sensor system have been described. The chapter ends with a brief description on the available sensor systems in the market for detection of the airborne mold spores.

In chapter 3 theoretical aspects for understanding the design and operation of the membrane-sealed bioreactor is presented. Starting with the basics of electrochemical impedance spectroscopy, this chapter explains in detail about equivalent circuit model employed for designing an impedance sensor. Also different impedance based biosensors that are currently used for rapid detection of various microbial organisms are discussed. In addition to this, a brief explanation is given regarding the molds metabolism.

Chapter 4 is dedicated to the bioreactor based mold sensor system, where the design and concept of autonomous operation of the sensor system is discussed. This chapter includes detailed explanation of the design, fabrication and assembly of membrane-sealed bioreactor. Also a novel mold detection method by integrating impedance and colorimetric principles has been introduced. Furthermore, the concept of bioreactor cartridge consisting of an array of membrane-sealed bioreactors for long-term measurements is presented. Later, a brief explanation regarding the design of an air sampling unit is mentioned. At the end, measurement setup comprising of sensor readout electronics and control unit for autonomous operation has been described.

Chapter 5 discusses various characterization results. At first, the bioreactor is characterized with the culture medium. Later, influence of reference pH indicator dye on the growth of mold is studied. Followed by this, detection of the mold growth by integrating impedance and colorimetric measurements is presented. Different silicon nitride

membrane designs are characterized and experiments are performed for investigating the distribution of spore particles among the bioreactors within the air sampling unit. Afterwards, an array of membrane-sealed bioreactors is used for monitoring the spore concentrations in the laboratory. As a final step, the mold sensor system is implemented in the archives where the indoor air is sampled for detecting different spore concentrations.

Chapter 6 deals with the detection of mold spores using their auto-fluorescence properties. This chapter starts with a brief introduction to the auto-fluorescence mechanism in biological samples or in mold spores. The designed sensor system allows studying the emission profiles of different mold species under ultraviolet excitation. Furthermore, this concept has been integrated into an optical sensor system for monitoring mold spores.

In chapter 7, a novel sensor sticker concept has been introduced for determining mold spore concentrations on fruits. In the first section, importance of monitoring mold growth on fruits during transportation has been explained. Later, the design of a sensor sticker which can be put on fruits is discussed. This is followed by a study of the effect of mold spores on development of mold on fruits. This sensor sticker concept was successfully tested by measuring different concentrations of mold spores on bananas.

In the final chapter 8, the presented thesis is summarized with main conclusions. Furthermore, an outlook is provided with perspectives of further improving the sensor system. Moreover, new ideas for continuation of the research topics have been discussed.

2 Mold Detection Methods

2.1 Molds and their characteristics

Molds are a part of fungi kingdom and are eukaryotic organisms. Eukaryotes are biological organisms whose cell components are enclosed within a membrane. The cells of eukaryotes consist of a nucleus, cytoplasm, intracellular vacuoles, and other membrane bound organelles [7]. Fungi are further classified into unicellular and multicellular organisms. Single-celled or unicellular microorganisms of fungi are termed as yeasts, whereas multicellular organisms are named as molds. Though molds are treated to be a part of plant kingdom, their cells do not contain photosynthetic pigments. Hence they have to obtain necessary energy required for their growth by digesting or by oxidizing other organic substances. For obtaining nutrients required for their growth, molds grow in the form of multicellular filaments that spreads over the nutrient medium [8]. These filaments are called as hyphae and are considered to be the vegetative body for the mold (Fig. 2). The hyphae is about 4-7 µm in diameter and consists of cytoplasm, nucleus, cell wall and other organelles. The hyphae might be continuous as one single branch or it could be divided into different segments by septa as shown in Fig. 2.

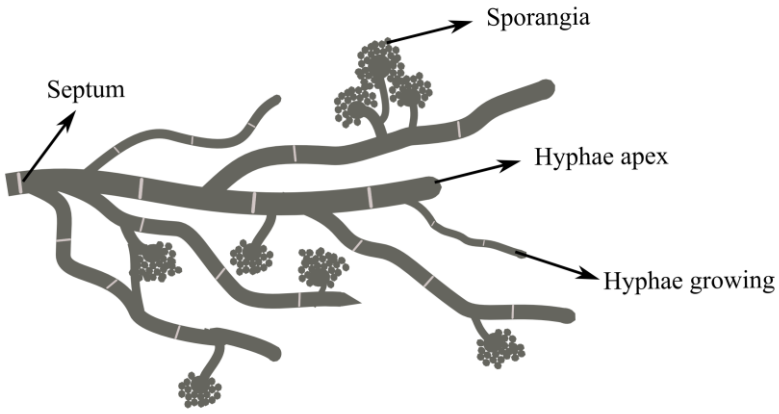

Figure 2: The hyphae of mold species growing in the form of filaments. Hyphae is dividied into small segments by septum and contain different cell components like mitochondira, ergosterol, nucleus, lipids, plasma membrane etc [8].

Mold grows with elongation of hyphae at their tips. Each part of the hyphae has the potential to elongate and form a new branch. There are two different ways how the hyphae starts to reproduce, namely asexual reproduction and sexual reproduction. In asexual reproduction, the mold reproduces either by fragmentation of hyphae or by formation of spores as represented in Fig. 3. In the case of fragmentation, the hyphae is divided internally into single cells. Each single cell then gets separated from the parent hyphae and starts to germinate forming a new branch of hyphae. The other means of reproduction is via spores. The most common mode of reproduction for molds is through the formation of asexual spores. In this process, spores are produced either at the tip of the hyphae (called conidiospores) or at a location inside hyphae (called sporangia), through mitosis process. These spores which are genetically identical to that parent get dispersed from the parent hyphae because of the wind or due to animals. Once the spores land on the nutrient medium, they start to germinate forming branches of hyphae.

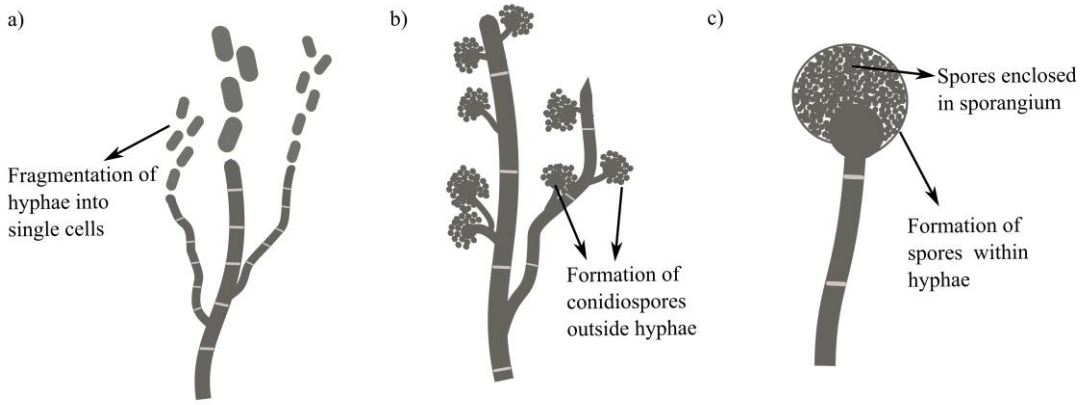

Figure 3: Different types of asexual reproduction a) fragmentation of the hyphae b) formation of conidiospores at hyphae c) formation of spores inside sporangia [7].

Sexual reproduction of mold comprises of three stages (Fig. 4) [7]. The first stage is called plasmogamy, where two haploid cells (containing half of chromosomes) from different hyphae fuse together forming a single cell with two nuclei. In the next stage (karyogamy), the two haploid nuclei fuse together forming a diploid nucleus of the zygote. Following karyogamy stage, meiosis cell division process takes places resulting in the production of haploid spores. These spores get transported from one place to another and start to germinate forming hyphae, thus repeating the cycle.

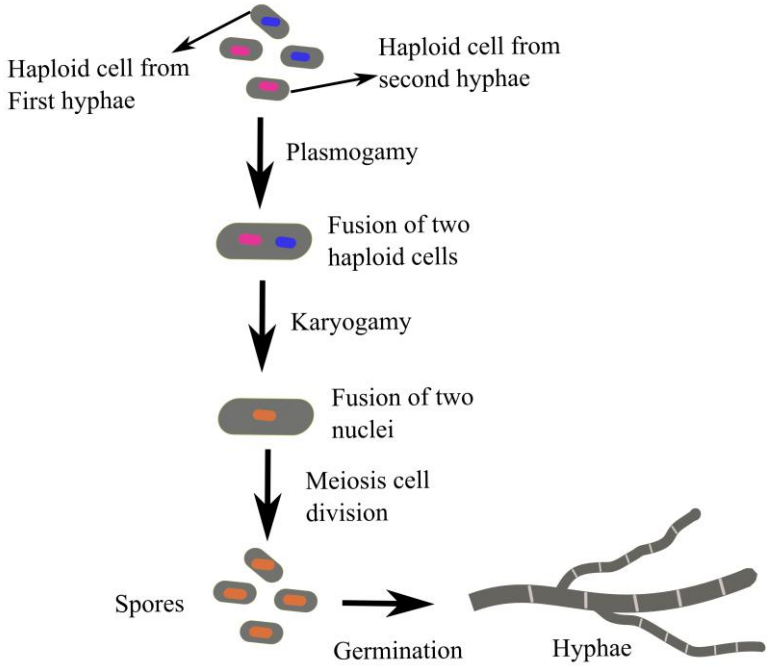

Figure 4: sexual reproduction of mold [7].

The growth of mold depends on various conditions, like temperature, humidity, availability of nutrients, presence of water in the nutrient medium, etc. Different mold species could have different requirements of the nutrients and other environmental conditions for their growth. Once all the nutrients are used up by the mold, they start to reproduce (via spores or by fragmentation) and are then transported to other locations, thus colonizing other organic substances. The spores vary in size from 1 µm to 100 µm. Spores that are transported via wind are called airborne spores and their sizes are in the range from 1 µm to 20 µm, bigger spores are heavier to be carried away by air currents. The mold spores remain dormant (not active) if the environmental conditions do not favor their germination. Once they have favorable growth situation with enough humidity, temperature and nutrient material, they start to germinate by degrading the substance that they reside on by developing filaments of branches (hyphae).

2.2 Indoor mold exposure and its effects

Molds can be found everywhere, in the indoor and in the outdoor. Mold spores are easily transported from outdoor to indoor environments with wind, through ventilating systems and via insects. As most of the indoor material including buildings, wooden floors, wooden walls, books, papers, food are of organic origin; they are easily prone to mold contamination. The possibility of mold growth is even higher if there

is condensation in the indoor, caused by humidity accumulation. Lack of proper air ventilation further increases the possibility of mold growth [9].

In the last decades, interest for the detection of mold growth inside the indoor environments has received much attention. This is because growth of mold not only destroys food, books, buildings, or other organic material present in the indoor but they are also responsible for health hazards in humans and animals [10]. Persistent exposure to the indoor mold could cause several infectious diseases like allergies, asthma, sinusitis, hypersensitivity pneumonitis etc. Recent data shows that approximately 10 % of the world population has developed immunoglobulin E (IgE) antibodies due to the inhaled mold [11]. Furthermore, about 5 % of the population is predicted to have developed allergic reactions due to the mold exposure [2]. Also, recent studies by the world health organization suggest that people living in damp homes where mold growth is visible in their houses were 75 % more likely to get effected with respiratory tract infections, persistent wheezing and cough [12][13].

In addition to the mentioned effects, the mold growth on food produces mycotoxins. Mycotoxins are chemical compounds released by the molds once they start to digest organic material [14]. These mycotoxin compounds are also called as secondary metabolites and are not consumed by the mold for their reproduction. Since they remain in the food, once they are consumed in large dosage they could cause severe human illness [15][16]. Also, as the mold grows they produce mobile volatile organic compounds (MVOC's) [17]. Depending on the exposure level and duration, these MVOC's could cause headaches, throat, eye and nose infections in humans and animals [18]. So the best way to avoid these effects is to prevent the growth of mold inside the indoor environment.

In industrial environments, especially in the food storage rooms, spoilage of raw material or food is often linked to the growth of mold inside the storage area. Hence for controlling the mold contamination, it is advisable to monitor the mold spore concentrations at the processing sites, storage rooms and also at the ventilator locations [19]. A major recommendation for maintaining the quality of food is to have a year-long mold monitoring system for measuring the mold spore contaminations. This not only allows in determining the variations in microbial concentrations over a period of time but also provides the possibility for the responsible personnel to act quickly if there is any contamination outbreak inside the indoor.

In archives, museums, residential homes, hospitals and schools, a major reason for mold growth is due to high humidity or due to accumulation of water because of leakages [20]. Even in these environments, it is important to adapt regular mold monitoring procedure to prevent damage of the stored material. To minimize the possibility for airborne spores reaching the indoor environments from outdoor, high

efficiency particulate air (HEPA) filtration systems are employed. Defects in HEPA filters could also result in increase of the mold contamination.

2.3 Methods for detection of indoor mold

To avoid diverse health risks and material damages caused by mold contamination, many measurement techniques have been developed to assess mold growth in the indoor environments [21][22]. Detection of mold is divided into two stages; the first stage is sampling which is then followed by an analysis stage. An overview of various sampling and detection techniques that are currently employed for assessment of mold contamination is presented in Fig. 5.

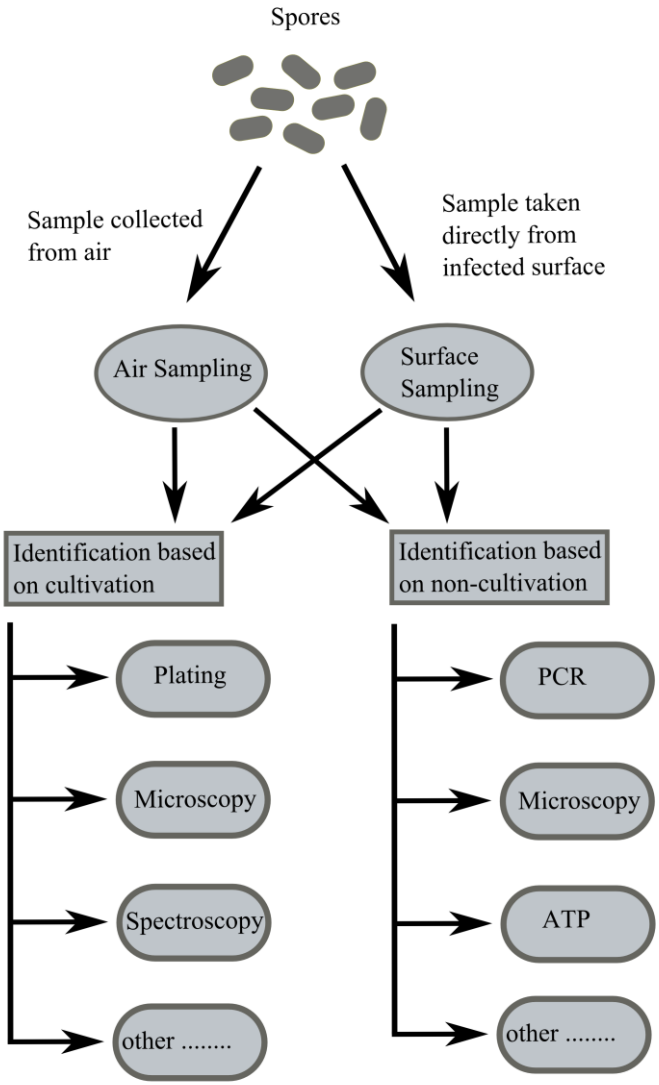

Figure 5: Flow chart illustrating different sampling and detection techniques employed for the monitoring mold contamination [21].

2.3.1 Sampling techniques

When a mold contamination is visually suspected, different techniques are employed for collecting the samples, which are later analyzed for quantification and identification of the mold [23]. There are two different types of sampling methods, surface sampling and air sampling. The type of sampling technique to be used depends on the damage evaluation. Hence prior to the sampling a thorough inspection of the damaged location is done. After visually evaluating the situation, the type of sampling method to be used is determined.

Surface sampling

In this sampling technique, the sample is directly taken from the surface. The easiest way of taking the sample is by using an adhesive tape (e.g. transparent Scotch tape) [24]. If any fungal growth is suspected or seen on a material, the adhesive tape is pressed onto the surface with the sticky side facing the surface. This allows the mold spores and the hyphae present on the surface to get attached to the sticky surface of the tape. The tape is then carefully removed and is either attached on a dry microscopic slide or transferred in a clean plastic bag to the laboratory for further analysis.

In addition to adhesive tapes, there are contact plates or Rodac strips, which are used for surface sampling and direct cultivation [25]. These contact plates contain culture medium filled until the rim of the plate. The culture medium is pressed directly against the surface of the contaminated material, thus allowing the spores to stick onto the culture medium. Later the plates with culture medium are closed and incubated for further analysis.

Direct plating is another type of surface sampling method. This method is considered to be effective if the material is already infected with mold [26]. For identification and enumeration of the mold, a small piece of the infected material is either transferred directly onto a culture medium or suspended in a dilution fluid and then plated onto the culture medium. The culture medium is then incubated for 5-7 days for further analysis.

Swab sampling is done using sterile swabs, where the tip of the cotton swab is dipped in sterile water and then rubbed over the surface of the material (suspected to have mold contamination) [27]. These swabs are then packed in a sterile plastic bag and are transferred to a laboratory. In the laboratory, the swabs are either directly rubbed over the culture medium or suspended in a peptone solution, which are later quantified using dilution plating.

Air sampling

Air sampling techniques are often used for the detection of mold that produces airborne spores. These mold species include *Aspergillus, Penicillium, Eurotium* and *Cladosporium*. Mold species like *Chaetomium, Trichoderma,* do not produce airborne spores. For such species, surface sampling is favored. There are two types of air sampling techniques, passive and active air sampling [28].

In passive air sampling, petri dishes containing the culture medium are opened and are exposed to the air for a certain period of time. This allows the particles present in the indoor to get settled in the culture medium (due to gravity). As this method depends on the sedimentation of the spores, this technique is also called sedimentation or gravity plating technique. Depending on the estimated density of spores the opened petri dishes are closed sooner or later. Typically the petri dishes are opened for 15-60 minutes. This method is only recommended for the initial or preliminary identification of the mold as it provides non-quantitative values. Passive air sampling is mostly used inside food production lines (e.g. inside an oven, or on food transport belts) where active air sampling is hard to do. Once the samples are collected, the petri dishes are closed and transferred to an incubator for further analysis.

For quantitative analysis of the mold, active air sampling is used. In this method, a defined volume of air is pumped either onto a petri dish containing the culture medium or onto an adhesive tape (or microscopic strip) [29]. For diverting spores onto a defined spot on an adhesive strip or on a petri dish, impactors are used. Petri dishes filled with the culture medium are impacted with air at a defined flow rate (for a defined time) and are later closed and incubated [30]. The incubated culture medium plates are later analyzed in the laboratory for identification and quantification of the mold spores. In general, 30-100 liters of air is collected onto the petri dishes. This volume could also be higher or lower depending on the density of spores present in the collecting environment [31]. In a very clean environment, for example in intensive care units (inside hospitals), high air volume is necessary because the spore concentration inside will be very less. In general, for detecting mold that is present at a very low level, high sampling volumes are required. On the other hand, in agricultural fields where the expected fungal contamination could be very high, less air volumes are sampled.

2.3.2 Analytical methods for mold detection

Different analytical techniques are employed for detection and enumeration of the mold as shown in Fig. 5. Based on the objective of investigation, the collected samples are analyzed either to detect the mold particles like spores and other mold fragments (e.g. hyphae), or the samples are investigated for the presence of specific secondary metabolites like MVOC's, mycotoxins, allergens, or other cell wall compounds [21][22]. Mostly, mold assessment is done based on the amount of spores or hyphae particles present in the air sample. If there is a need to detect a specific mold (e.g. mold species which is associated with severe health risk) then specific quantification is done based on the cell components or using secondary metabolites of that particular mold species. Different methods employed for the mold detection are microscopic analysis, cultivation technique, Polymerase chain reaction (PCR) method, immunoassay methods, bioluminescence based methods and chemical methods. The following section explains each method in detail.

Microscopic analysis

Microscopic mold detection relies on the visual examination of suspicious samples collected either using the surface or the air sampling techniques. The sample preparation for the optical detection process is very easy; first a tiny droplet of water or dispersion fluid is placed on a microscopic slide. Later a small piece of mold (growing on a material) is transferred onto this liquid drop using a sterile needle. As a final preparation step, this drop is covered with a microscopic cover slip and thus allowing the liquid to form a uniform layer. Optical analysis can be done with the liquid or after the liquid gets evaporated. Samples taken on an adhesive tape either by using an impactor or via tape lift method are also prepared in a similar manner. After placing the adhesive tape on the microscopic slide, a drop of dispersion liquid is placed on top of the tape and is later covered with a cover slip. The prepared microscopic slides are placed under a microscope for visual identification and enumeration of the mold.

Easy sample preparation steps and shorter detection times are the major advantages of the optical detection method. To ease the effort of laboratory personals, several image processing software's were developed and are available in the market for automating the spore counting process [32]. There exists an automated spore and pollen counting device for the outdoor environment [33][34]. Though the optical method is faster and easier, it has some disadvantages. With this technique both viable (living or active) and non-viable (dead or not active) spores are quantified. As it is not possible to distinguish between the viable and the non-viable mold spores this method does not allow the detection of mold growth. Having the information about the quantity of spores is not enough to confirm the risk of the mold growth because

only viable spores are responsible for the mold growth inside an indoor environment [35].

Cultivation technique

The cultivation or culture-based method is a standard approach used for the detection of mold growth. These methods do rely on the mold growth, where the mold samples are collected on a sterile nutrient or culture medium, which is filled in a petri dish. Once sample is collected on the culture medium, the petri dishes are closed and are transferred into an incubator chamber to provide the necessary environmental condition (e.g., temperature and humidity) required for the mold to grow. The sample or the viable mold spores collected will start to decompose the culture medium and start to grow in the form of colony (each visible spot of mold growth on the culture medium is termed as a colony). These colonies are later counted in terms of colony forming units per cubic meter of air sample (CFU/m^3 or CFU/ml for sample diluted in liquid) and are used for quantification. Sample preparation for the culture-based methods is labor intensive. Samples can be collected either directly from the air on the culture medium (using impactors) or can be transferred onto the culture medium in liquid form. In general, mold spores that are collected on the nutrient medium by air sampling techniques are cultured directly. This allows the possibility for direct quantification in terms of CFU per cubic meter of air sample (which is the standard).

An-other scenario, where the samples are collected using surface sampling techniques, several preparation steps are required. Firstly, the collected sample has to be dispersed in a liquid. Later, different dilutions are made so as to decrease the concentration of the mold species in the liquid. Finally, a defined amount of liquid (e.g., 100 µl) is transferred and distributed homogeneously over the culture medium. The petri dishes are closed and the medium is incubated. Once visual colonies are formed, they are counted for quantifying in terms of CFU per milliliter.

Automated image processing software tools are available to count the number of colonies growing on the culture medium, which reduces the manual effort [36]. Cultivation technique is one of the easiest and most economical ways for the detection and identification of molds. One of the major disadvantage of using this method is the time it takes for the mold species to grow (which is normally days) forming a visual colony for counting.

Major advantage of using culture-based analysis is that only the viable mold species are detected. Also, since various microorganisms prefer different nutrients for their growth, it is possible to make the culture medium specific to one particular microorganism. For example growth of bacteria in the medium can be inhibited by addition of chloramphenicol to the culture medium.

Polymerase chain reaction based mold detection

Molecular based methods have received major attention for the detection and identification of mold because of their fast analysis. Polymerase chain reaction (PCR) based DNA sequencing is the most frequently applied molecular technique for the purpose of species identification [37][38]. Both surface sampling and air sampling methods can be used for sample collection. After sample collection, there are multiple steps involved in DNA sequencing method. Firstly, the mold cells or spores have to be lysed for extracting the genomic DNA. Once the DNA has been extracted, the location of interest (in the Gene) has to be amplified using PCR. With PCR, the DNA fragment or template is amplified exponentially. As a last step, the amplified DNA is detected (base-pair sequence of the amplified DNA is determined) either by using electrophoresis or hybridization techniques [39].

Major advantages of the molecular based detection techniques in comparison to the standard morphology or physiological method is that it offers rapid detection and is reproducible. The quantitative PCR method is mostly used for specific identification of certain mold species. Moreover, both viable and non-viable mold spores are quantified using the PCR method.

Although this method has a good specificity, sample preparation is very complex, and requires experienced professionals. Extracting DNA from the mold spores or cells itself needs several laborious steps like, lysis of the mold cells (by mechanical, chemical, or enzymatic disruption of cells), separation of the DNA from other fragments (by centrifugation or filtration), washing DNA to remove salts and other proteins attached to the fragments. Later for PCR, several reagents have to be mixed in proper concentrations and the sample should be placed in a thermocycler. Once the sample is amplified, it should be transferred to the electrophoresis chamber for analysis. Because of these multiple steps, this method is often prone to contamination and moreover this method is expensive.

Immunoassay method

Immunoassay is a biochemical method applied for measuring the presence of an analyte through antibody-antigen interactions [40]. This method relies on the ability of an antibody to identify and bind to a specific location of the mold. Immunoassays are carried out in multiple steps. Firstly, a solution comprising of antibodies is placed in a reaction chamber and is incubated for a certain period. After incubation, the antibodies in the solution get adsorbed onto the walls of the reaction chamber. The remaining solution is washed off using a buffer solution. Later sample with analyte or antigens (such as mold spores or parts of hyphae, or mold cells) is added to the reaction chamber. After a predefined incubation time, the target antigen binds to the antibody and

gets adsorbed to the walls of the reaction chamber. The reaction chamber is then washed with a buffer solution to remove molecules other than the adsorbed antigens. As a final step for measurement, a colorimetric substrate is added to the reaction chamber. This substrate interacts with the antibody, thus generating a color intensity signal which is proportional to the target antigen (which is attached to the antibody).

As immunoassays have faster detection times and are highly accurate in detecting specific antigens, they are often used in the food industries for monitoring and detecting contaminants present in food, air or water. Although this method is successful and can be used for on-site detection of contaminants, there are complications in developing or obtaining the required antibodies with high specificity for the vast variety of the mold species present in our ecosystem. Also, several sample preparation steps are involved in this method, thus requiring experienced laboratory professionals.

Bioluminescence based methods

Adenosine triphosphate (ATP)-bioluminescence is a rapid detection method which can be employed for detection and enumeration of different microorganisms present in the air or that are growing on a surface [41][42]. ATP is a molecule found in all living organisms or cells and can be quantified by a luciferase based bioluminescence reaction. In this reaction, luciferin is oxidized by the luciferase in the presence of ATP and magnesium. This oxidation reaction results in an emission of light where the emitted light intensity is directly proportional to the amount of ATP present inside the cells.

Detection of microorganism using this method starts with a lysis process, where the ATP content present inside the organisms or cells is extracted. Various chemical and physical lysis methods can be employed for extracting the ATP. Later, a bioluminescent assay is used for measuring the presence of ATP. This method is fast and thus can rapidly determine the amount of living microorganisms present in a sample. As all viable microorganisms have ATP in their cells it is not possible to exactly quantify the mold species. Also to automate this method is complex because the microorganisms have to be lysed, should be mixed with different substrates and enzymes are required for the bioluminescence reaction.

Chemical methods

For analyzing cell wall components and secondary metabolites released by the mold (like mycotoxins and microbial volatile organic compounds) different chemical methods are employed [43]. For identification of the mold based on their molecular composition, various spectroscopic techniques such as Fourier transform infrared spectroscopy (FTIR) and mass spectroscopy have been introduced [44]. Depending

on the molecular composition of the mold, they absorb infrared light, thus generating a spectrum. This spectrum can be used for the identification of different microorganisms like mold or bacteria. Likewise, mass spectroscopy is another analysis method in determining the fingerprint for microorganisms by ionization methods [45]. Though spectroscopic methods are accurate and allow identification of specific mold species, they are confined to laboratory use because of their complexity and cost. Moreover, samples should be prepared in a clean environment as these methods are sensitive to contaminants.

Mold detection is also possible by analyzing Ergosterol. Ergosterol is a major sterol component present in cell membranes of mold (hyphae or spores). By measuring the quantity of Ergosterol it is possible to determine the mold biomass. Ergosterol can be detected using either liquid-phase chromatography or gas chromatography in combination with the mass spectroscopy [46]. Though Ergosterol is found only in the mold cell walls, it is present in small amounts hence recovering this component from the cell walls is very complex [47].

Another possibility for the detection of mold is by monitoring the microbial volatile organic compounds (MVOC's) emitted by the mold during their growth [48]. So far over 500 different types of MVOC's have been identified. MVOC's emitted are sampled or captured onto special adsorbents using solid-phase micro extraction technique [49]. Later they are analyzed either by using gas chromatography or by using mass spectroscopic techniques for determining the figure print of that particular MVOC. This method is not suitable for the mold detection because it was proved that MVOC's emitted by the same mold species are influenced by several factors. For example, the type and amount of MVOC's emitted depends on the nutrient medium on which the mold is growing, on the age of the mold and also on the climatic conditions during the mold growth. Furthermore, low levels of MVOC's are emitted thus making sampling process complex.

2.4 Common molds in archives

Most commonly found mold species in archives are *Eurotium Amstelodami, Aspergillus Peniciloides, Aspergillus Restrictus* and *Cladosporium Cladosporiodes*. These molds produce airborne spores that are easily transported from one place to another via winds or with insects. Eurotium Amstelodami is one of the major indoor mold species. Their airborne spores sizes vary from 10 μm to 20 μm and are relatively bigger when compared to *Aspergillus* and *Cladosporium*. Their spores are spherical in shape with rough outer surface. *Cladiosporium Cladosporiodes* are common both in indoor as well as in outdoor environments. Their spores are small in size (around 1-2 μm) and are easily transported through air. *Aspergillus* species require less water to grow when compared to *Cladosporium* and *Eurotium*. So *Aspergillus* species is mostly found

on dry paper or dry files. Their spore sizes vary from 2-7 μm and are ellipsoidal in shape.

Eurotium and *Cladosporium* molds are common in the archives with condensation problems or archives with high humidity (relative humidity greater than 70 %). Archives that are located in basements with no proper climate control will provide suitable conditions for these species to grow (because of high humidity). Both these species utilize dampness (water) and degrade organic matter present in the archives.

2.5 State of art

Using the microscopic optical detection principle an autonomous pollen and spore monitoring sensor system for outdoor environments has been designed and realized [33]. This system uses light microscopy to extract an optical fingerprint of various airborne particles like pollens, spores and other dust or soot particles. As a first step, the airborne particles are collected onto a substrate. Later, the samples are illuminated with white light for obtaining three dimensional images. In addition to the white light, an UV light of 395 nm wavelength is integrated to determine the autofluorescence property of the pollens and spores. The collected pictures are analyzed using different pattern recognition procedures to extract specific features of pollens, spores and soot. The pattern recognition software finally determines the amount of airborne particles.

Although this optical method has some advantages like it is faster and easier, a major disadvantage is that it cannot give information about the mold growth. This is because with the optical method both viable and non-viable pollens, spores are detected. Though both viable and non-viable spores could cause allergic reactions once inhaled, only viable spores are responsible for further contamination.

Milliflex rapid detection system is a sensor system available in the market, which can be used for rapid detection of microorganism by using the ATP-bioluminescence principle [50]. There are three major steps involved in identifying microorganisms using this sensor system. First step is sample collection on a membrane. In the second step, the membrane is transferred onto a spraying station where all the required reagents for the bioluminescence reaction are applied automatically across the membrane. As a last step, the membrane is transferred to a camera module for image analysis. Although this method can rapidly determine the amount of ATP present in the living organisms, it is not an automated sensor system. The collected sample (in a membrane) has to be transferred to three different modules for enumeration. Moreover, using the ATP-bioluminescence method all the viable microorganisms are detected thus making it hard to quantify the mold species.

Bruker Daltonics demonstrated an instrument (MALDI Biotyper, Bruker Daltonics, EW Leiderdorp, The Netherlands) for the detection of the mold based on the mass spectroscopy [51]. With this instrument it is possible to identify the protein fingerprint of individual microorganisms. The obtained protein fingerprint characteristics are different for each species, which helps in identification of specific microorganisms. Though this instrument is efficient and rapid, it is not an autonomous sensor system and moreover several sample preparation steps are involved before microbial identification. Furthermore, these spectroscopic techniques are confined to laboratory use because of their cost and complexity.

The existing sensor systems are complex, costly and are not fully autonomous. For some of these systems, the sample preparation steps must be done in the laboratory before detection. Hence, in this thesis the design, realization and characterization of a fully autonomous sensor system, which is based on a culturing method has been described.

3 Theoretical Considerations

A biosensor is a device that is employed for detection and quantification of biological species or molecules present in a medium. There are different types of biosensors, which are categorized based on the measurement principle involved [52]. Electrical, chemical and optical ways (e.g., Fluorescence, Bioluminescence, Surface plasmon resonance) are mostly used for measuring or detecting a particular species (or molecule) present in a solution [53]. Over the last decade electrochemical biosensors have generated a tremendous interest in the detection and quantification of biological species. As these electrochemical biosensors rely on the measurements of current or voltage for the detection of target molecules, they are easier to miniaturize and can be readily integrated into an electronic sensor system. Currently, this technique is widely being used for label free and real time detection of DNA, Proteins and in immunoassays [54–57] .

Based on how the electrical measurements are done, the electrochemical biosensors are classified into different categories, voltammetric, amperometric, potentiometric and impedance based biosensors. The voltammetric and amperometric sensors utilize a redox reaction of an electroactive species [58,59]. By applying a constant potential between the reference electrode and the solution, the current flow is measured at a working electrode. Because of the redox reaction there is a change in the current flow, which is measured at the working electrode. Using this measurement principle a glucose sensor has been realized [60]. This sensor uses glucose oxidase enzymes for oxidizing glucose to gluconic acid. Because of this oxidation reaction there is generation of free electrons, which leads to an increase in the current flow at the working electrode. The measured current is linearly proportional to that of the glucose concentration. In addition to the glucose measurement there are other examples for detection of DNA and other biological molecules [61,62]. All of these sensors utilizing the voltammetric and amperometric principles involve the use of redox reactions (i.e, redox enzymes have to be added for the initiation of the reaction). This could result in the corrosion of electrodes and are unstable for long-term usage, therefore.

The potentiometric sensing method involves measuring the potential of the bulk solution enclosed between the electrodes. The reference electrode maintains a constant potential, whereas the working electrode measures the changes in the potential dif-

ference between its surface and the bulk solution. As the ionic concentration of the bulk solution changes, the potential difference measured varies. Therefore, the measured difference in the potential gives an assessment of the ionic concentration of the bulk solution [63]. Usually the working electrodes used in the potentiometric sensing are ion selective, thus measuring only one particular type of ion. Currently, there exists several ion-sensitive field effect transistors using this principle to measure pH changes in a solution [64]. The potentiometric sensing doesn't require redox reactions, hence there is a much less risk of electrode corrosion when compared to the voltammetric and amperometric methods. One of the major disadvantages of the potentiometric sensing method is that it requires an ion sensitive electrode [65]. Because of this, the sensor should be calibrated every time before a new measurement is done. Also this method is sensitive to external factors like temperature, humidity.

In recent years, electrochemical impedance spectroscopy (EIS) has become one of the attractive analytical techniques used in the biological analysis or in the field of biosensors [66]. Electrochemical impedance spectroscopy utilizes the electrochemical kinetics happening at the electrode-bulk solution interface for determining the conduction mechanisms involved in the system [67]. Typically, in the EIS the impedance response is measured over a wide range of frequencies. For monitoring the impedance changes occurring in the bulk solution a small AC signal is applied between the reference and the sense (or working) electrodes, and the resulting current flowing through the system is measured. The measured impedance of the system depends on the molecular interactions happening at the electrode-bulk solution interface, which varies depending on the concentration of the ions inside the bulk solution. Thus by measuring the impedance spectrum it is possible to determine various diffusion and conduction mechanisms, molecular interactions and concentration changes happening inside the bulk solution [68].

As the EIS is based on simple electrical measurements, this method can be easily automatized and integrated into standard electronic circuits. Moreover, there is no need of any redox enzymes as this method uses intrinsic impedance properties of the bulk for determining the concentrations. Also, when compared to the potentiometric method, no ion sensitive electrodes are necessary. Hence this method can be used for label-free detection of different biological molecules. In addition to the biological applications, EIS technique is broadly employed in material research for monitoring material degradation, corrosion monitoring, in fuel-cell based sensors etc.

3.1 Overview of electrochemical impedance spectroscopy

3.1.1 Electrochemical impedance representation

For the electrochemical impedance spectroscopy experiments, a minimum of two electrodes are required, which are referred as sense and reference electrodes. A basic electrochemical cell is shown in the Fig. 6. The bulk solution which has to be analyzed is suspended between the sense and the reference electrodes. When a small external potential (V) is applied between the two electrodes, current (I) starts to flow through the electrochemical cell.

The current (I) flowing through the electrochemical cell due to the applied potential difference (V) is contributed by two different charge carriers i.e., electrons present in the electrodes, and ions within the bulk solution. Within the electrochemical cell, there exists two different regions which offer resistance to the flowing current. The first is called interfacial region which appears at the electrode-bulk solution interface. In this region there is a shift in the charge carriers i.e., from the electrons in the metal electrodes to the ions in the bulk solution. The second region opposing the flow of current is within the bulk solution. Also in this region there exists a resistance to the ionic migration.

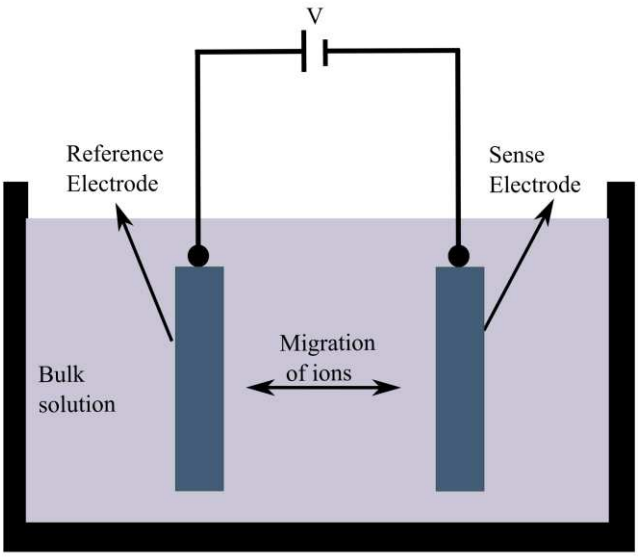

Figure 6: A simple electrochemical cell for impedance spectroscopy [66]

There are two major physical processes involved in the electrochemical impedance spectroscopy: charge-transfer and diffusion of charged ions [66]. Different phenomenon happening during the impedance spectroscopy (with an applied potential V), at the electrode-bulk interface and within the bulk solution is represented in Fig. 7a.

These phenomena can be explained in detail by using an electrical equivalent circuit model called Randles circuit as shown in Fig. 7b. This circuit model allows the explanation and prediction of the frequency-dependent behavior of the electrochemical cell.

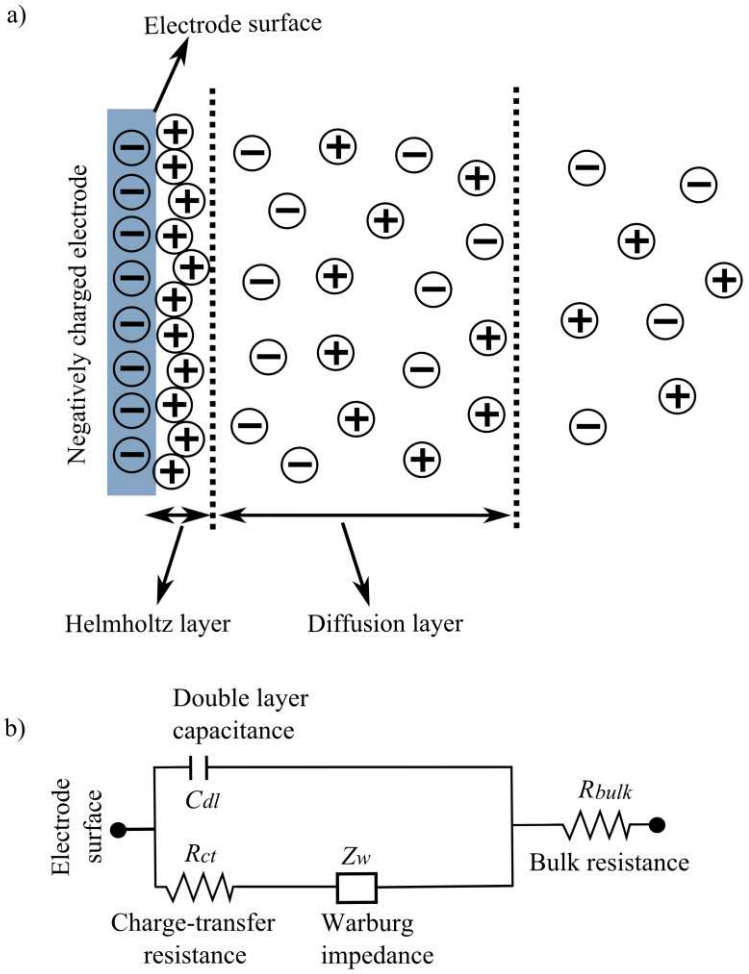

Figure 7: a) Electrochemical interactions happening at the electrode-bulk solution interface b) Randles electrical equivalent circuit model [66]

In brief, R_{bulk} represent the resistance of the bulk solution. R_{ct} is the interfacial or charge-transfer resistance at the electrode-bulk interface, C_{dl} is the double layer capacitance that exists at the electrode and the bulk interface. Z_w is the Warburg or mass transport impedance. In the following sections detailed emphasis is provided on individual circuit elements.

Electrochemical double layer capacitance C_{dl}

At the electrode-bulk interface there exists a charge carrier transition from electrons to ions, resulting in the formation of an electrical double layer. As soon as the electrodes are bought in contact with the bulk solution, the ions and other charged species present in the bulk come in contact (or get adsorbed) with the electrode surface. Because of this, charges in the electrodes and ionic charges get separated, thus creating a potential drop across the separated distance, resulting in the formation of the double layer capacitance C_{dl}. This separation distance of charges is very small (in the scale of nanometers). The double layer capacitance measured will be in parallel with the measured double layer or charge-transfer resistance R_{ct}.

The capacitance of the double layer mainly depends on the intrinsic properties of the bulk solution such as, dielectric constant, permittivity, concentration of conducting ions in the bulk, dipole moment, the size and shape of ions within the bulk, etc. Also, the value of double layer capacitance depends on various other factors, like electrode type, shape, heterogeneity at the electrodes surface, the type of oxide deposited on electrodes, medium temperature, other adsorbed impurities on the electrode surface etc. The experimentally measured double layer capacitance values for ionic aqueous solutions are typically in the range of 10-60 μF/cm^2[66].

The double layer capacitance at the electrode interface is composed of different layers as shown in the Fig. 7a. Maxwell-Wagner, Helmholtz, Stern have developed theories to explain the dynamics of the double layer. In brief, the double layer mainly comprises of three adjacent layers, inner Helmholtz layer, outer Helmholtz layer and the diffuse layer.

The inner Helmholtz layer (IHL) is the closest layer to the electrode surface and consists of adsorbed molecules or ions. The layer adjacent to the IHL is the outer Helmholtz layer (OHP) and is comprised of electrostatically attracted ions or molecules. The diffuse layer also comprises of the electrostatically attracted ions, which are distributed at some distance away from the electrode. The double layer thickness is the distance measured from the electrode surface till the external boundary of the diffuse layer, where the potential measured is equal to that of the bulk solution. The double layer capacitance is the series combination of the Helmholtz capacitance and the diffuse capacitance as shown in Eq. 1.

$$\frac{1}{C_{dl}} = \frac{1}{C_{Helmholtz}} + \frac{1}{C_{Diffuse}} \qquad \text{Eq. 1}$$

Where, $C_{Helmholtz}$ is the Helmholtz capacitance and is expressed as [66]

$$C_{Helmholtz} = \frac{\varepsilon.\varepsilon_0}{L_{Helmholtz}} \qquad \text{Eq. 2}$$

$L_{Helmholtz}$ is the Helmholtz layer thickness which is in the range of 1-2 nm [66]. ε is the relative permittivity and ε_0 is the absolute permittivity. The Helmholtz capacitance is relatively constant with the concentration of ions and is in the range of 1-60 μF/cm^2 (for different bulk solutions). As the value of $L_{Helmholtz}$ is much smaller than the diffuse length, the Helmholtz capacitance is 4 to 5 times larger than the diffuse layer capacitance [66].

On the other hand, the diffuse layer capacitance is dependent on the applied potential (ϕ_0), conducting species concentration present in the bulk solution (n_b), relative permittivity of the bulk (ε), diffuse layer thickness (λ_{Debye}) and charge of the ionic species (Z), and is given by the Eq. 3 [66].

$$C_{Diffuse} = \frac{\varepsilon\varepsilon_0}{\lambda_{Debye}} \cosh\left(\frac{Zq\phi_0}{kT}\right) \quad \text{Eq. 3}$$

$$\lambda_{Debye} = \sqrt{\frac{\varepsilon\varepsilon_0 kT}{8\Pi q^2 \sum z^2 n_b}} \quad \text{Eq. 4}$$

Where q is the charge of an electron, k is the Boltzmann constant, T is the absolute temperature. λ_{Debye} is the Debye length, which gives information about the thickness of the diffuse layer. The diffuse layer thickness is determined using the formula shown in Eq. 4. The diffuse layer thickness varies with the ionic concentration of the bulk. Bulk solution with high ionic concentrations (~0.1 M) will have a thin diffuse layer of about 10 nm. Whereas if the bulk solution has very low ionic concentrations (10^{-7} M), the diffuse layer is thicker (in the range of 1 μm) [66].

Electrochemical charge-transfer resistance R_{ct}

Whenever the electrode-bulk interface is disturbed from its standard equilibrium there will be a flow of electric charge from the electrode to the bulk or vice versa. The resistance offered by the system to this flow of charge is termed as the charge-transfer resistance R_{ct}. There are two major reasons why an interface is disturbed from its equilibrium. Firstly, if there is an electrochemical reaction taking place within the system then the charges generated from this reaction will disturb the equilibrium. In the second situation, the presence of electric or charge gradients inside the bulk could charge the interface which inturn will change the equilibrium of the interface [66].

When the electrode interface is driven away from its equilibrium then the electrode gets polarized. With polarization of the electrode, there will be flow of current. The amount of current flowing through the electrochemical cell is determined by the diffusion of reactants (towards and away from the electrode surface) and by the kinetics

of the electrochemical reaction. The current flow as a function of applied potential is given by the Eq. 5 [66].

$$i = i_0 \left(\frac{C_{ox}}{C_{oxb}} e^{\frac{\alpha z F (V - V_0)}{RT}} - \frac{C_{Red}}{C_{Redb}} e^{\frac{(\alpha - 1) z F (V - V_0)}{RT}} \right) \quad \text{Eq. 5}$$

Where, i_o is exchange current density, C_{ox} and C_{oxb} are the concentrations of oxidant at the electrode surface and bulk respectively, C_{Red} and C_{Redb} are the concentrations of reductant at the electrode surface and bulk respectively, F is Faraday's constant, T is the absolute temperature in Kelvin, α is the transfer coefficient, R is the gas constant, z is the number of electrons involved in the reaction, V is the applied potential and V_o is the equilibrium electrode potential.

Considering the case where the concentrations of charges are equal in the bulk and at the electrode surface then the Eq. 5 can be simplified to Butler-Volmer equation (Eq. 6) [66].

$$i = i_0 \left(e^{\frac{\alpha z F (V - V_0)}{RT}} - e^{\frac{(\alpha - 1) z F (V - V_0)}{RT}} \right) \quad \text{Eq. 6}$$

The charge transfer resistance R_{ct}, can be determined using the following expression [66].

$$R_{ct} = \frac{RT}{z F i_o} \quad \text{Eq. 7}$$

Exchange current density (i_o) can be determined either using Eq. 5 or by the Eq. 8 [66].

$$i_0 = z F A k_0 c_{ox} e^{\frac{-\alpha z F}{RT} (V - V_0)} \quad \text{Eq. 8}$$

Where K_0 is the kinetic rate constant, A is the area of the electrode.

Bulk solution impedance R_{bulk} and C_{bulk}

Using the electrochemical impedance spectroscopy it is also possible to investigate the motion of ions, polarized molecules and other charged species present in the bulk solution. In the EIS, two different processes happen, one at the electrode-bulk interface (i.e., process involving R_{ct} and C_{dl}) and the other process happens inside the bulk solution. During the EIS, electric current starts to flow through the electrochemical cell, this current flow in the bulk medium is transported by the migration of ions, or by conductive species, or via dipoles present in the bulk. This conduction mechanism varies based on the type of bulk medium used. For example if the medium is a polar

liquid then the conduction is purely ionic. Whereas, when the medium is solid (conducting) then the conduction mechanism is via ions and also by the electrons.

The bulk solution resistance is determined from the following equation Eq. 9 [66].

$$R_{bulk} = \rho \frac{d}{A} \quad \text{Eq. 9}$$

Where A is the surface area of the electrodes exposed to the bulk solution, d is the thickness of the sample and ρ is the resistivity of the bulk material. The bulk resistance can also be expressed in terms of concentration of the conducting species C_i, charge of the species z and their mobility u as [66]

$$R_{bulk} = \frac{1}{\sum zuc_i} \quad \text{Eq. 10}$$

If the bulk medium is aqueous then there exists only resistive component, but if the bulk solution is dielectric then the electrical equivalent for the bulk is a complex circuit comprising of a capacitive component C_{bulk} in parallel to the resistive component R_{bulk}.

Warburg or Mass transport impedance Z_w

In addition to the Helmholtz and the diffuse layers which are present at the electrode surface, there exists an additional layer called diffusion layer. The diffusion layer starts at the external boundary of the diffuse layer and extends into the bulk solution. The mass transport impedance is the impedance offered by the system to the movement of charge ions or species present in the diffusion layer and in the bulk solution. The mass transport impedance is also called as Warburg impedance (Z_w). This impedance represents the amount of charges that have been transported from the electrode to the bulk and from the bulk to the reaction site. Because of the concentration gradient inside the bulk solution the charged species get transported from higher concentration location to the lower concentration location via diffusion or migration or via convection. The Warburg impedance can be calculated using the following equation [66]

$$Z_w = \frac{RT(1-j)}{z^2F^2AC^{dif}\sqrt{2\omega D}} \quad \text{Eq. 11}$$

Where R is the gas constant, T is the absolute temperature in Kelvin, z is the amount of transferred electron charges, A is the surface area of the electrode, F is the Faradays constant, C^{dif} is the concentration of diffusing species or ions in bulk solution, D is the diffusion constant.

3.2 Impedance based biosensing

Impedance based biosensors can be divided into two categories. Affinity-based impedance biosensors and microbial metabolism based impedance sensors. In the affinity-based biosensors, the concentration of an analyte (i.e., molecule or ion that has to be analyzed) in a solution is estimated by using antibodies or probe molecules, which selectively bind the analyte. In the case of microbial metabolism based impedance sensors, microorganisms are allowed to grow in the culture medium and the impedance of the culture medium is monitored at regular time intervals. Based on the measured impedance growth curves, it is possible to determine the concentration and the type of microorganism. Detailed explanation regarding these two types of impedance biosensors are explained in the following sections.

3.2.1 Affinity based impedance biosensing

The affinity-based biosensing is one of the most frequently used impedance methods for detection of an analyte in a sample. The different steps involved for the detection of analyte using this method are explained in [69]. The affinity-based biosensors require immobilization of probe molecules or antibodies on the electrode surface. The antibodies are selected such that they can specifically bind to the target analyte. Once the antibodies are immobilized, the sample consisting of analyte molecules is placed on the surface. The analyte molecules start to diffuse through the sample and move towards the electrode surface where they start to bind to the antibodies present on the electrode surface. By performing impedance measurements it is possible to determine the concentration of the captured analyte. Other optical detection methods can also be employed instead of the impedance measurements, but in the case of optical methods an additional label has to be added to the analyte for detection, thus increasing the process steps. The impedance based method doesn't require any label and hence it is also called as label-free detection method.

The Randles electrical equivalent circuit can be used for modeling the electrode-sample interfacial interaction for the affinity-based sensors. The interfacial impedance comprises of the double layer capacitance (C_{dl}) and the charge transfer resistance (R_{ct}). R_{bulk} is the solution resistance. The affinity-based impedance biosensors use the changes in the interfacial impedance for determining the concentration of the analyte. The change in the impedance happens due to the attachment of the analyte to the probe molecules. With the attachment of the analyte onto the probe molecule, the double layer capacitance decreases and the charge transfer resistance increases thus changing the measured impedance.

There are two reasons why the double layer capacitance decreases with the attachment of the analyte molecule to the probe [70–72]. Firstly, with the attachment of the

analyte molecule the thickness of the double layer is increased resulting in the decrease of C_{dl}. Secondly, there is a shift in the dielectric constant at the interface (ε_r for organic molecules is around 2-3, whereas for water it is 80). Because of the reduction in the dielectric constant at the interface the double layer capacitance (C_{dl}) decreases. Attachment of the analytes to the probe molecules leads to an increase in R_{ct}. This is because once molecules get attached to the electrode surface they will block the flow of current through the interface.

In addition, attachment of analyte to the probe molecules could result in ionization of the immobilized molecules on the electrode surface. Because of ionization there is a change in charge density profile at the electrode-solution interface, thereby changing the interfacial impedance (R_{ct} and C_{dl}).

Based on this principle, several impedance sensors have been designed. Reference [38,73], shows an example of an antigen-antibody based impedance sensor. Moreover, bacterial spores, biological cells, proteins have been successfully detected by utilizing the affinity-based detection principle. Designing probe molecules that are selective to the analyte is complex, because of which this method has less selectivity. This is a major disadvantage for the affinity-based biosensing.

3.2.2 Metabolism based impedance biosensing

The microbial metabolism based biosensing is a classical impedance microbiological technique that is applied to detect and quantify the analyte or microorganisms. This method is based on the measurement of changes in the electrical impedance of the culture medium where microorganisms (bacteria, cells) are being cultured (grown) [74]. A major advantage of growth based impedance sensing is its ability to differentiate between the viable and non-viable microorganisms. As only viable organisms decompose the culture medium and start to grow, the impedance changes measured is associated only to these viable organisms. Most of the impedance sensors that have been designed so far using this principle are applied for monitoring the bacterial growth [75–77].

For impedance based biosensing, two or more electrodes are located beneath the culture medium. Once the culture medium is inoculated with the microorganisms, the electrical property of the medium is measured at regular time intervals. As these microorganisms grow, they release ionic metabolites into the culture medium resulting in the impedance change. Most of the microorganisms utilize oxygen and glucose provided with the culture medium for their growth and produce either acidic or basic by products resulting in either decrease or increase of the culture medium impedance.

For example, when bacterial cells start to grow they convert glucose to lactic acid, this increases the ionic conductivity of the medium, thus decreasing the measured impedance. A microchip has been designed with integrated electrodes to analyze the growth of bacteria using the metabolism based impedance detection principle. According to [78], the impedance change measured during the growth of different concentrations of *L.innocuea* bacteria depends on the initial concentration of bacteria. The rate of impedance change not only depends on the initial concentration but also on the type of the microorganism growing in the medium. So by selecting a specific culture medium, it is possible to quantify and identify mold species.

3.3 Mold metabolism and pH change

In this section, a detailed explanation regarding the molds metabolism is presented. As the mold grows there is a change in the ionic concentration of the culture medium. This is caused by the metabolic products, which are extracellularly released into the culture medium during decomposition of the organic matter (present in the culture medium). Depending on the type of mold species and the medium on which the mold is growing, these byproducts could be acidic or basic. This will either decrease or increase the pH (hydrogen ion concentration) of the culture medium.

Mold growth results in the production of several acids like lactic acid, gluconic acid, oxalic acid, citric acid, amino acids etc [7]. Because of the molds ability to produce different kinds of acids, several molds are being used in industries for production of organic acids in industrial scale. As it is easier to separate mold organisms (by low cost filtration methods) from the culture medium, they are widely used for acid production compared to bacteria (requires centrifugation and other costly filtration techniques for separation).

Mold metabolism happens in the presence of oxygen, hence it is aerobic. Molds break down the carbohydrates present in the culture medium aerobically, which are utilized for their growth. During this process they secrete intermediate products. The amount of intermediate products excreted by molds depends on the culture medium [7].

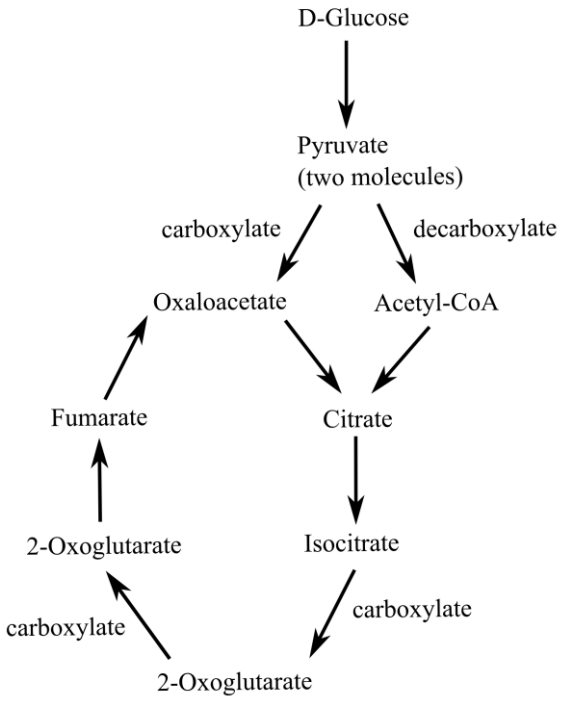

Figure 8: Production of organic acids during the growth of mold [7]

Production of organic acids as intermediate products results in the decrease of the culture medium pH. The acids that are responsible for lowering the pH of the culture medium are citric acid, lactic acid, gluconic acid, oxalic acid etc [79]. With the decrease in pH, the ionic concentration in the medium increases thus the impedance of the culture medium decreases.

Fig. 8 shows the synthesis mechanism of these acids. For example, production of the citric acid from glucose is done within the molds intracellular components (cytosol and mitochondrion) and is later exported out of the cell [7]. Glucose is consumed by the cytosol (a cellular component in the mold) and is digested into two molecules of pyruvate (a three carbon acid). One pyruvate molecule is decarboxylated within mitochondria (another cellular component in the mold) into acetyl-CoA. The other pyruvate molecule is carboxylated within cytosol to oxaloacetate. Oxaloacetate is then transported into the mitochondria, where it reacts with acetyl-CoA forming citric acid. This citric acid is then transported out of the mitochondria and the cellular membrane into the culture medium as a metabolic byproduct resulting in acidification of the culture medium. Unlike citric acid, Gluconic acid is formed outside the cell wall of the mold. Glucose is oxidized to gluconic acid via glucose oxidase enzyme. Gluconic acid also reduces the pH of culture medium.

Fig. 9 shows the production of amino acids during the mold growth. Glutamate is one of the major amino acids, which is produced within the intracellular components and

is later transported out of the cell. Increase in the pH of the culture medium is due to the formation of amino acids [79]. Synthesis of amino acids starts with the degradation of glucose to glutamate via citrate and oxoglucotarate. Citrate which is formed inside the mitochondria is decarboxylated forming 2-Oxoglutarate. 2-Oxoglutarate in the presence of ammonium forms glutamate which is then secreted out of the cellular membrane. Other amino acids which could be released during molds metabolism include tryptophan, tyrosine, isoleucine.

Mold species investigated in this work (Eurotium, Aspegillus, Cladosporium) produce acidic by products during germination phase (initial phase where spores start to germinate). This decreases the pH of the culture medium. During growth phase (spores start to grow into mold by forming hyphae) there is production of amino acids, resulting in the increases of culture medium pH. After growth phase, the mold growth reaches saturation, thus the pH of the medium remains constant.

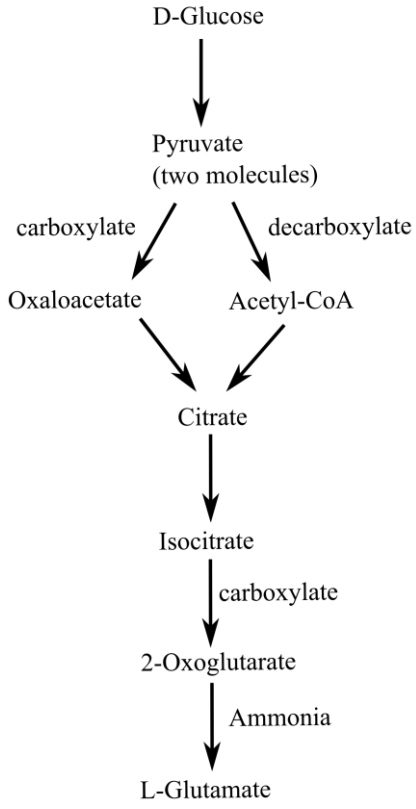

Figure 9: Production of amino acids during the growth of mold [7]

4 Bioreactor Based Mold Sensor System

4.1 Autonomous sensor system

The described mold sensor system in this thesis is targeted to monitor archive or library environments at regular time intervals. Mold infestation to the library material e.g. documents, books, files (as shown in Fig. 10) is one of the major concerns in archives [80]. Mold spores enter the archives through ventilators, or via humans or due to animal interventions and start to decompose the organic material present within the archives. Once infested with mold, it either involves expenses to restore the damaged material or in some cases the material is completely lost or irreplaceable.

Figure 10: a) Contaminated archive inside Bochum library, Germany b) mold growing on files.

Files, books or other stored materials inside archives are often not edited or opened for long durations, so archives are not accessed or opened on a regular basis. During this period (when archives are not opened) if there is a contamination within the archive then there is a danger that it could be unnoticed for a long duration. The risk of mold infestation is much higher for archives that do not have a climate controlled environment and for the archives that are located in the basements. The possibility of humidity accumulation in such locations is higher when compared to the climate con-

trolled archives (higher humidity makes the mold to grow fast). If the contamination is not detected at its initial state then the infestation could spread throughout the archive thus creating losses, both in terms of materials and money. Moreover, exposure to the airborne mold spores can lead to severe respiratory illnesses in humans and animals. To avoid this potential danger it is needed to monitor the spore concentrations inside archives at regular time intervals. To do so an autonomous sensor system would be highly attractive. The autonomous sensor system should be able to perform steps from sampling to detection of the mold spores without any manual interventions. Once the mold growth is detected, the autonomous sensor system should warn the end user. This allows the possibility of real-time intervention to prevent further damage.

4.1.1 Design of sensor system

The sensor system has been designed based on the initial investigations of mold spore detection, which were carried out by BMA Labor GmbH at Bochum archives. Major considerations of the sensor system include:

1) The sensor should be able to measure the mold growth from the archive air sample. Investigations revealed that in a contaminated archive the spore concentration could vary from 1000 – 3700 CFU/m^3. So the designed sensor should be able to detect this concentration. The designed sensor uses impedance microbiology technique to detect and quantify the mold spores.
2) Multiple measurements (twice or thrice per week) could be helpful and in some cases is necessary for better evaluation of spore concentrations within the archive. So the designed sensor system should consists of an array of sensors that can be activated at desired time interval. For the first realization sixteen sensors arranged in 4 X 4 array was chosen.
3) Mold species responsible for archive contamination produces airborne spores; so air-sampling technique has been employed for collecting spores onto the sensors. An air-sampling unit has been designed that diverts spores present in the indoor air onto each of the sixteen sensors.
4) The sensor system should be able to perform sampling and detection without any manual intervention. A control unit ensures step-by-step functionality such that the system is automatized.

   The schematic view of the autonomous sensor system is presented in Fig. 11.

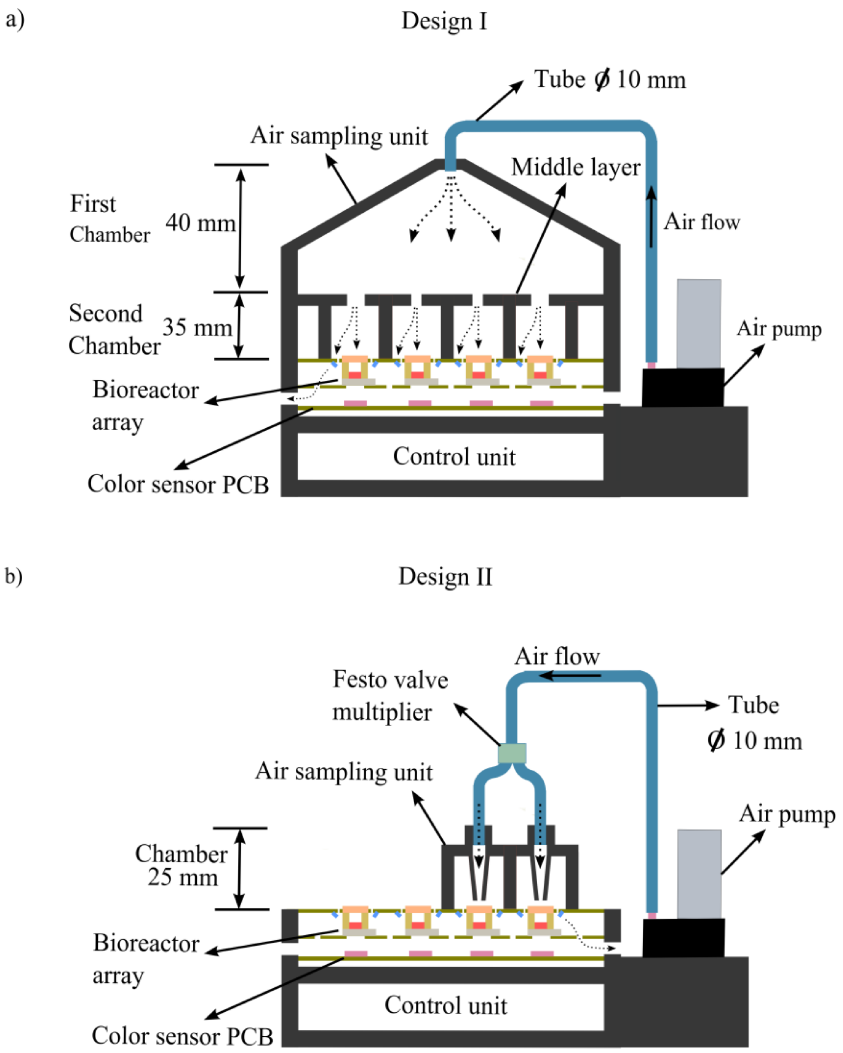

Figure 11: Design of the autonomous mold sensor systems with a) air sampling unit design–I b) focused air sampling unit.

The designed sensor system for monitoring archive mold spore contamination comprises of an air sampling unit, an air pump, a replaceable bioreactor cartridge, and a control unit [81]. An air pump is used to pump the indoor air of desired volume into the air sampling unit. The air sampling unit divides the sampled air over the bioreactor cartridge. The bioreactor cartridge consists of 16 membrane-sealed bioreactors which are preloaded with the culture medium. Once the spores present in the air sample get in contact with the culture medium, they start to germinate by digesting the nutrients present in the culture medium. During this digestion process they release secondary metabolites into the culture medium. These metabolites will change the ionic concentration of the culture medium, thus changing the pH of the medium. Because of the pH change the impedance of the culture medium changes. Sensor elements are integrated within the bioreactor (beneath the culture medium) to measure

the impedance change in the medium. For internal calibration (to determine the absolute pH value of the culture medium), a colorimetric reference measurement is integrated within the sensor.

As the proposed sensor system is targeted at monitoring archive environments at regular time intervals, for example twice or thrice a week, an array of bioreactors are used. These bioreactors are arranged in 4x4 array, which is termed as a bioreactor cartridge. The bioreactor cartridge is replaceable, i.e. if all the 16 bioreactors have been used the cartridge is exchanged with a new one. Each bioreactor is preloaded with the culture medium and is sealed with a thin silicon nitride sacrificial membrane. Sealing the bioreactor with the sacrificial membrane will not only protect the culture medium from contamination but it also allows activating the bioreactor at a desired time. The silicon nitride membrane has heater elements integrated on it. Whenever a measurement is desired, the membrane is activated by applying a short current pulse. Because of the applied current, a temperature gradient is formed within the membrane, resulting in the development of thermal stress. Once the thermal stress reach the fracture strength of silicon nitride membrane, the bursting of membrane occurs.

The bioreactor cartridge is housed within the air sampling unit. The air sampling unit ensures uniform spore particle distribution among all the bioreactors in the cartridge. In addition, the sensor system consists of readout electronics for quantification of mold spores. The communication electronics in the control unit ensures that the sensor system sends an email warning alert to the user as soon as the mold growth is detected.

4.1.2 Concept of autonomous operation

The process steps involved for autonomous detection of mold spore contamination is illustrated in Fig. 12. The control unit ensures that the sensor system performs all the individual steps in a systematic manner. In the first step, one of the bioreactors (out of 16) is activated. The activation is initiated by applying a current pulse for a short duration such that the silicon nitride membrane bursts. Once the membrane opens, desired volume of indoor air (varying from 30-500 liters) is pumped into the air sampling unit. The sampling volume to be pumped through the sensor system can be scaled up or down depending on the application. After pumping the desired volume of air, the air pump is turned off. The spore particles, which are present in the air sample, get in contact with the culture medium of the activated bioreactor. The other bioreactors remain protected with the silicon nitride membrane and thus stay inactive. The settled spores start to grow and cause impedance changes in the culture medium. The impedance and the color of the culture medium are monitored hourly and the values are stored in the data logging unit.

Based on the concentration of the mold spores the rate of impedance change varies. With the designed sensor, it is possible to determine the initial concentration of the mold spores within 24 hours. If mold growth is detected, the control unit stops the detection process. The detection process is stopped in order to prevent the danger of further contamination from the sensor system. If no mold growth is detected, the control unit activates another bioreactor after a certain pre-defined time interval. This process is repeated until all of the 16 bioreactors in the cartridge have been used. Once the bioreactor cartridge is used it is replaced with a new one.

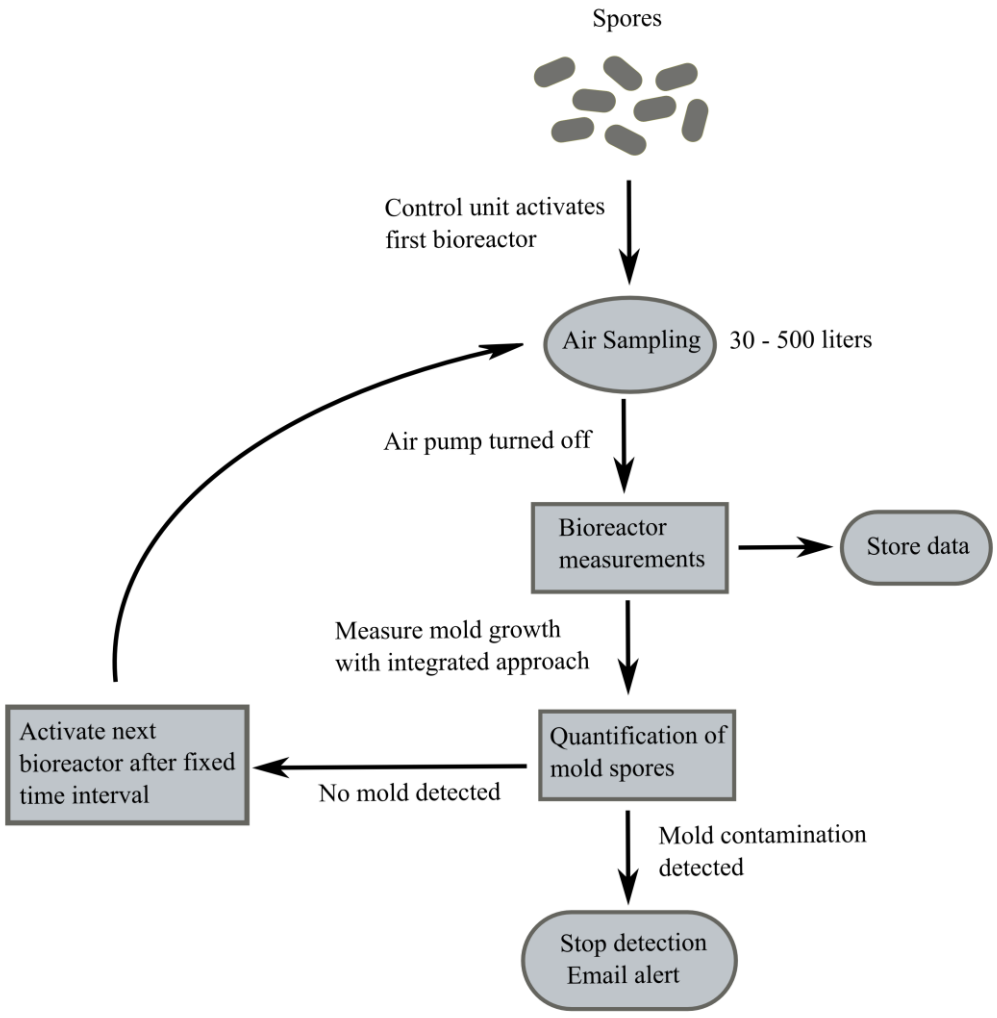

Figure 12: Process steps implemented for autonomous detection of mold spores.

4.2 Bioreactor

As discussed in Chapter 2.3, mold detection methods like PCR, molecular methods, ATP-bioluminescence, MVOC's, FTIR, etc., are not suitable for designing an out-of-lab sensor system. These methods require several sample preparation steps making them complex to be integrated into an autonomous sensor system. Moreover, reagents employed in these methods are not stable for longer durations thus making a reliable long-term monitoring sensor system with these methods are complicated.

Hence in this thesis, the standard culturing method is automated for making an autonomous sensor system suitable for out-of-lab mold detection. The detection principle is a based on impedance microbiology, which is based on the measurement of electrical properties of the culture medium as the mold spores germinate. One of the major advantages of designing a sensor by using a culture medium technique is that it specifically detects viable mold spores. As in the archive environments, only viable mold spores are responsible for contamination, the used method allows in realizing an effective autonomous sensor system. The bioreactor used for the detection of mold spores consists of three components, an impedance sensor, a reaction cavity and a protective membrane. The schematic view of the bioreactor is as shown in Fig. 13. The bioreactor is assembled in three stages. Firstly, the impedance sensor is fabricated using traditional silicon technology. Secondly, the reaction cavity made of borosilicate glass is glued onto the sensor. The reaction cavity is loaded with the culture medium and as a final step it is sealed with the membrane.

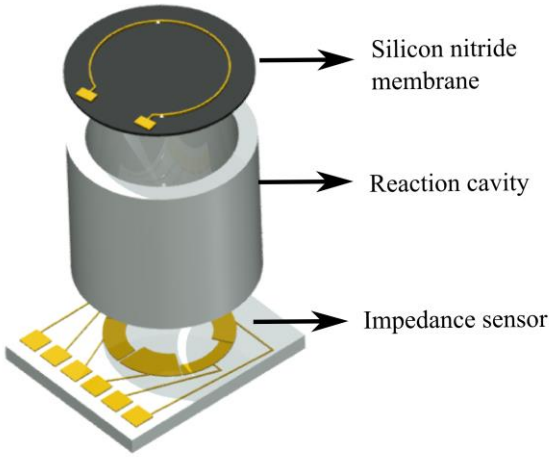

Figure 13: Schematic view of the bioreactor comprising Impedance sensor, reaction cavity and a silicon nitride membrane.

4.2.1 Impedance sensor design

Detection of the mold spores is done with an integrated approach of impedance and colorimetric principles [82]. The designed sensor comprises of electrodes to monitor impedance changes and a color sensor for measuring the color transition of the culture medium (color change happens at known pH values as the mold grows). For measuring the impedance changes within the culture medium a minimum of two electrodes are required. A symmetrical two-electrode configuration has been implemented on the chip for measuring the impedance changes. The schematic view of the electrode design is shown in Fig. 14.

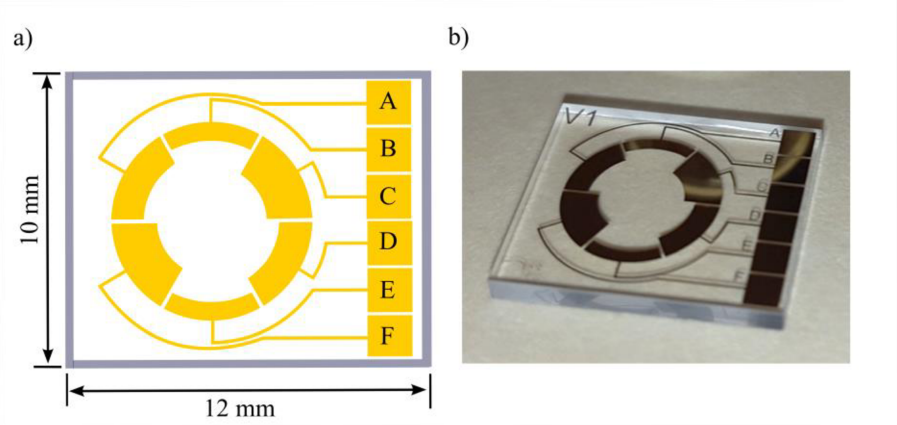

Figure 14: Impedance sensor with three different electrode configurations (AD, BE and CF) for measuring impedance changes in the culture medium a) schematic view b) picture of the sensor.

As the area of the electrode has a direct influence on the sensitivity of the sensor, three different electrode configurations (BE, AD and CF) with different electrode areas were designed (see Fig. 14). Three different configurations have been tested to get more experimental feedback on the used electrical equivalent circuit model. Moreover by using three different designs the frequency-dependent behavior of the sensor has been explained.

The electrode areas for three different configurations BE, AD and CF are 2.5 mm^2, 3.5 mm^2 and 4.5 mm^2, respectively. For the optical path, which is used for measuring the color of the culture medium, a minimum of 3.5 mm distance is included between the electrodes. So the electrodes were designed to have a distance of 3.5, 4.5 and 5.5 mm between the edges for CF, AD and BE configurations, respectively. By implementing all the electrode configurations on the same sensor chip, it is possible to compare their performances at the same time and for the same medium. The outer dimension of the chip is 10 mm x 12 mm. A borosilicate glass that has an inner diameter of 7 mm is glued (UHU plus schnellfest, 2-k-epoxi, biocompatible) onto the sensor. This glass

cavity acts as a reaction chamber and has a capacity to store 400 µl of the culture medium.

4.2.2 Fabrication of impedance sensor

The designed impedance sensor is fabricated using standard clean room fabrication technology. The sensor is manufactured on a glass wafer to provide optical transparency for color measurements. Gold is used for the electrodes and for the contact pads. The fabrication process of the sensor is schematically shown in Fig. 15. Starting with the inspection of the glass wafer for any optical defects, a thin layer of titanium with a thickness of 100 nm is deposited using a physical vapor deposition (PVD) process. On this titanium layer 500 nm of gold is deposited using sputtering technique. As gold is noble metal, its adhesion to substrate materials is very poor. The titanium layer deposited beneath the gold acts as an adhesion promoter. This layer ensures a stable adhesion of the gold to the glass substrate.

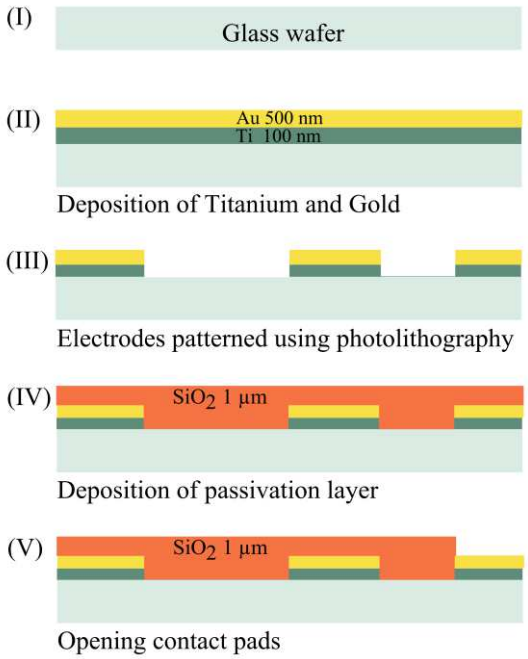

Figure 15: Schematic view of sensor fabrication process

After depositing gold, electrodes were patterned using photolithography and wet chemical etching. Once the electrodes are patterned, 1 µm of silicon dioxide layer is deposited using plasma enhanced chemical vapor deposition (PECVD) technique. The silicon dioxide layer acts as a passivation layer, thus isolating the electrodes. This passivation layer is important as it prevents a short circuit between the electrodes if a conductive medium is used. As a final step, the contact pads were opened by etching silicon dioxide. As shown in Fig. 14, all the contact pads are located at one end of the

sensor making it easier for wire bonding. The impedance sensors have been fabricated by microFAB Service GmbH.

4.2.3 Equivalent circuit and principle

To understand the frequency-dependent behavior of the sensor and also to explain and predict the sensor behavior, it is a standard practice to analyze the impedance data obtained from the measurements by fitting it to an electrical equivalent circuit model. There exists several equivalent circuit models to represent the physical processes happening during the impedance change. Full Randles equivalent circuit is one of the models to represent the impedance sensor. This model includes the physical processes of charge-transfer and diffusion of charged ions, which occur in the culture medium during the growth of mold [66].

The full Randles equivalent circuit for one of the electrode configurations of the designed impedance sensor is shown in Fig. 16. R_{sol} and C_{sol} represent the resistance and capacitance of the culture medium, respectively. R_{ct} is the charge-transfer resistance at the electrode-culture medium interface. C_{dl} is the double layer capacitance formed due to the separation of charges at the electrode-culture medium interface. Z_w is the impedance offered by the culture medium to the diffusion of ions, and is called as Warburg or mass transport impedance. C_s is the parasitic capacitance that exists between the substrate and the electrodes. C_s is present only if the substrate material is conductive (e.g., silicon). If the substrate material is made of glass, which is an insulator, the substrate capacitance is neglected. C_c represents another parasitic capacitance between two adjacent electrodes. R_s is the resistance offered by the substrate. Other parasitic capacitances from external wires, packages are not shown in the Fig. 16.

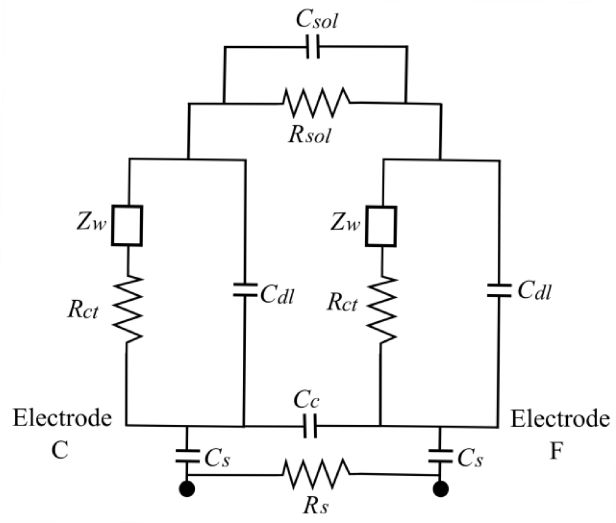

Figure 16: Electrical equivalent circuit for the designed impedance sensor [82].

As explained in chapter 3.1.2, for impedance analysis two different processes are to be considered, charge-transfer and the diffusion of charged ions. In frequency range from 1 kHz to 1MHz, the charge-transfer process is dominant, hence in this frequency range the main contribution to the total impedance value is from charge-transfer resistance and double layer capacitance. At lower frequencies (<1 kHz), Warburg impedance contributes a major part to the overall impedance of the system. This is because diffusion processes dominates at low frequencies.

The principle of mold detection can be explained using the electrical equivalent circuit model. As the mold grows the ionic concentration of the culture medium will change (due to the pH change). Because of this the measured interfacial impedance will vary. For example, if the pH of the culture medium is lowered, then the amount of polar molecules inside the culture medium increases. This will decrease the charge-transfer resistance and increase the double layer capacitance. Thus the overall interfacial impedance of the culture medium decreases. Similarly, if there is an increase in the pH, the interfacial impedance of the culture medium increases. Hence by observing the interfacial parameters it is possible to detect changes happening in the culture medium.

4.3 Bioreactor with integrated optical reference

Currently there are no sensors for detection of the mold growth using impedance measurements but there exist several sensors in literature applying culture medium based impedance sensing for detection of bacterial growth [75–77]. All the published work applying impedance measurements has a major drawback of lacking a reference measurement within the sensor system. Although by utilizing the electrodes, pH changes can be monitored (by measuring the impedance), it is not possible to determine the absolute pH value. For determining the absolute pH value, a calibration step is necessary before the impedance measurements. Moreover, for different culture mediums used within the system this calibration step has to be repeated before the start of every measurement.

To avoid this additional calibration step, a novel method has been investigated by integrating a colorimetric reference within the sensor. This colorimetric method allows the determination of the absolute pH values of the culture medium. In addition, the sensitivity of the sensor, which is the impedance change per unit pH, can be determined without the necessity of calibration step [83,84]. By using this approach different mold species, which are common in archives environment like, *Eurotium amstelodami, Aspergillus penicilloides, Aspergillus restrictus* and Cladosporium cladosporiodes have been detected.

4.3.1 Colorimetric principle

To integrate a reference measurement within the sensor, a standard pH indicator dye has been added to the culture medium. A pH indicator is a chemical reagent used for detection of hydronium or hydrogen ions [85]. With the growth of mold the pH of the culture medium changes and because of the integrated pH indicator, the color of the culture medium changes at specific pH values.

The pH indicators are in general either weak acids or weak bases with an acid dissociation constant ($\underline{k}_a$). Acid dissociation constant is also called as acidity constant and is a quantitative measure of the acids strength in a solution [86,87]. In aqueous solution, the pH indicators reaction (Bronsted acid-base reaction) can be expressed as

$$H_{Inidcator} + H_2O \underset{aqueous\ solution}{\Longleftrightarrow} Indicator^- + H_3O^+ \qquad \text{Eq. 12}$$

Where, $H_{Indicator}$ is the cation or acid form of the pH indicator and $Indicator^-$ is the conjugate base or anion of the pH indicator. From Eq. 12 it is clear that the indicator dye dissociates into a conjugate base (anion) of the acid. In addition hydrogen ion reacts with the water molecule forming a hydronium ion. The dissociation constant of the pH indicator dye is given by the following equation [88,89].

$$K_a = \frac{[Indicator^-][H_3O^+]}{[\ H_{Inidcator}][H_2O]} \qquad \text{Eq. 13}$$

Where, $[Indicator^-]$, $[H_3O^+]$, $[H_{Indicator}]$ and $[H_2O]$ are expressed in terms of concentrations (mol/L). $\underline{k}_a$ is mostly expressed in logarithmic values as pK_a [88].

$$pK_a = -\log_{10}\left(\frac{[Indicator^-][H_3O^+]}{[\ H_{Inidcator}][H_2O]}\right) \qquad \text{Eq. 14}$$

The more positive the value of pK_a, the weaker is the acid (for example, for water the value of pK_a is 14 whereas for HCL it is -7). Weaker acids have smaller extent of dissociation when compared to the strong acids. Thus strong acids dissociate completely in aqueous solutions [90].

The pH of the solution is expressed (by Henderson-Hasselbalch equation) in terms of acid dissociation constant, the concentrations of indicator acid and its conjugate indicator base as [88]

$$pH = \ pK_a + \log_{10}\left(\frac{[Indicator^-]}{[\ H_{Inidcator}]}\right) \qquad \text{Eq. 15}$$

Eq. 15 states that, when pH of the solution is equal to the pK_a of the indicator, then the concentrations of the indicator acid and its conjugate base are same. If the pH of the

solution is above pK_a of the indicator then (from Eq. 15) the concentration of the conjugate base is greater than the concentration of the acid. Thus the color of conjugate base is dominated in the solution. Similarly, if the pH of the solution is below pK_a of the indicator dye, then the concentration of the acid is higher than the conjugate base. Hence the color of cation dominates the solution [91].

By adding a pH indicator dye to the culture medium, the color of the medium changes as the mold grows. This principle is shown in Fig. 17, where Fig. 17a and 17b shows the growth of *Aspergillus* species on PDA culture medium with no pH indicator dye in it. As there is no indicator dye the color of the culture medium remains unchanged after the growth of mold (Fig. 18a is taken after 24 hours of mold growth, Fig. 17b is taken after 96 hours of mold growth).

Fig. 17c and 17d shows the growth of *Aspergillus* species on the culture medium which has methyl red indicator dye. Methyl red indicator has a pK_a of 5 [91]. When the pH of the culture medium is less than 5 then the cation of methyl red dominates in the culture medium, resulting in a red color. As the pH of the medium increases above 5, the anion or conjugate base of methyl red dominates in the culture medium. This transforms the color to yellow. In Fig. 17c the culture medium is orange in color as it has a pH of 5.5 (when no mold is growing), as the mold grows the color of culture medium is turned to yellow after 96 hours (where pH is 8.0).

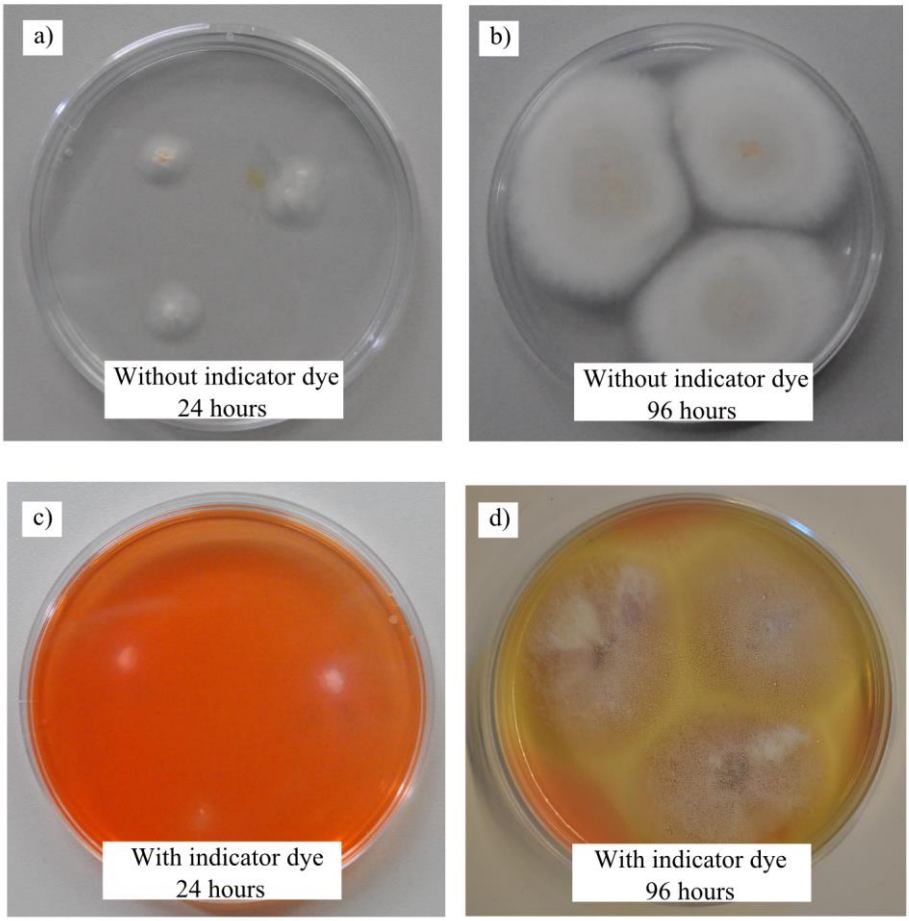

Figure 17: Growth of aspergillus species on PDA culture medium. Culture medium without indicator dye a) picture taken after 24 hours of mold growth b) picture taken after 96 hours of mold growth. Culture medium with methyl red indicator dye c) picture taken after 24 hours of mold growth d) picture taken after 96 hours of mold growth.

4.3.2 Detection method

For integrating the colorimetric reference measurement within the bioreactor, the culture medium is prepared with a pH indicator dye and is transferred onto the reaction cavity of the bioreactor [84]. Measuring the color of the culture medium is done by using a programmable color sensor (TCS3200). The color sensor is placed beneath the bioreactor and is controlled by the control unit of the sensor system. Schematic view and the setup for detection of color sensor are shown in Fig. 18. Once illuminated with the white light (using an LED), the color of the culture medium is measured in terms of RGB intensities. As we are discussing to perform experiments in the archives which have a temperature range from 18 to 25 °C, the influence of temperature on the color sensor is minimum and can be neglected. All the measurements are done at room temperature (25 °C).

To determine the offset values and the sensitivity of the sensor, the impedance sensor is calibrated by using the color transition region of the pH indicator. For methyl red indicator dye this region is between pH 4.5 and pH 6.5. To calibrate the impedance sensor, the measured absolute value of pH using the color sensor is assigned to the impedance reading of the sensor. The sensitivity of the sensor is determined by measuring a unit change of pH using the color sensor and this value is assigned to the corresponding impedance change measured by the impedance sensor.

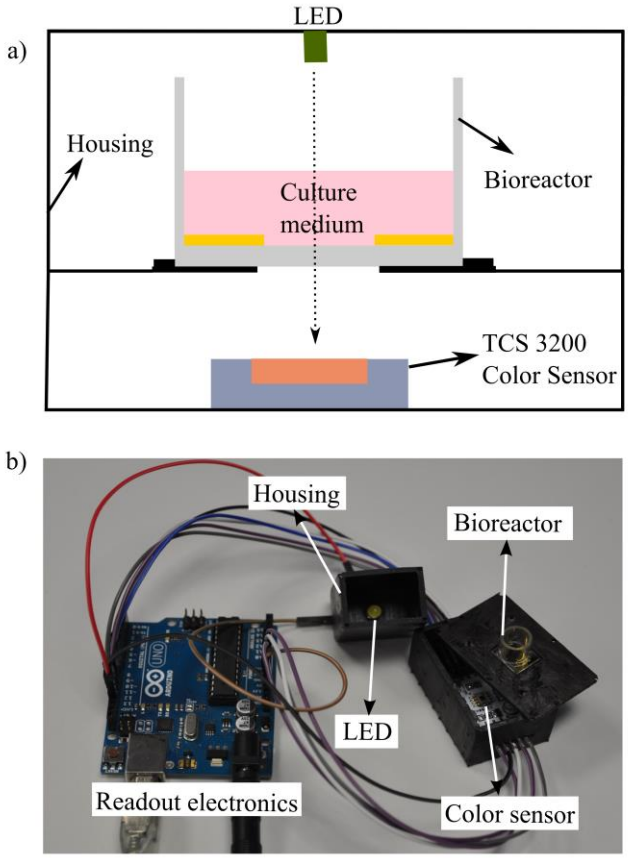

Figure 18: a) Schematic view for measuring color change of the culture medium during mold detection b) photo of experimental setup [82].

4.4 Electrically actuated silicon nitride membrane

4.4.1 Membrane design and principle

As the goal of the designed sensor system is to monitor archive mold spores at desired time intervals, it is necessary that the culture medium loaded within the bioreactor is protected from contamination. To prevent mold spores reaching the culture medium before the measurement is initiated the bioreactor is sealed with a thin sacrificial membrane [92]. This sacrificial membrane can be actuated electrically and

is made of silicon nitride. Sealing the bioreactors arranged in the cartridge (array of 16 bioreactors) with the silicon nitride membrane not only prevents the culture medium from contamination but it also provides the possibility to activate the desired bioreactor at a defined time.

The silicon nitride membranes have electrodes integrated on its surface. Whenever a measurement is required, a short current pulse is applied to the electrodes. Because of this current pulse, thermal stresses are developed within the membrane, which results in the bursting of the membrane. This concept of using electrically actuated membranes as one-shot valves (in the field of microfluidic systems) and for encapsulation of sensitive material has been studied by different research groups [93–97]. We used this principle but we have used other material to the electrodes to improve the bursting behavior. In our membranes titanium tungsten electrodes are used instead of traditional gold or platinum electrode which were used in other studies (this prevents the melting of electrodes before the membrane bursts) [94].

The schematic view of the silicon nitride membranes are shown in Fig. 19. The silicon nitride membrane is 500 nm thick and has a diameter of 7 mm. The activation electrodes are 22 µm wide and were made of titanium tungsten alloy (90 % tungsten and 10 % titanium). The titanium tungsten electrodes are 300 nm thick. Three different electrode designs have been fabricated on the silicon nitride. Design I has circular-electrodes, design II consists of cross-electrode design, and design III has parallel-electrode design with semicircular rounding. In the third design, an additional layer of electrode material is coated on the top of membrane (at the center) to make the membrane burst outwards. These three designs have been patterned on the membrane to investigate the bursting behavior. Contact pads for application of current pulse are located at the lower end of the membrane as shown in Fig. 19.

The principle of operation is based on the development of thermal stresses [98,99]. Upon electrical actuation, the electrodes get heated up resulting in dissipation of heat to the electrode surroundings (to the air on top of electrode and to the silicon nitride membrane beneath). This heat dissipation in the electrodes will introduce temperature gradient within the membrane. Because of this temperature gradient there is a development of thermal stress. If the value of thermal stress reaches the fracture stress of the silicon nitride membrane, then the membrane breaks. Once the membrane breaks apart, the sensor is activated i.e., the spores present in the environment can get in contact with the culture medium. Depending on the amount of spores growing in the bioreactor the impedance of the culture medium changes, which is used for quantification.

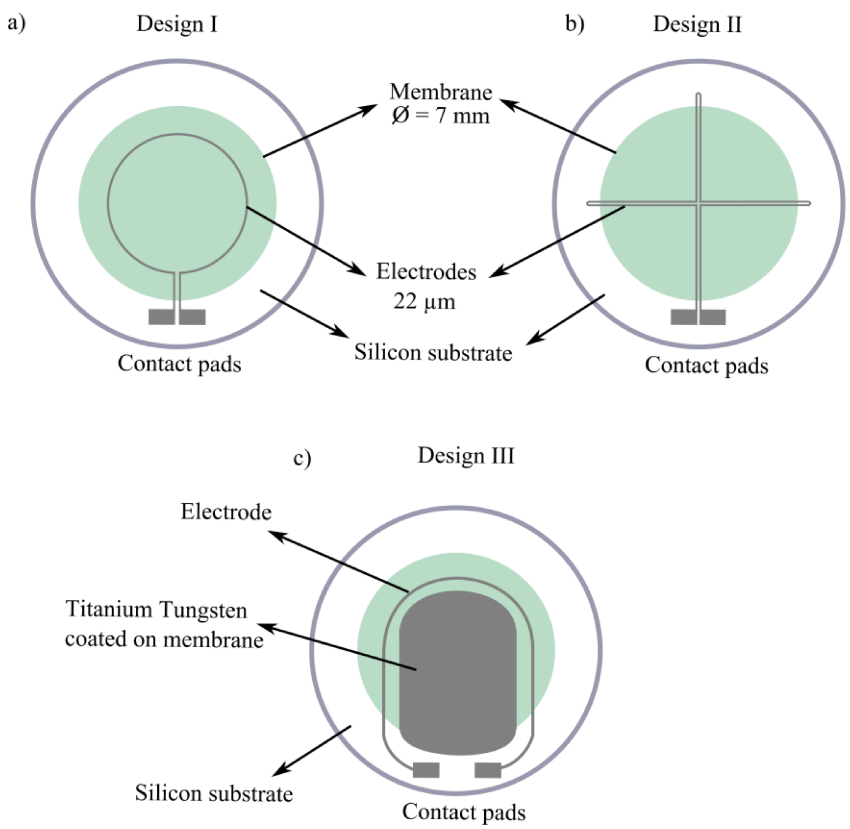

Figure 19: Silicon nitride membrane with different designs of titanium tungsten electrodes a) circular-electrode design b) cross-electrode design c) parallel-electrode with semicircular rounding.

4.4.2 Numerical modeling

Comsol Multiphysics has been used to model the electrically actuated silicon nitride membrane [94,100,101]. This model allows studying the membrane behavior when it bursts. Numerical modeling helps in predicting the time and current required for bursting the membrane. For simulations, joule heating physics in combination with solid mechanics has been employed [102].

Joule heating which is also called ohmic or resisitive heating, describes the process of production of heat due to the flow of electric current through a resistor or a conductor. In this process, the electrical energy flowing through a conductor is converted to heat energy. For actuating the membrane a short current or voltage pulse is applied to the electrodes, because of the applied current there is a production of heat. Joule heating physics has to be applied to the model to simulate the generated heat. Followed by Joule heating, the temperature distribution profile within the membrane is calculated. Each material has different temperature dependent properties, because of this, thermal stresses are developed within the material. Finally the mechanical

stresses developed due to the temperature gradient within the membrane are determined.

For designing the membrane model in Comsol, there are possibilities to use 1-D, 1-D Axis symmetric, 2-D, 2-D axis symmetric, 3-D modes. In this work, a 3D mode has been chosen to design the silicon nitride membrane. The geometrical model for the silicon nitride membrane designed within comsol with three different electrode designs are shown in Fig. 20.

As the reaction cavity of the bioreactor has an inner diameter of 7 mm, the membrane is designed to have same dimensions. One of the major requirements for the membrane is to make sure that the burst area (opening area after the membrane bursts) is as large as possible. This will increase the exposed surface area of the culture medium to the air sample. To achieve this, three different electrode patterns have been designed on the membranes. The circular electrode is designed to open up the membrane around the perimeter of the electrode at the center. The cross electrode has been designed to cut the membrane into four quadrants, with opening at the center. The parallel electrode design consists of additional layer of metal deposited on the membrane to make the membrane burst outwards. The width of the electrode has been chosen to be 22 μm. Investigations by microFAB Service GmbH showed this to be the optimal electrode width. Higher electrode width results in buckling at the edges of the electrode, as electrode material induces compressive stress on the membrane. Lower electrode width decreases the amount of current through the electrode thus increasing the bursting time.

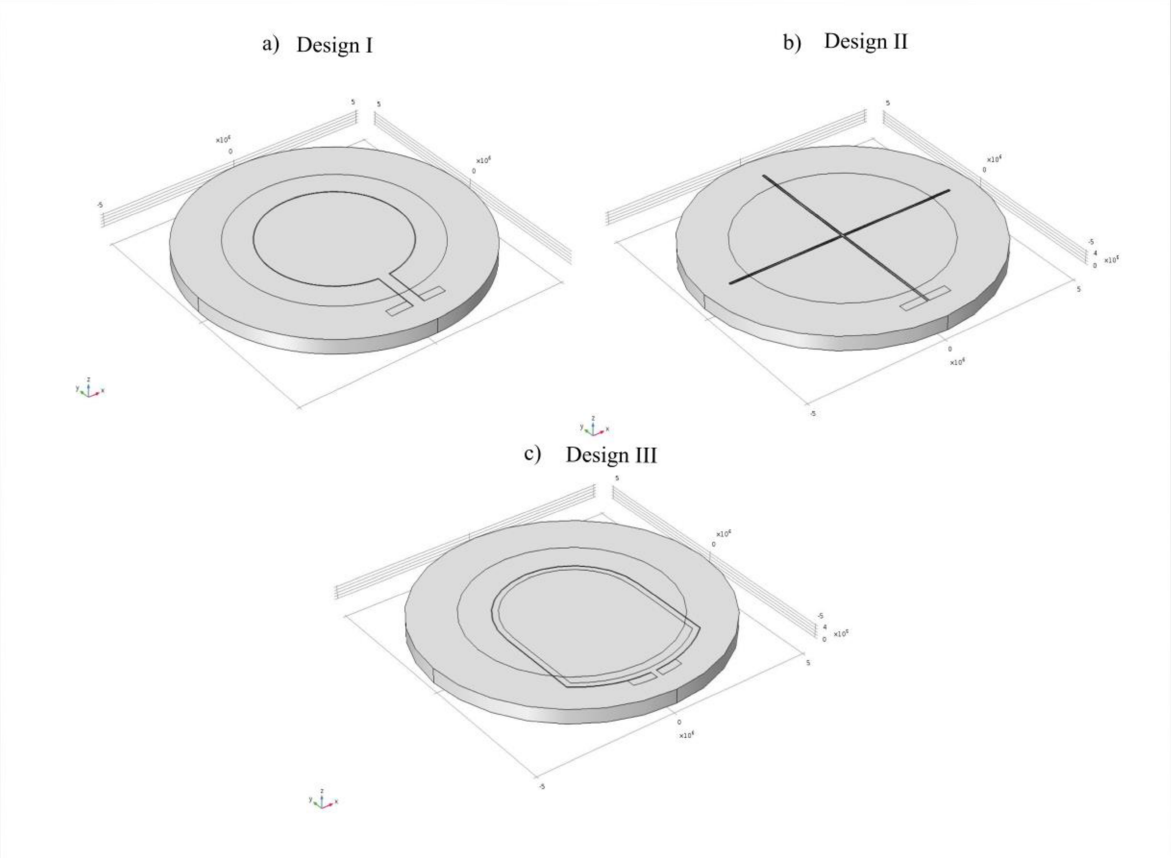

Figure 20: Designed membrane models in comsol multyphysiscs for studying the bursting behavior of the silicion nitride membranes a) circular b) cross-section c) semi-circular with electrode coating

After designing the model geometry, materials have been assigned to the model from comsol material database. Three different materials have been assigned to the model i.e., silicon for the substrate, silicon nitride for the membrane and titanium tungsten for the electrodes. After assigning the materials, Joule heating and solid mechanics physics are applied to the model. The source term is either an electrical potential or an electric current and is applied between the contact pads of the electrodes. The material offers resistance due the flow of electric current resulting in the generation of heat. This joule heating is expressed as [94,103,104]

$$\rho C \frac{\partial T}{\partial t} = \nabla.(\mathrm{k}\nabla\mathrm{T}) + \sigma(\nabla\mathrm{V})^2 \qquad \text{Eq. 16}$$

Where, ρ is the density of the material, σ is the electrical conductivity of the material, C is the thermal capacity of the material, k is the thermal conductivity of the material and T is the temperature.

Comsol solves the above equations by considering two major boundary conditions. The first one is the heat transfer to the air above the membrane via radiation which is determined by Eq. 17 [94,103].

$$\varphi = \sigma_B(\mathrm{T}^4 - \mathrm{T}_0^4) \quad \text{Eq. 17}$$

Where σ_B is the Boltzmann's constant, and T is the temperature after application of electric current, T_0 is the room temperature. The second boundary condition is the heat transfer via conduction and can be expressed as [94,103]

$$\phi = \frac{1}{2}\sqrt{\frac{k\rho C}{t}}(T - T_0) \quad \text{Eq. 18}$$

With the applied electrical potential, Comsol solves the above mentioned joule heating equations (Eq. 16, Eq. 17 and Eq. 18) to determine the temperatures at different locations on the top of membrane. As silicon nitride membrane is poor conductor, the heat diffusion within the membrane is small. This results in a temperature gradient within the membrane.

Because of this temperature gradient there is development of stress in the material. Solid mechanics physics in Comsol uses stress-strain relation equations to determine the value and position of stress on the membrane. If this stress reaches the fracture strength of the material then the membranes burst. The maximum stress is determined by using the Eq. 19 [94].

$$\sigma_{maximum} = \beta E/(1 + v) \quad \text{Eq. 19}$$

Where E is the Young modulus, v is the Poisson ration and β is a constant. From the literature it is shown that the fracture strength of silicon nitride material is in the range of 2 to 5 GPa [105–107]. By using the Comsol model, the stress values are determined for the applied electrical potential. If the determined stress is higher than the fracture strength, the membrane breaks. The stress-strain relations implemented in Comsol is expressed in the following equation.

$$\sigma = D.\varepsilon \quad \text{Eq. 20}$$

Where σ is the stress, ε is the strain and D is the elasticity of the material.

4.4.3 Fabrication of silicon nitride membranes

The silicon nitride membranes are fabricated on a silicon wafer using standard photolithography process. The process steps involved in the fabrication of the membranes are schematically shown in Fig. 21a. Fabrication starts with the deposition of 500 nm thick silicon nitride on silicon wafer using low-pressure chemical vapor deposition (LPCVD) technique. Later, 300 nm thick titanium tungsten alloy is sputtered on the

deposited silicon nitride layer. After sputtering, the titanium tungsten layer is patterned to obtain 22 µm wide electrodes using photolithography technique. 500 nm thick silicon dioxide layer is thermally deposited on the back of the wafer. This layer serves as the etch mask for deep reactive ion etching. As a final step, deep reactive ion etching is done from the back of the wafer to etch the silicon wafer completely, thus leaving the silicon nitride membrane.

The fabricated silicon nitride membranes with three different electrode designs are shown in Fig. 21b, 21c and 21d. The membranes have been fabricated by microFAB Service GmbH. The deposited silicon nitride on the silicon (using LPCVD technique) has a residual tensile stress of 200 MPa. Because of the tensile stress the silicon nitride membrane are perfectly flat.

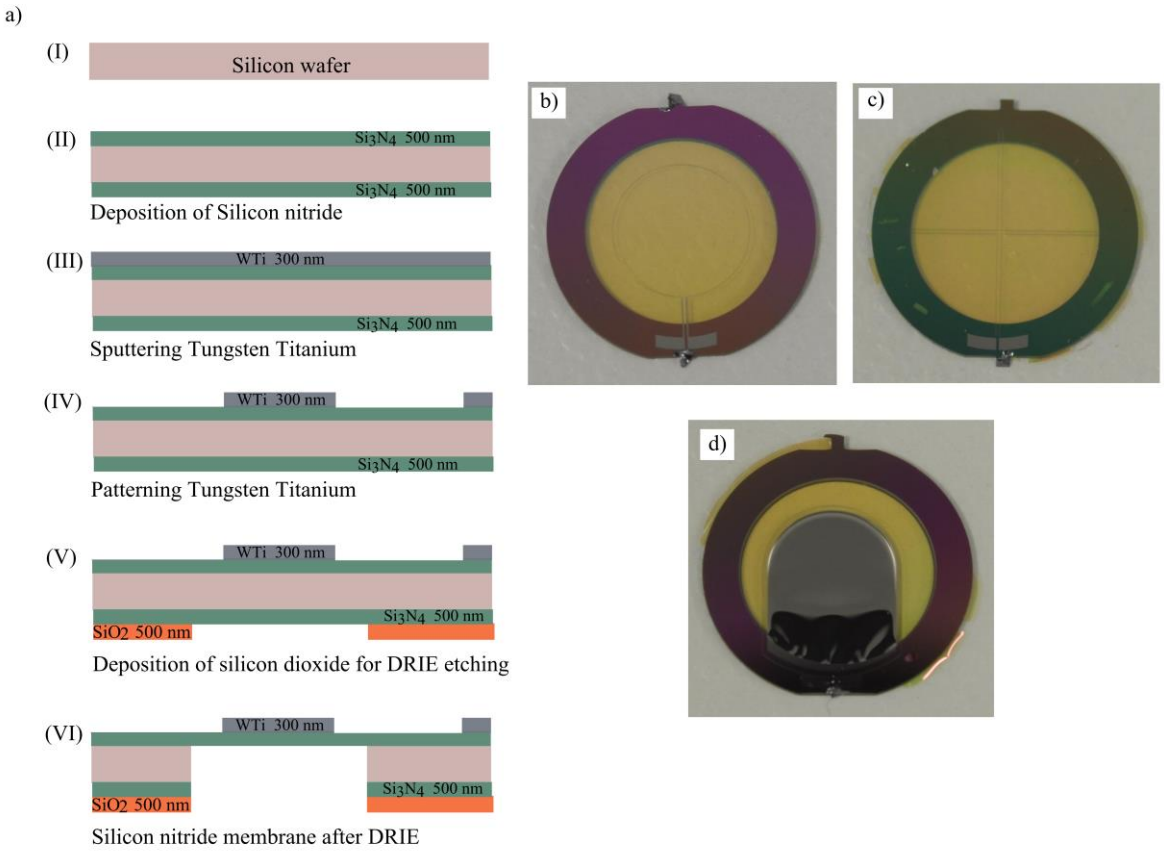

Figure 21: a) Process steps involved in the fabrication of silicon nitride membranes, b), c) and d) shows photograph of the membranes with three different electrode designs.

4.5 Bioreactor assembly

4.5.1 Membrane sealed bioreactor

The fabricated impedance sensor and the silicon nitride membrane are assembled together forming a membrane-sealed bioreactor. As a reaction cavity, a cylinder made of borosilicate glass is used. The borosilicate glass cylinder has a height of 10 mm with inner diameter of 7 mm. The outer diameter and the wall thickness of the cylinder are 10 mm and 1 mm, respectively. The cylinders with mentioned dimensions are manufactured by Hilgenberg-GmbH. The impedance sensor, reaction cavity and silicon nitride membrane are glued together forming a membrane-sealed bioreactor. The process steps involved during the assembly of a membrane-sealed bioreactor are shown in Fig. 22.

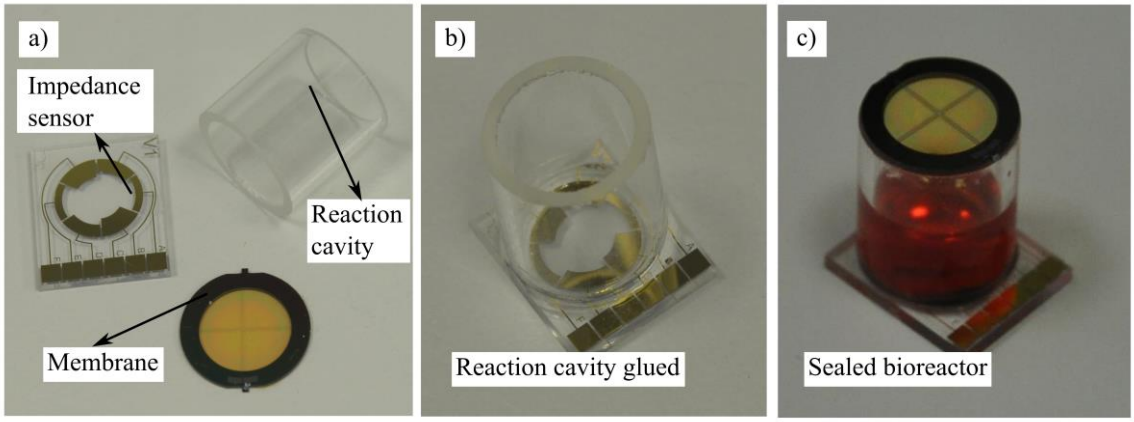

Figure 22: Process steps involved in assembling the membrane-sealed bioreactor a) individual components of bioreactor b) borosilicate glass cavity is glued onto the impedance sensor c) addition of sterile culture medium and sealing the bioreactor with the silicon nitride membrane.

Before assembling the bioreactor, all the components are treated with UV-C light to disinfect the surfaces. As a first step, the borosilicate cylinder (reaction cavity) is glued onto the impedance sensor using UHU plus schnellfest, 2-k-epoxi glue, which is biocompatible. Later, the culture medium prepared with pH indicator is added into the reaction cavity. Before loading into the reaction cavity, the culture medium is sterilized in an autoclave. As a final step, the silicon nitride membrane is glued onto the borosilicate glass using glue (UHU plus schnellfest, 2-k-epoxi). In order to prevent contamination of the culture medium, the complete assembly process of the bioreactor is done in a sterile flow box cabinet.

4.5.2 Bioreactor cartridge

Once the membrane sealed bioreactor has been successfully tested and characterized for the detection of mold spores, the concept of using an array of bioreactors has been considered. Multiple bioreactors can be employed for long-term monitoring of archive environment. This bioreactor array comprising of 16 bioreactors connected in a 4x4 format is referred as bioreactor cartridge. In addition to the 16 membrane-sealed bioreactors, the bioreactor cartridge consists of two PCB boards. First PCB board is called the sensor board and is used for contacting the impedance sensors. The second PCB board is called membrane board, which provides electrical contact to the membranes. The assembly of bioreactor cartridge is schematically shown in Fig. 23.

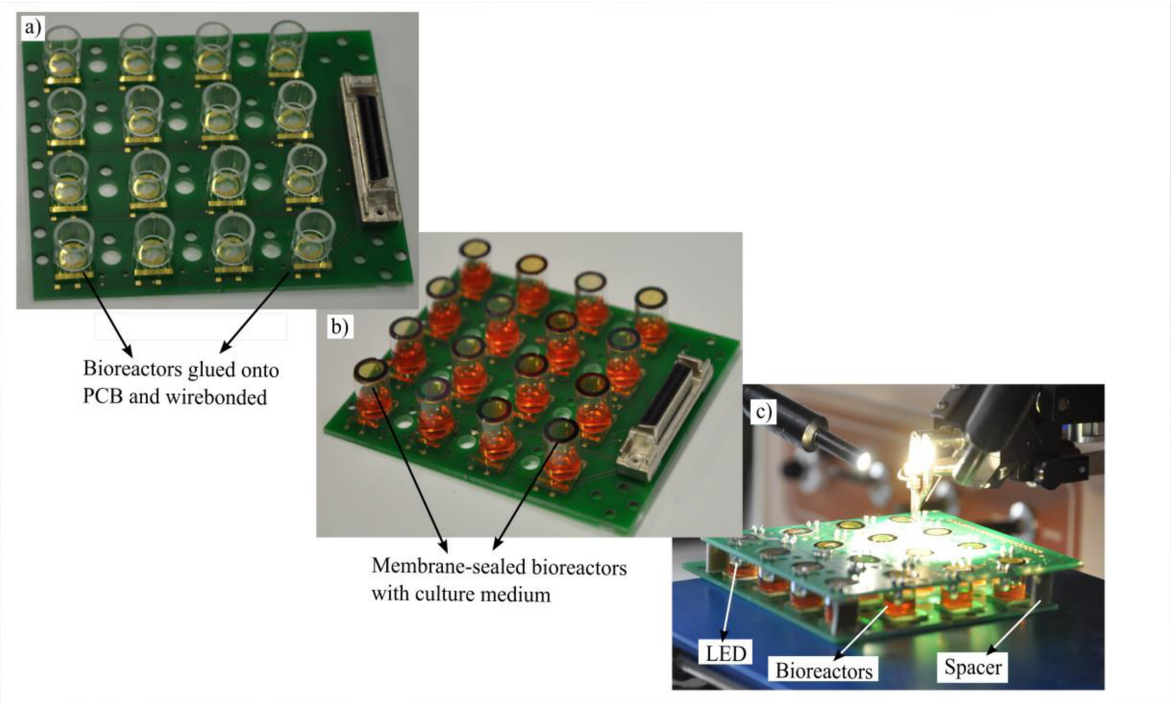

Figure 23: Process steps involved in assembling the bioreactor cartridge a) 16 impedance sensors are glued and wire bonded onto the sensor PCB board b) Culture medium is loaded and the reaction cavities are sealed with the membranes c) membranes wire bonded onto the membrane PCB

The assembly of the bioreactor cartridge starts with gluing sixteen impedance sensors onto the sensor PCB board. The contact pads of the impedance sensors were wire bonded to the contact pads existing on the sensor PCB board. This will allow contacting individual sensor using a connector pin, which is soldered on one side of the PCB board (see Fig. 23a). Later, reaction cavities are glued onto each of the impedance sensor and the sensor board is exposed to UV-C light for disinfecting the reaction cavities. Now, sterilized culture medium prepared using PDA and pH indicator dye is loaded into individual reaction cavities.

After loading the culture medium into sixteen bioreactors, the reaction cavities are sealed with the silicon nitride membranes. The last two assembly steps i.e., loading of culture medium and sealing the reaction cavities with the membranes are done in a sterile flow box to avoid contamination. As a final step in assembling the cartridge, the contact pads of the silicon nitride membrane are wire bonded onto the membrane PCB board. This will allow electrical actuation of the individual membranes.

4.6 Air sampling unit

The mold species that are responsible for archive contamination produces air borne spores. So air sampling technique has been employed for collecting the mold spores. An air sampling unit has been designed to divert the spores present in the air into the bioreactors. The following sections explain the design and simulation of the air sampling unit.

4.6.1 Design and manufacturing of air sampling unit

The air sampling unit encloses the bioreactor cartridge comprising of 16 bioreactors and distributes the incoming spores uniformly among all the bioreactors. Two different versions of air sampling units have been realized. In the first version the incoming air is not focused onto the reaction cavities, whereas in the second version (focused air sampling unit) the air sample is focused into the bioreactor. Two designs have been represented schematically in Fig. 24a and 24b. In the first version, the air sampling unit is divided into two chambers. The first chamber is 40 mm tall and has an inlet (diameter of 10 mm), which is connected to the air pump via a tube. The second chamber has a height of 35 mm and divides the sampling unit into 16 equal sized compartments (18 mm x 18 mm). Each compartment has its own inlet with a diameter of 6 mm and encloses one bioreactor as shown in Fig. 24a. The incoming air from the air pump is distributed equally into 16 compartments by the first chamber. The second chamber ensures that there is no cross contamination between the bioreactors.

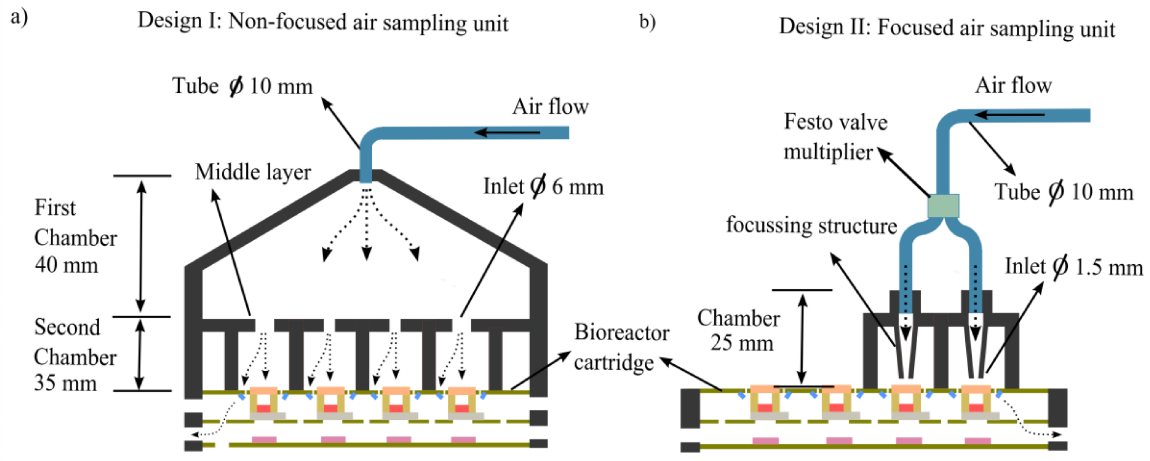

Figure 24: Schematic view of air sampling units a) Design I b) focused version

To improve the catching efficiency, a second version of air sampling unit is designed after observing the results from the first version. The second version air sampling unit is 40 mm x 40 mm in dimensions and consists of four inlets (each with a diameter of 6 mm). Each inlet focuses the incoming air into the reaction cavities of the bioreactor and has an outlet diameter of 1.5 mm. This version of air sampling unit requires an additional connector tube which multiplexes one inlet tube (from the air pump) to four outlets (inlets to the air sampling unit).

The air sampling units are manufactured using stereolithographic technology. Stereolightography or 3D print technology is a rapid prototyping method based on additive manufacturing principle [108]. In this method, the designed 3D geometry is converted into slices of 2D data and is loaded into the printing software. A 3D printer consists of a UV laser, a photo reactive resin and a platform which moves in vertical direction. As a first step, the platform is dipped into the resin. UV laser exposes the resin selectively forming the first 2D layer on the platform. The platform is later moved step by step upwards and for each step a new layer is built upon the existing layer. After printing the complete device, the part is cleaned to remove the unexposed resin and post processed under UV-light. Post processing allows the resin to be cured completely, thus forming a solid part. Fig. 25 shows two versions of the air sampling units manufacture using 3D print technology. Different colors are due to the used polymers (PA2200 polymer gives black color to the device)

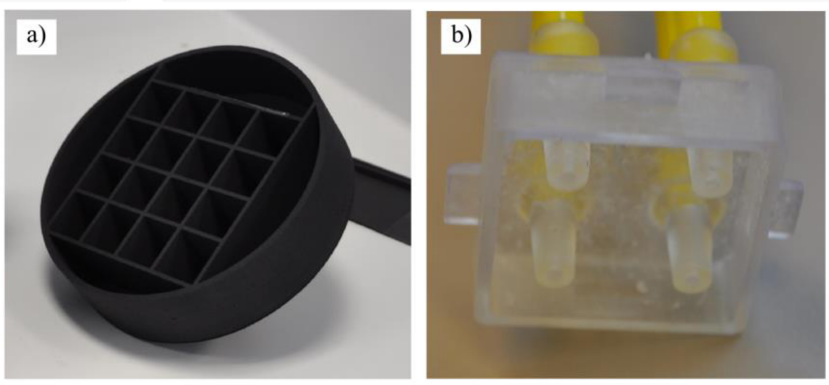

Figure 25: 3D printed air sampling unit a) non-focused version b) focused version.

4.6.2 Simulation

Comsol Multiphysics is used to model the air flow and spore particle distribution within the air sampling unit. For simulation, turbulent flow (k-ε) physics is implemented along with particle tracing module [102]. The air sampling unit is connected to a pump with an inflow velocity of 5 m/s. There exists a turbulent flow inside the inlet tube as the Reynolds number is larger than 2300. The flow model simulates the air flow distribution in each compartment of the air sampling unit. For studying the spore particle distribution, a particle tracing physics is applied to the model. Spore sizes have been varied from 2-30 µm and the quantity of spores at the inlet has been varied to determine the distribution at each outlet of the sampling unit. The geometry of air sampling unit (version I) designed in comsol is shown in Fig. 26. Different design parameters like height of the chambers, size of inlet and outlet diameters, have been varied to find the optimal air flow and spore particle distribution within the air sampling unit.

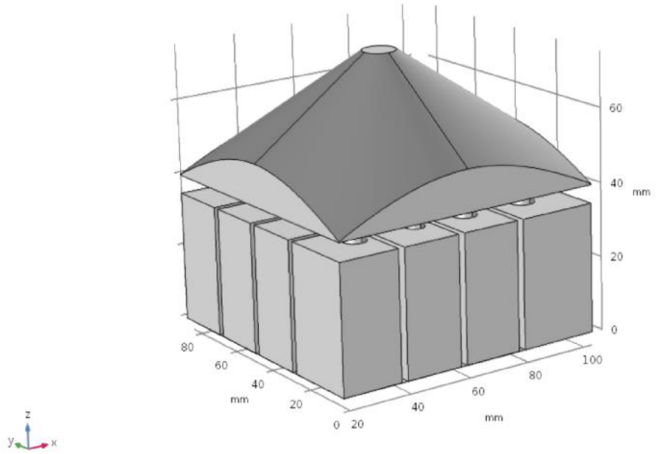

Figure 26: 3D model designed in Comsol Multiphysics simulation software.

4.7 Measurement system

4.7.1 Sensor readout electronics

Impedance sensor readout

For measuring impedance values from the bioreactor, a network analyzer (AD5933 integrated circuit) from analog devices is used. AD5933 has an on-board 12 bit frequency generator which is also called as direct digital synthesis core (DDS). DDS of AD5933 is capable of producing sine wave excitation signals from 1 Hz to 100 kHz. A 12-bit analog-to-digital converter and a digital signal processing (DSP) core, useful for measuring unknown impedance are integrated within the IC. The AD5933 IC requires a 5.5 V power supply and is controlled via Arduino ATmega 2560 microcontroller using I^2C interface. AD5933 can measure complex impedance in the range from 100 Ω to 1 MΩ. The excitation signals generated using this IC has peak-to-peak amplitude of 1.98 V. In this work, a potential divider is employed to trim this excitation voltage to 200 mV (peak to peak) [109,110].

To measure an unknown impedance of the culture medium (using AD5933), the impedance sensor is excited with a known frequency (generated by on-board DDS). Once excited, the impedance sensor gives a response signal which is sampled and processed by on-board ADC and DSP core. After processing using discrete Fourier transform algorithm, the IC provides a real and imaginary data for the measured impedance, which is read by ATmega 2560 via I^2C interface. One IC is used for generating the excitation signal and for measuring the impedance of all the sixteen bioreactors. DPDT relays are used to route the excitation signal (to the sensor) and response signal (from the sensor).

The block diagram presented in Fig. 27a shows the implementation of AD5933 for measuring culture medium impedance. Each time before an unknown impedance is measured a calibration step is performed, which measures the value of known impedance (3.3 k Ω). This step is integrated to check the functionality of the IC. Moreover, the collected impedance data is stored using a sparkfun data logger. To cross check the measured impedance reading, a CompactStat impedance analyzer (Ivium Technologies, The Netherlands) is used.

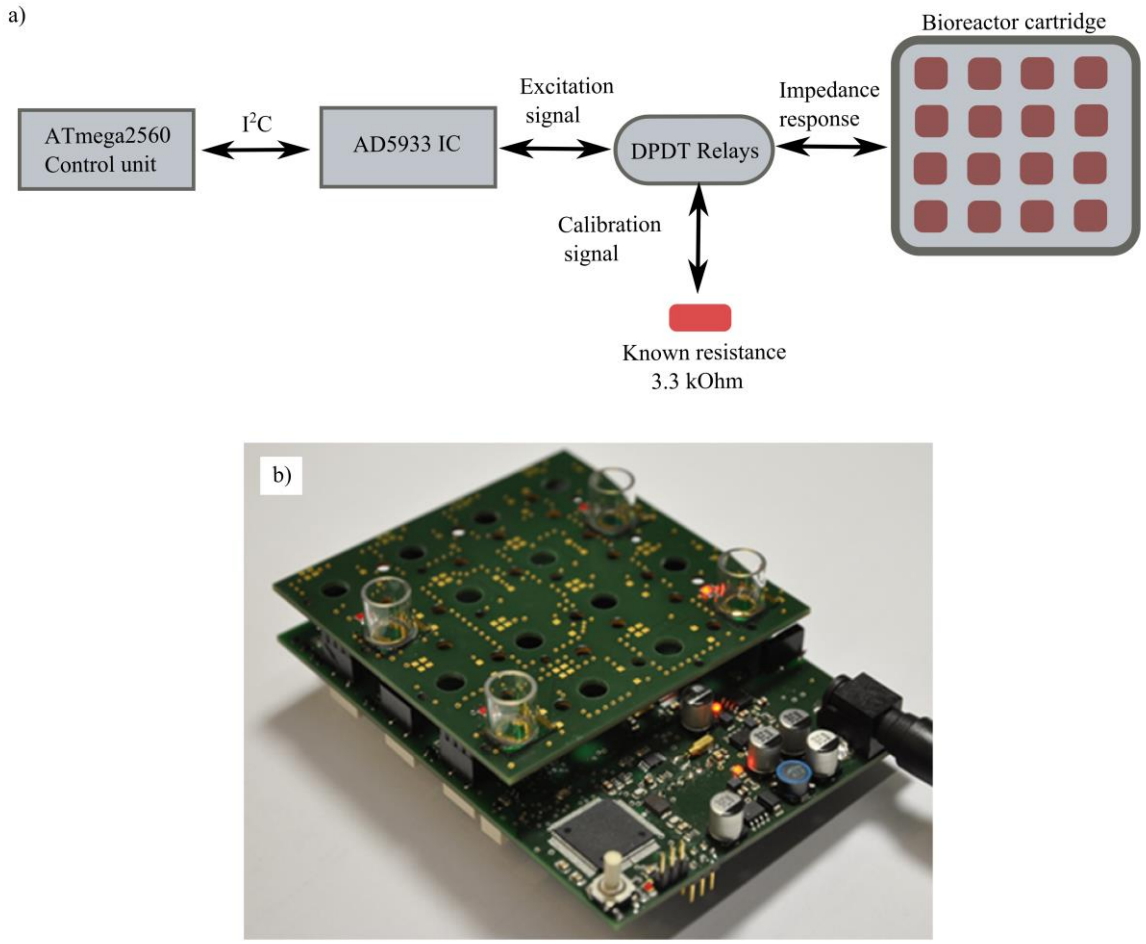

Figure 27: a) Block diagram showing the principle of impedance measurement using the network analyzer b) photo of implemented network analyzer with control unit.

Color sensor readout

As a reference measurement, a colorimetric principle is integrated within the sensor. In order to measure the color of the culture medium, a programmable color sensor TCS3200 is used. TCS3200 is manufactured by Texas advanced optoelectronic solution (USA) and requires an operating voltage of 5 V. Each color sensor has 64 photodiodes, which are connected in an array. Out of these 64 photodiodes, 16 have red (R) filter, 16 have green (G) filters, 16 have blue (B) filters and 16 photodiodes have no filters on them. Photodiodes with R, G and B filters measure the intensities of corresponding color, whereas photodiodes without filters are used to measure the intensity of white light. Thus by selecting red, green or blue filers, the RGB intensity values of the culture medium (ranging from 0 to 255) are determined [111].

In the sensor system there are sixteen color sensors mounted on a PCB such that each color sensor is placed beneath the bioreactor as represented in Fig. 28a. The color

sensors mounted on PCB are shown in Fig. 28b. All of the color sensors are controlled via ATmega 2560, which is programmed to measure the readouts from the color sensor. Light required for measuring the color is provided by white LEDs which are integrated on the membrane PCB board (see Fig. 28c).

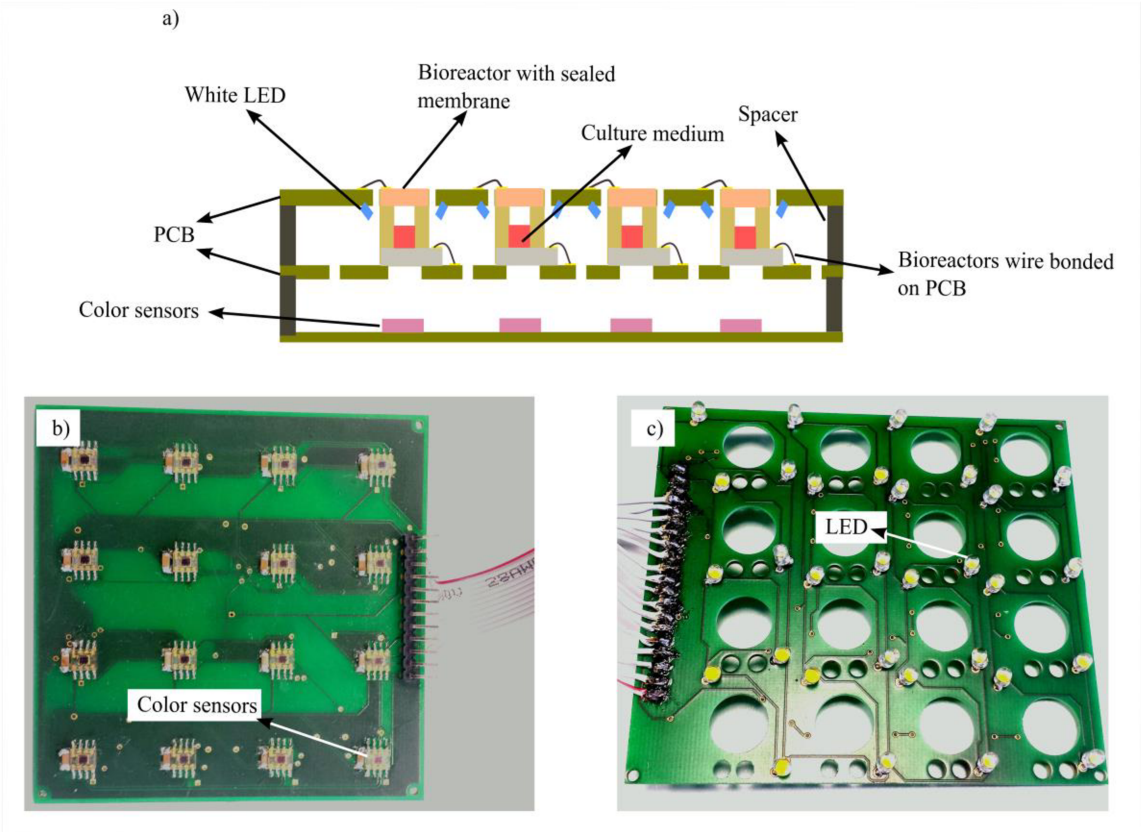

Figure 28: a) Schematic view of the color sensor positioned beneath the bioreactor cartridge for measuring the color of the culture medium b) PCB board with 16 TCS3200 color sensors c) Membrane PCB board with white light LED's.

4.7.2 Control unit

AVR microcontroller (ATmega 2560) designed by Atmel is used as the control unit for the sensor system. Control unit is programmed for autonomous operation of the sensor system. The schematic view of various modules which are controlled via the control unit is represented in Fig. 29.

Individual bioreactors are activated via the control unit by bursting the membranes. For bursting silicon nitride membrane a DC-DC converter (INNOLINE R15-100B, RECOM), which can provide a maximum output of 135 V and 20 mA is used. To protect the control unit and other electronics, the high voltage converting side (from DC-DC converter) is isolated from the low voltage side using solid state relays (CPC1510).

Sixteen solid state relays are used for each membrane and are controlled via the control unit through a de-multiplexer (74HCT4067).

After activating the bioreactor, the control unit activates the air pump. For sampling indoor air, a membrane micro diaphragm air pump (NMS030.1.2 KPDC) manufactured by KNF Neuberger GmbH is used. This pump operates at 12 V and provides a constant air flow of 11.5 liters/min. A high side electronic MOSFET switching circuit which is controlled by ATmega 2560 (control unit) is implemented to switch on and off the air pump.

Once desired amount of air has been sampled, the control unit activates sensor readout electronics to perform impedance and color measurements. The measured impedance and color data is automatically logged into micro SD card by using Sparkfun data logging unit. Moreover, there is an Ethernet module (W5550 Ethernet chip) to store the impedance and color data in cloud server, which can be monitored by the user at any time. If a mold growth is observed, the control unit commands the Ethernet module to send an email alert to the user.

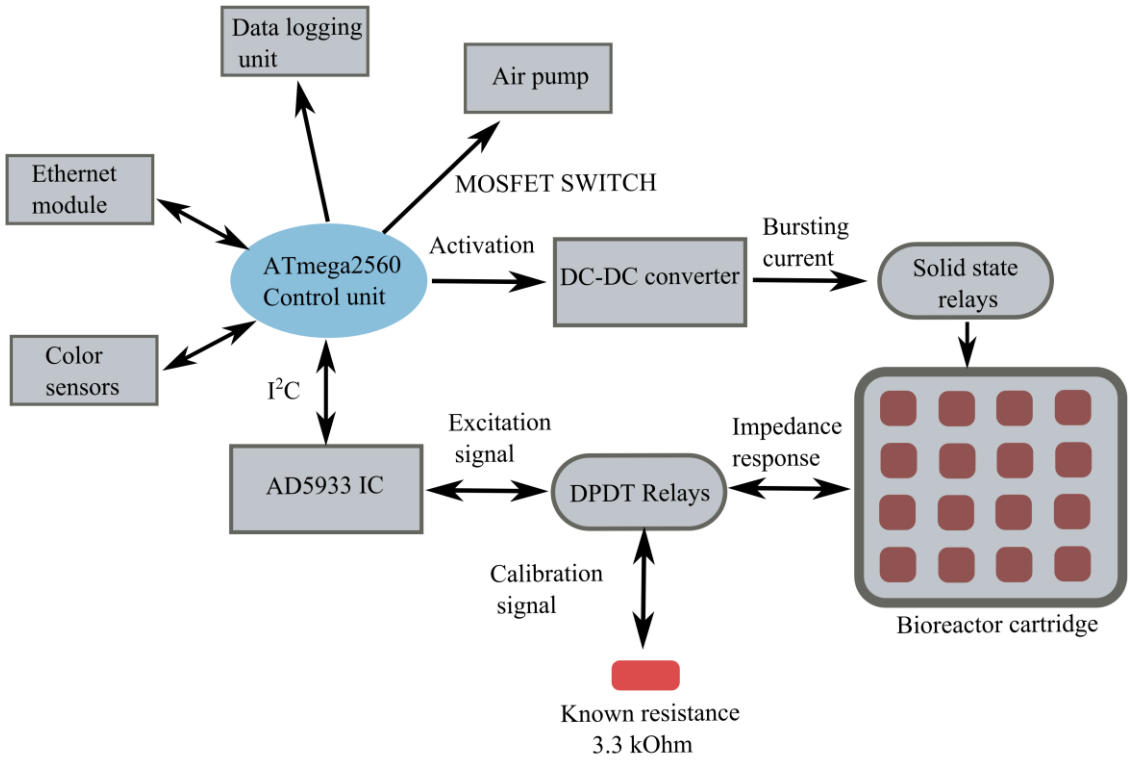

Figure 29: Schematic view of various modules controlled by the control unit.

4.7.3 Reagents, growth media and mold suspension

All necessary reagents and chemicals utilized in this work for preparation of the culture medium were bought from Carl Roth GmbH, Germany. Culture medium with reference pH indicator is prepared within the laboratory and is sterilized using an autoclave. All mold species investigated in this thesis like *Eurotium amstelodami, Aspergillus penicillioides, Aspergillus restrictus, Fusarium incarnatum* and *Fusarium Oxysporum* were provided by BMA Labor GmbH, Bochum, Germany. For producing airborne spores, the mold species were cultured in PDA agarose at 25 °C in an incubator for 8 weeks. Spore suspensions of desired concentration were prepared in the laboratory by using sterile deionized water in combination with sodium chloride and tween.

4.7.4 Experimental setup

For the experiments, the bioreactor cartridge is connected to the 3D printed air sampling unit as shown in the Fig. 30. A double side adhesive tape is used to connect the cartridge to the sampling unit and copper wires are used to prevent the cartridge delaminating from the air sampling unit. Autonomous sensor system for detection of mold spore contamination is shown in Fig. 31. Two prototypes have been designed for implementing the sensor system in archives.

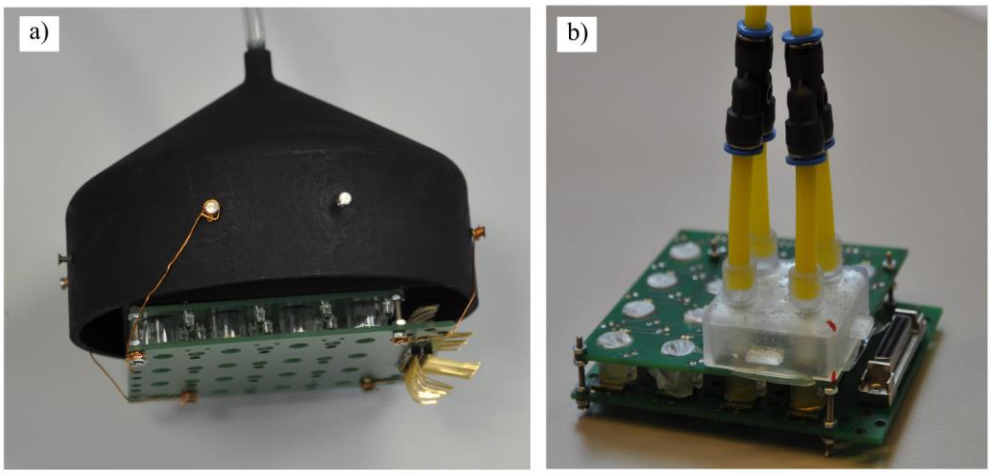

Figure 30: a) Bioreactor cartridge connected to non-focused air sampling unit b) Bioreactor cartridge connected to focused air sampling unit.

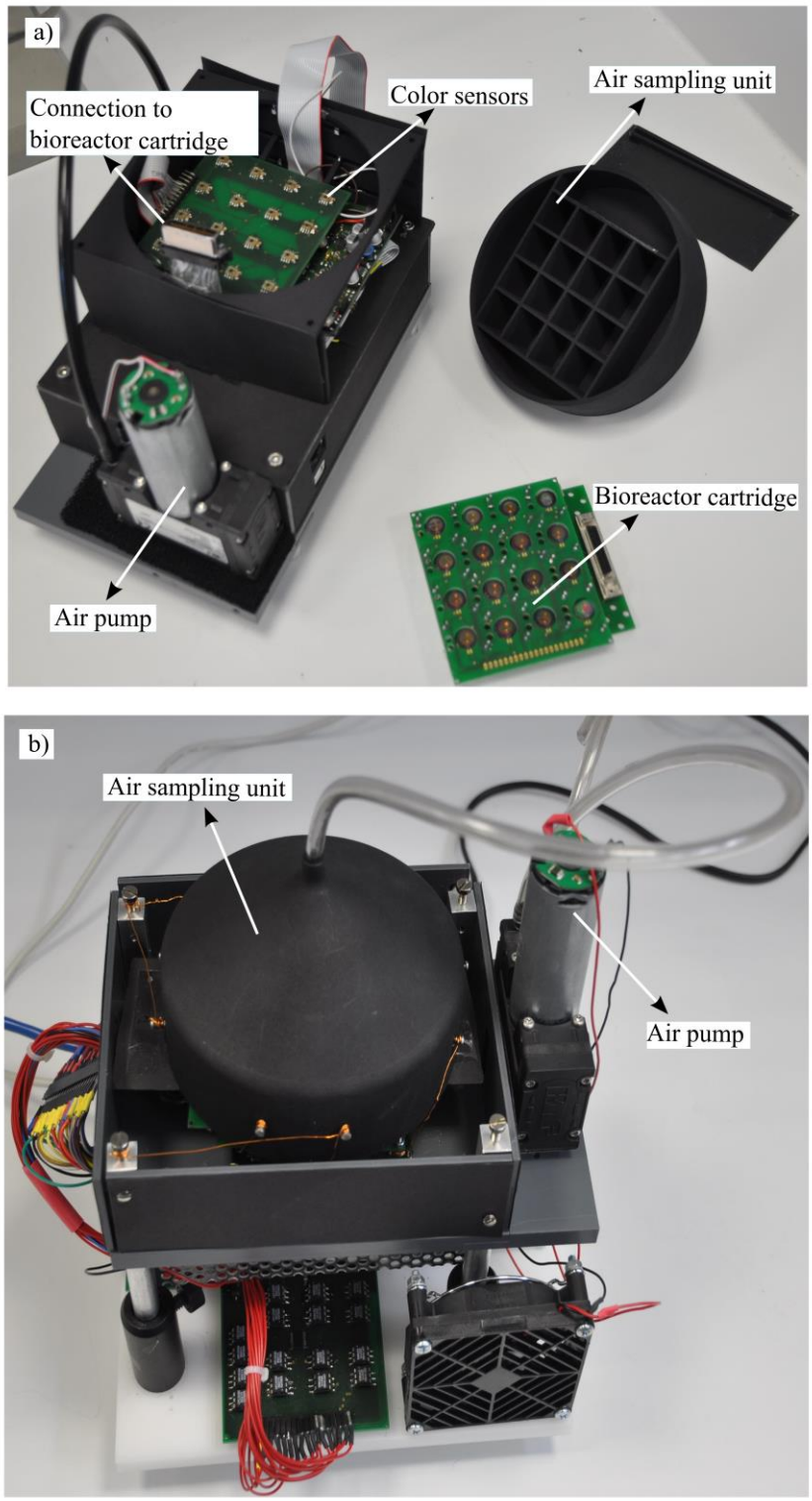

Figure 31: Autonomous sensor system for detection of mold spore contamination a) first prototype b) second prototype.

5 Results and discussion: bioreactor sensor system

5.1 Characterization of impedance sensor

The designed impedance sensor has been tested with three different electrode configurations (BE, AD and CF, see Fig. 14). As explained in chapters 4.2.1 and 4.3.3, the active areas of the electrodes have been varied for providing different sensitivities to the sensor. The electrode surface areas are 2.5 mm², 3.5 mm² and 4.5 mm² for BE, AD and CF electrode configurations, respectively. The surface area of the electrode has an influence on the double layer capacitance (C_{dl}) and the charge-transfer resistance (R_{ct}), whereas the distance between the electrode pairs has an influence on solution resistance (R_{sol}) and solution capacitance (C_{sol}). For characterizing the sensor, 200 µl of PDA agar culture medium is transferred into the reaction cavity. The PDA culture medium has an initial pH of 5.5 ± 0.2 (measured with a commercial pH meter at room temperature of 23 ± 1 °C; Hanna pH 209). The impedance response of the culture medium measured with all the three electrode configurations is represented graphically in Fig. 32 (Bode Plot) and Fig. 33 (Nyquist Plot) [82].

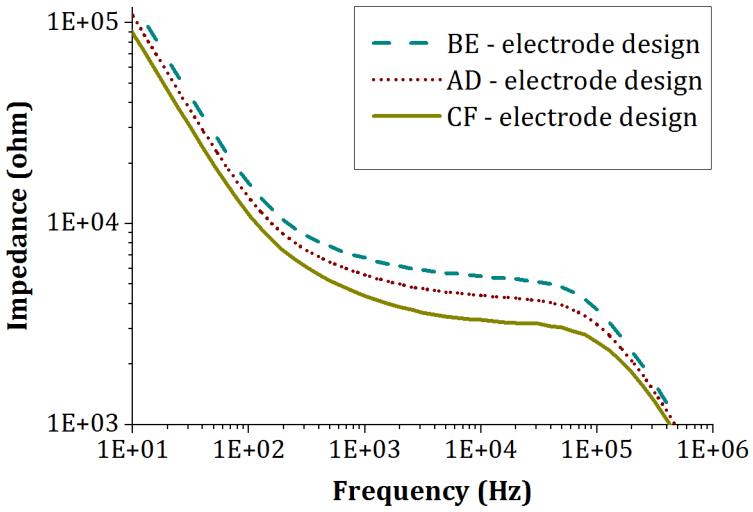

Figure 32: Impedance response of the PDA medium measured with all the three electrode configurations, represented in Bode plot

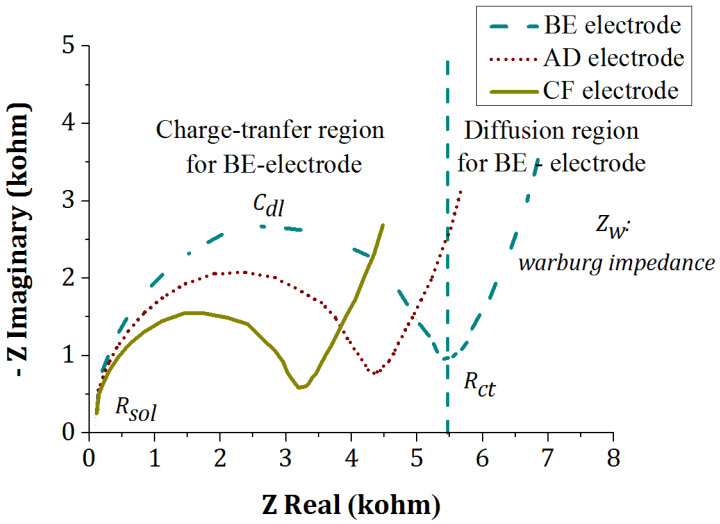

Figure 33: Impedance response of the PDA culture medium measured with all the three electrode configurations and represented in Nyquist plot. Vertical dotted line in the graph shows the separation region of charge-transfer and diffusion processes for BE electrode design.

Impedance spectrum is measured at 23 ± 1 °C (at a relative humidity of 45 ± 5 %) and in the frequency range from 1 Hz to 1 MHz using an impedance analyzer (compactStat, The Netherlands). In the Bode plot the absolute value of the impedance is plotted, showing detailed information of the measured impedance versus frequency. In the Nyquist plot the imaginary component of the impedance is plotted against the real component. Nyquist plots provide insight into various physical processes happening in the culture medium during impedance analysis. As indicated in Fig. 32, the impedance measured has a frequency-dependent behavior. This frequency-dependent behavior of the sensor is explained using the electrical equivalent circuit model presented in chapter 3.1.2 (Fig. 7).

The total impedance of the culture medium measured by the sensor is contributed by all the electrical circuit elements (R_{ct}, C_{dl}, R_{sol}, Z_w, and other parasitic capacitances). Depending on the circuit element that provides maximum contribution to the total impedance, the impedance spectrum can be classified into three frequency regions. Each frequency region corresponds to a different physical process, which is indicated by a vertical dotted line in the Nyquist plot (Fig. 33). At lower frequencies (i.e., below 1 kHz), diffusion process plays a crucial role, hence in this region major part of the impedance is contributed by the Warburg impedance. In the frequency range from 1 kHz to 100 kHz, charge-transfer process plays a crucial role. Hence in this region, the double layer capacitance and the charge-transfer resistance are the major contributors to the total impedance. Because the charge-transfer resistance is in parallel to the double layer capacitance the frequency response can be seen as a semicircle (when

plotted in the Nyquist plot). In the high frequency region (i.e., above 1 MHz), major part of the impedance is contributed by the solution (R_{sol} and C_{sol}). With the mold growth, the ionic concentration of the culture medium changes which results in the impedance change. As the sensor system is designed for mid frequency region (1 kHz to 100 kHz) only charge-transfer phenomena are considered. So the impedance change is studied by observing the changes in R_{ct} and C_{dl}.

To determine the values of each circuit component, the measured impedance data is fitted into the electrical circuit model using the Iviumsoft program (provided by Ivium technologies, The Netherlands). The obtained circuit parameters are compared for all the three electrode configurations and are represented in Table 1.

Table 1. Circuit parameters obtained by fitting the measured data to the electrical equivalent model at different pH values

Parameter	**BE-Electrode Design**		**AD-Electrode Design**		**CF-Electrode Design**	
Active area (mm^2)	2.5		3.5		4.5	
pH	5.5	4.5	5.5	4.5	5.5	4.5
R_{ct} (kΩ)	6	5.5	4.8	4.1	3.7	3.0
C_{dl} (nF)	19	21	24	28	30	36

The BE-electrode design, which has the lowest surface area, has the lowest double layer capacitance of 19 nF and highest charge-transfer resistance (6 kΩ). As the total impedance is the combination of resistive and capacitive elements, the BE-electrode design has the highest impedance of all the three electrode designs (as show in Fig. 32). The electrodes with larger surface areas have higher double layer capacitance (24 nF and 30 nF for AD and CF, respectively) and lower charge-transfer resistance (4.8 kΩ and 3.7 kΩ for AD and CF, respectively). As CF electrode has the highest double layer capacitance and the lowest charge-transfer resistance, the total impedance is lower when compared to other electrode configurations BE and AD (see Fig. 32).

Only the C_{dl} and R_{ct} values are determined from the model. As glass is used as the substrate material, which is an insulator, the parasitic capacitance (C_s) and the substrate resistances are neglected. The values of other parasitic capacitances (C_c) are negligible compared to the double layer capacitance. Also, the solution resistance and capacitance will change, but in the frequency range of 1 kHz to 100 kHz, their contribution to the total impedance is very small compared to the double layer resistance. Hence they are neglected.

To determine the sensitivity of each electrode configuration, the pH of the culture medium is lowered from 5.5 to 4.5 (1 unit change) by adding citric acid. With the ad-

dition of citric acid the amount of polar molecules within the culture medium increases. With higher polar molecules there is an increase in the dielectric permittivity, resulting in the decrease of double layer thickness. As the double layer thickness decreases, the double layer capacitance increases and the charge-transfer resistance decreases. The circuit parameters of different electrode designs when the pH of the medium is lowered from 5.5 to 4.5 are indicated in Table 1.

With a variation in the pH from 5.5 to 4.5, the double layer capacitance of CF electrode increases from 30 nF to 36 nF and the charge-transfer resistance decreases from 3.7 kΩ to 3 kΩ. This results in a total impedance change of 20 % per unit pH value. For BE and AD electrodes, the double layer capacitance changes from 19 nF and 24 nF to 21 nF and 28 nF, respectively. Similarly, the charge-transfer resistance values decreases from 6 kΩ and 4.8 kΩ to 5.5 kΩ and 4.1 kΩ, respectively. So for BE and AD electrode designs, there exists a total impedance change of 10 % and 15 % per unit pH value, respectively. From the measurements it is clear that CF electrode design shows highest sensitivity of 20 % impedance change per unit pH change.

5.2 Influence of reference indicator dye on mold growth

A colorimetric measurement which is integrated within the sensor acts as an optical reference. For integrating the colorimetric reference measurement within the sensor, the culture medium is prepared with a pH indicator dye. As the mold grows, the pH indicator dye with known color transition region changes the color of the culture medium. Depending on the mold species being investigated, different pH indicator dyes can be integrated within the culture medium to obtain detectable optical changes.

For the archive mold species which are being investigated in this thesis, there will be an increase in the pH of the culture medium (from 5.5 to 8.0) as the mold grows. So the pH indicator dye used should have a color transition region within this pH range. For our experiments, Methyl red dye which has a color transition range from 4.5 to 6.5 is used as a reference pH indicator dye. One major challenge of using a pH indicator within the culture medium is to ensure that this indicator dye does not inhibit the growth of mold species. Usage of methyl red dye is proven to show acute toxicity to aquatic organisms [112–114]. However, not much information or research is available regarding the toxicity of the methyl red dye to the archive mold species.

To determine whether the methyl red dye inhibits the growth of the mold species experimental investigations are done. From these experiments the best suitable concentration of dye is determined. For the experiments, various PDA culture mediums are prepared by integrating different concentrations of methyl red. Same concentration of archive mold spores (10^3 CFU/ml) is pipetted at three different spots on the petri dish and the petri dish is incubated at 23 °C (at RH of 45 %). All the investigated

mold species were grown with varied dye concentrations. The diameter of the colony is measured every day to determine the influence of the indicator dye. Fig. 34 represents the results, which show that a concentration of 0.1 % dye is acceptable because it does not significantly inhibit the growth of mold species (when compared to the growth of mold species on the culture medium without any dye). Measurements were repeated three times for determining these results. The culture medium prepared with concentrations higher than 0.1 % seems to be toxic to the mold species as their growth is inhibited when compared to their growth in medium without dye. Fig. 35 shows the examples of other indicator dyes with different color transition regions, which can also be integrated within the culture medium. Pictures of mold species growing on PDA culture medium with methyl red indicator dye is presented in Fig. 36.

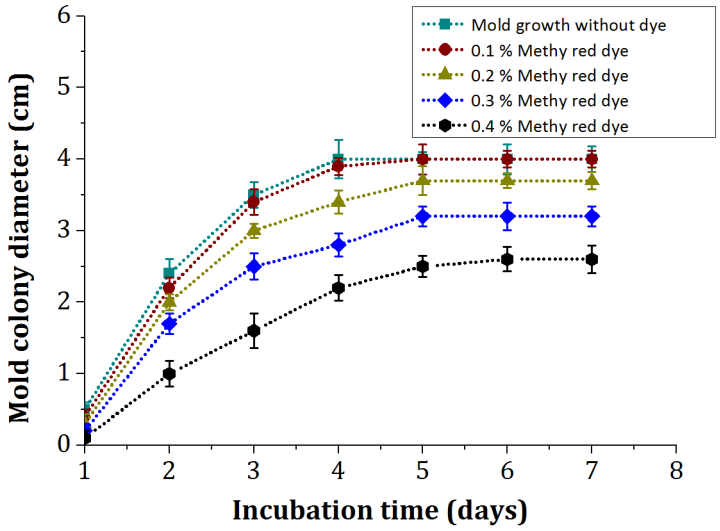

Figure 34: Mold colony diameter measured by integrating different concentrations of methyl red indicator dye within the culture medium.

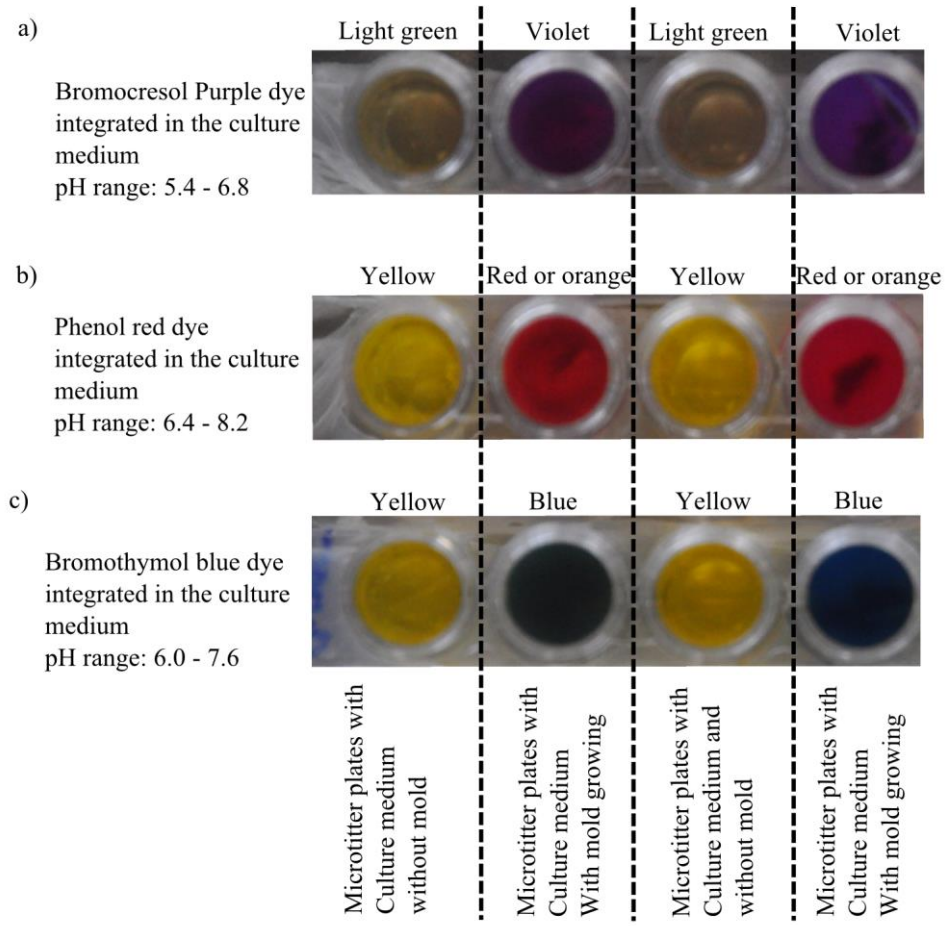

Figure 35: Mold growing in a PDA culture medium with different indicator dyes a) Bromocresol purple b) Phenol red c) Bromothymol blue.

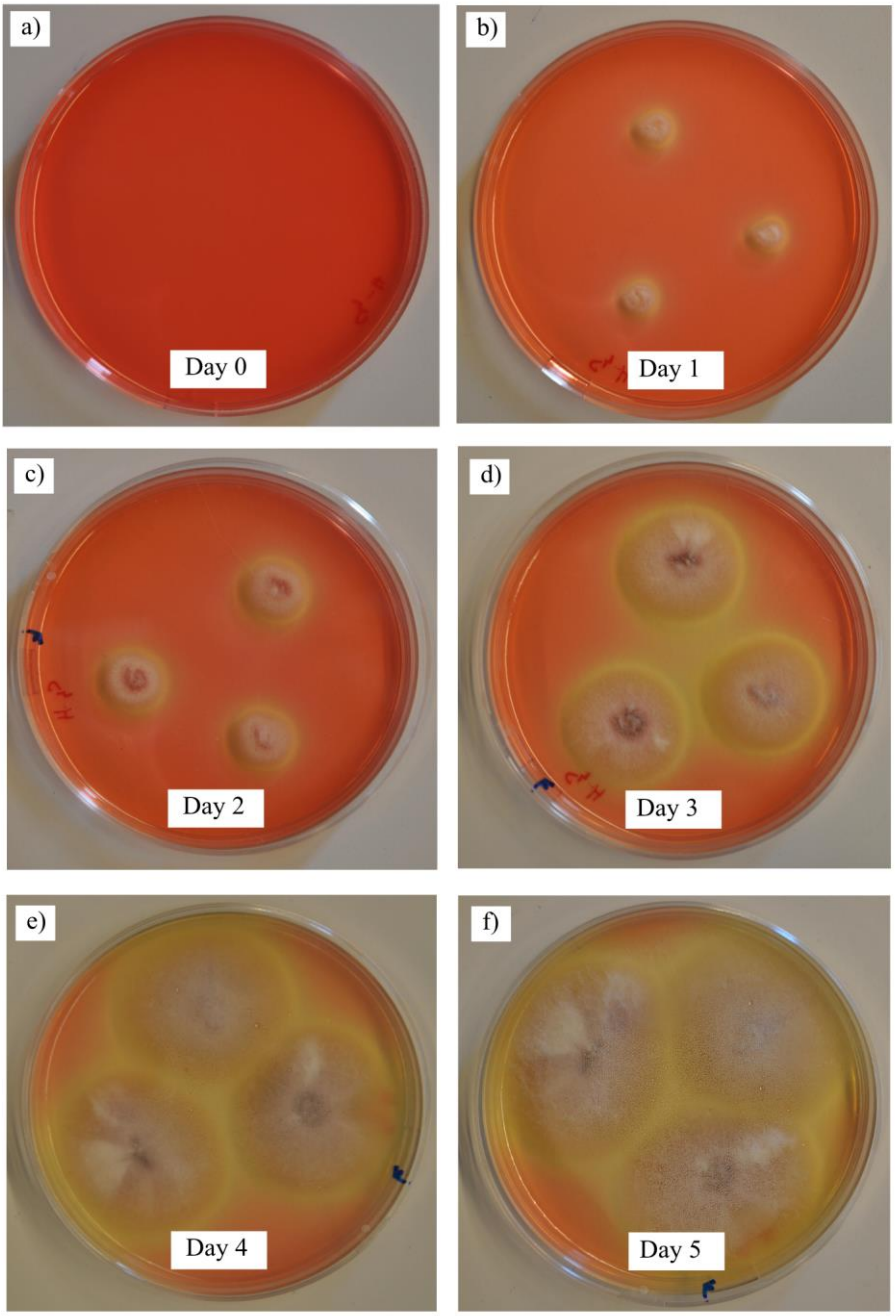

Figure 36: Mold growing in PDA culture medium with methyl red indicator dye. At initial state i.e on day 0 the color of culture medium is orange; as the mold grows there is an increase in the pH resulting in the change of mediums color to yellow.

5.3 Detection of mold growth using impedance and colorimetric measurements

This section describes the detection of mold growth using the bioreactor. Before beginning the measurements, mold spores of desired concentration are pipetted (100 µl) into the reaction cavity of the bioreactor. The bioreactor is then placed in the flow box till the solution (pipetted DI water) evaporates. After evaporation, the spores will be in direct contact with the culture medium. At this point the initial measurement (0 hour) is recorded. Different archive species like *Eurotium amstelodami, Aspergillus penicilliodes, Aspgergillus restrictus, Fusarium species* have been successfully detected using the bioreactor.

Fig. 37 shows the impedance response of one of the mold species *Eurotium amstelodami* measured on chip, with a spore concentration of 10^3 CFU/mL (colony forming units/mL). The impedance spectra measured is in the frequency range of 10 Hz to 1 MHz [82]. As CF electrode configuration provides highest sensitivity (compared to BE and AD), the impedance response is measured using CF electrode design. As represented in the Fig. 37, with the growth of mold the impedance of the culture medium changes. This is because the nutrients present in the culture medium are metabolized and are utilized by the spores to grow. During this metabolism the molds release byproducts changing the pH (i.e., increase) of the culture medium. More explanation regarding the released byproducts has been explained in Chapter 3.3.

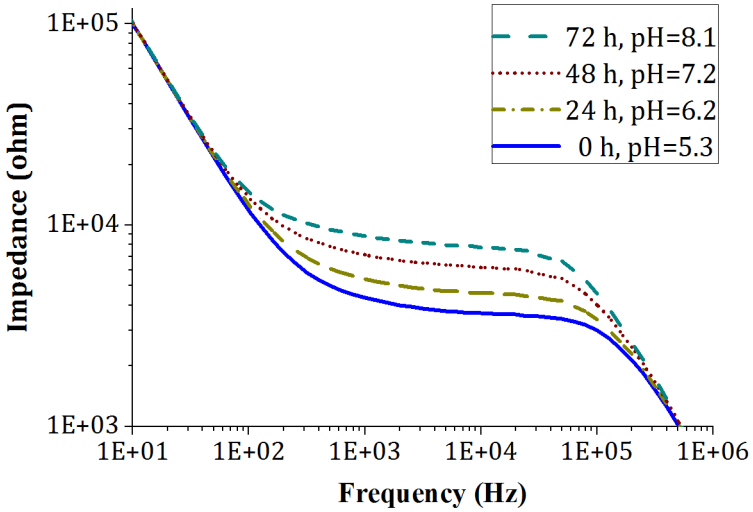

Figure 37: Impedance growth curve recorded using the mold sensor during the growth of *Eurotium amstelodami* mold species with CF electrode configuration.

As the pH of the culture medium increases, the amount of polar molecules inside the culture medium decreases. Because of this the ionic concentration within the medium decreases. This decreases the double layer capacitance, which simultaneously increases the charge-transfer resistance. Thus the total impedance of the culture medium increases with time as indicated in Fig. 37. The frequency-dependent behavior of the impedance curves has been explained using Randles equivalent circuit parameters in the chapter 5.1. The impedance measurements are fitted into the circuit model to determine the charge-transfer resistance and the double layer capacitance. At initial state before the mold growth, the values of double layer capacitance and charge-transfer resistance are 30 nF and 3.7 kΩ, respectively. The measurements done after 24 hours, decreases the double layer capacitance to 24 nF and increases the charge-transfer resistance to 4.4 kΩ. This results in an impedance change of 23 % within 24 hours, when measured at 10 kHz. Measurements were repeated six times and the results show a standard deviation of lower than 10 %. Similar behavior is observed for the measurements done with other electrode configuration (AD and BE electrode designs), but as they have lower sensitivities the impedance change for fixed time is lower when compared to CF electrode design.

Because of the pH change, the ionic concentration of the culture medium stored within the reaction cavity changes. This change is observed in the values of C_{dl} and R_{ct}. If there is a change in volume of the culture medium, C_{dl} and R_{ct} values will not be affected, instead the value of R_{sol} will change. As the value of R_{sol} is much smaller when compared to the double layer impedance (C_{dl} and R_{ct}), its contribution to the total impedance value is negligible. Thus the impedance change measured depends on the ionic concentration of the culture medium and is less influenced by the volume of the culture medium.

As it is not possible to assign an absolute value of pH to the measured impedance data without pre-calibrating the impedance sensor an independent colorimetric reference measurement is integrated within the sensor. Integrating the colorimetric reference allows to determine the absolute pH value of the culture medium and the sensitivity (percentage of impedance change per unit pH) of the sensor. As explained in section 5.2, a pH indicator dye added to the culture medium changes the color of the medium as the pH of the medium transits specific values. For methyl red indicator dye this color transition region is between 5.5 and 6.5.

Impedance sensor with the integrated colorimetric principle is shown in Fig. 38. The bioreactor consisting of culture medium which is prepared with methyl red indicator dye is indicated in Fig. 38. As the initial pH value of the PDA culture medium is 5.5, the medium with methyl red dye has an initial color of red or orange. So when there is no mold growing, the color of the culture medium is red or orange. Once there is mold growth, the pH of the culture medium increases. The color of the medium thus chang-

es from orange to yellow once the pH of the medium increases to 6.5. This color change of the medium is measured to determine the absolute change in the mediums pH.

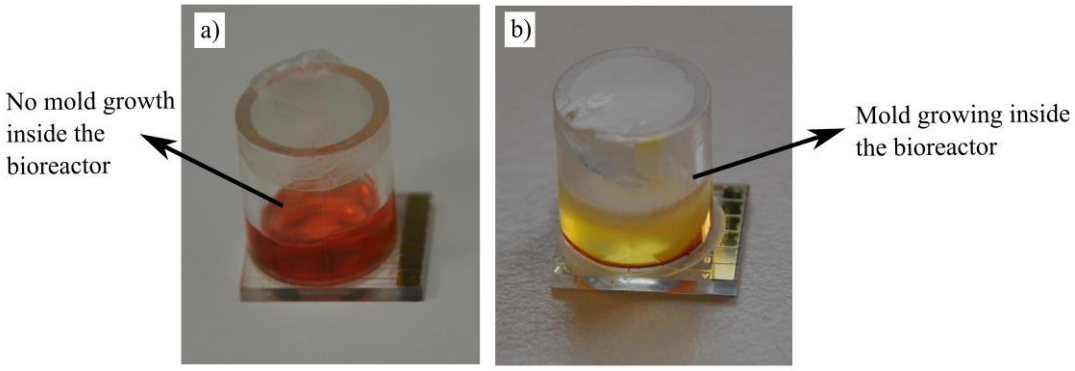

Figure 38: Detection of *Fusarium* mold species using the bioreactor a) initial orange or red color of the medium when there is no mold growth (pH is 5.5) b) culture medium turned yellow because of increase in the pH to 6.5 with the growth of mold.

The measured RGB intensity values of the culture medium with methyl red indicator using the TCS3200 color sensor for different pH values are represented in Fig. 39. If other indicator dyes (for example, bromothymol blue or phenol red) are used in the culture medium, then the measured RGB intensities will vary. Using the methyl red indicator dye the color of the culture medium changes from red to yellow in the pH range from 4.5 to 7.0. This color transition is observed due to the change in the intensity of the green component of the visible spectrum. Fig. 39 represents all the three RGB components of the culture medium with methyl red dye. As the pH of the medium is changed, the R and B components remain constant, whereas the green components of the visible spectrum changes.

From the calibration curve (Fig. 39), the absolute pH value of the culture medium can be determined. To determine the sensitivity of the sensor, a unit change in pH is measured using the color sensor and this value is assigned to the corresponding impedance values measured using the impedance sensor. The colorimetric measurement can be used to determine the pH of the culture medium till the saturation point of the dye is reached. In the case of methyl red, the color gets saturated at pH of 7.0.

Once the sensor is calibrated using the reference measurement, further changes in the pH are determined using the impedance measurements. The active region for determining the sensitivity of the sensor (in terms of pH unit) is between pH 5.5 to pH 7.0. Using the impedance spectra (Fig. 37) and the pH calibration curve (Fig. 39),

within the region where both optical and impedance methods are active, a relation of 0.9 kΩ/ pH unit is determined.

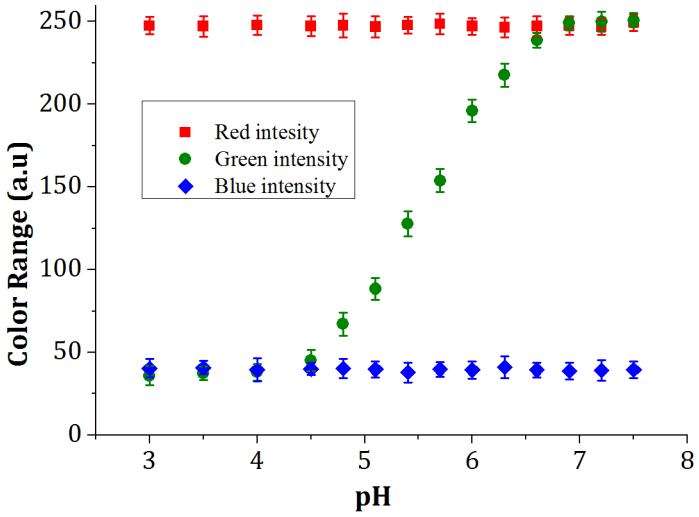

Figure 39: RGB intensity values measured from the color sensor for methyl red indicator dye at different pH values.

In the described mold experiment, with the growth of mold species, the RGB intensities are measured using the color sensor. The measured green component changes its intensity from 118 to a value of 210 after 24 hours. Using the pH calibration curve (Fig. 39), an interpolation is found for corresponding intensity. For the value of 118 the corresponding pH value is 5.3, whereas for the value of 210 the pH is 6.2. The corresponding impedance values measured using the impedance sensors are 3.65 kΩ at G=118 (corresponding pH = 5.3) and 4.5 kΩ at G=210(corresponding pH=6.2). From the mentioned values, the resulting impedance change is 23 % per unit pH change.

Mold species responsible for contamination of archives like *Eurotium amstelodami, Aspergillus penicillioides, Aspergillus restrictus* and *Fusarium* species have been successfully implemented on chip to determine the sensor performance. Depending on the initial concentration and the type of mold species the rate of impedance change varies. By utilizing the impedance rate the quantification of mold species is done to determine the mold spores initial concentrations. The impedance growth curves for two different concentrations of *Aspergillus penicillioides* mold species are shown in Fig. 40. There are three different growth stages for the mold. First stage is called lag phase or germination phase, where the spores start to germinate. At this stage the hyphae is not yet visible. The spores secrete acids at this stage resulting in decrease of the medium impedance. Second stage is the growth phase, where the spores start to grow into the mold. Due to mold growth there is formation of amino acids resulting in increase of the culture medium impedance. Last stage is called stationary phase. In

this stage mold growth has reached to saturation. So the medium impedance remains constant or varies slightly.

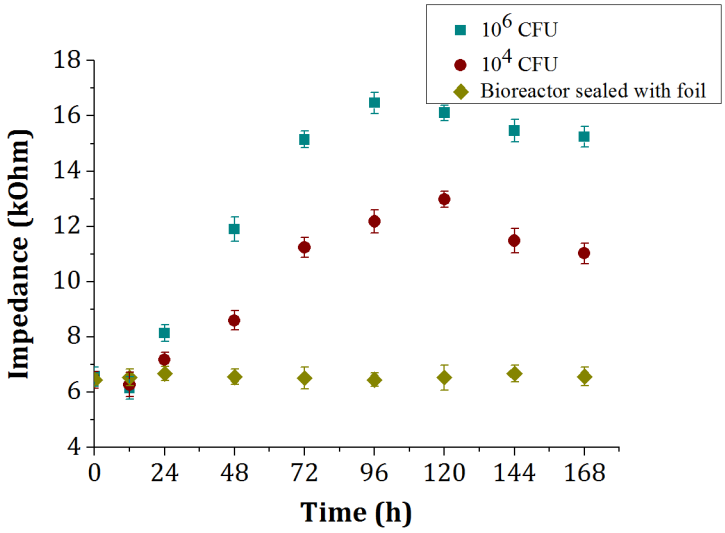

Figure 40: Impedance response of two different concentrations of Aspergillus penicilliodes mold species measured using the bioreactor with CF electrode configuration at 10 kHz.

The quantification results for different mold species are represented in Fig. 41, where the measured percentage of impedance change is plotted as a function of initial concentration of mold spores for a detection time of 24 hours. The impedance is measured at a frequency of 10 kHz and the error bars represent the standard deviation from 6 measurements.

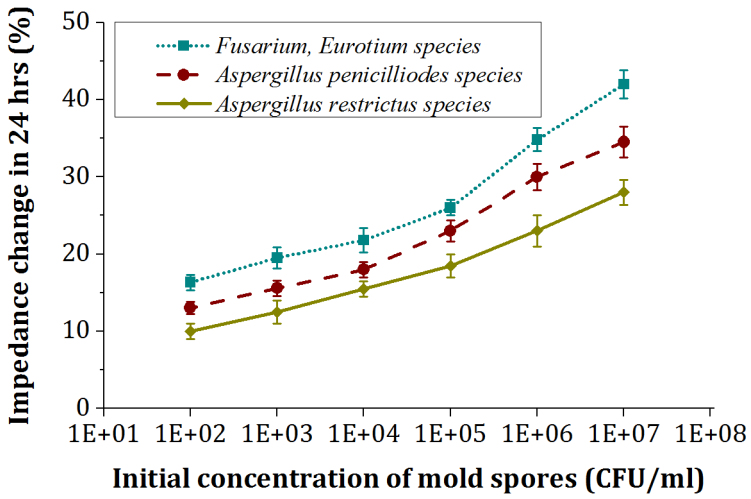

Figure 41: Percentage of impedance change measured within 24 hours as a function of initial concentration of mold spores determined using CF electrode configuration at 10 kHz.

As indicated in the measurement results, if the initial concentration of spores is high, the impedance change is faster thus resulting in higher impedance change for a constant detection time. Also mold species *Fusarium* and *Eurotium* grow relatively faster and produce pH changes quickly when compared to other mold species *Aspergillus penicilliodes* and *Aspergillus restrictus*. Considering Aspergillus restrictus, if it's initial concentration is 10^3 CFU/ mL then within 24 hours the impedance of the culture medium is changed by 12 %, whereas if the concentration of the spores is 10^6 CFU/ mL, then there is an impedance change of 23 % within 24 hours. If Eurotium species of 10^3 CFU/ mL is cultured in the bioreactor, then it produces an impedance change of 19 % within 24 hours and for a concentration of 10^6 CFU/ mL there is an impedance change of 35 % within 24 hours. This shows that different mold species having same initial spore concentrations produces different impedance changes within a constant time period. Although this thesis work is not aimed at differentiating the mold species, the quantification results show that monitoring mold growth rate gives a first indication of mold type. Also the quantification results show that by using CF electrode configuration the initial concentration of spores can be determined within 24 hours.

5.4 Characterization of silicon nitride membranes

Bursting behavior of the designed silicon nitride membranes have been simulated using Comsol Multiphysics. From the simulations the current required for the membrane to burst is predicted. As explained in Chapter 4.4.2, for simulating the temperature and stress distribution pattern within the membrane, Joule heating physics in combination with structural mechanics has been used. With the Joule heating physics, the temperature development within the membrane is determined. The structural mechanics model uses the temperature difference and calculates the thermal stresses developed within the membrane. If the thermal stresses developed within the membrane reach the fracture strength of silicon nitride then the membrane bursts.

The fracture strength of silicon nitride has been shown in literature to be in the range from 2-5 GPa. By using this range as a reference value for the fracture strength, simulations have been done to find the bursting current of the silicon nitride membrane. The simulation results provide a good indicator to determine the locations within the membrane where the temperature is highest. Moreover, with the simulations it is possible to find out the most likely rupture location on the membrane.

The simulated temperature distribution and their corresponding stress profiles developed within the membrane for all the three electrode designs are represented in Fig. 42. From the simulation profiles, it is observed that on applying a current pulse (e.g., 10 mA for cross-electrode design), the temperature around the electrode reach-

es to a maximum value (around 1200 K-1800 K). For all the electrode designs, the highest temperature region is around the circumference of the electrodes. This is because silicon nitride is a poor heat conductor and hence the heat diffusion within the membrane is low. Because of this when a current pulse is applied, there is a formation of temperature gradient within the silicon nitride membrane. This temperature gradient induces stresses in the membrane.

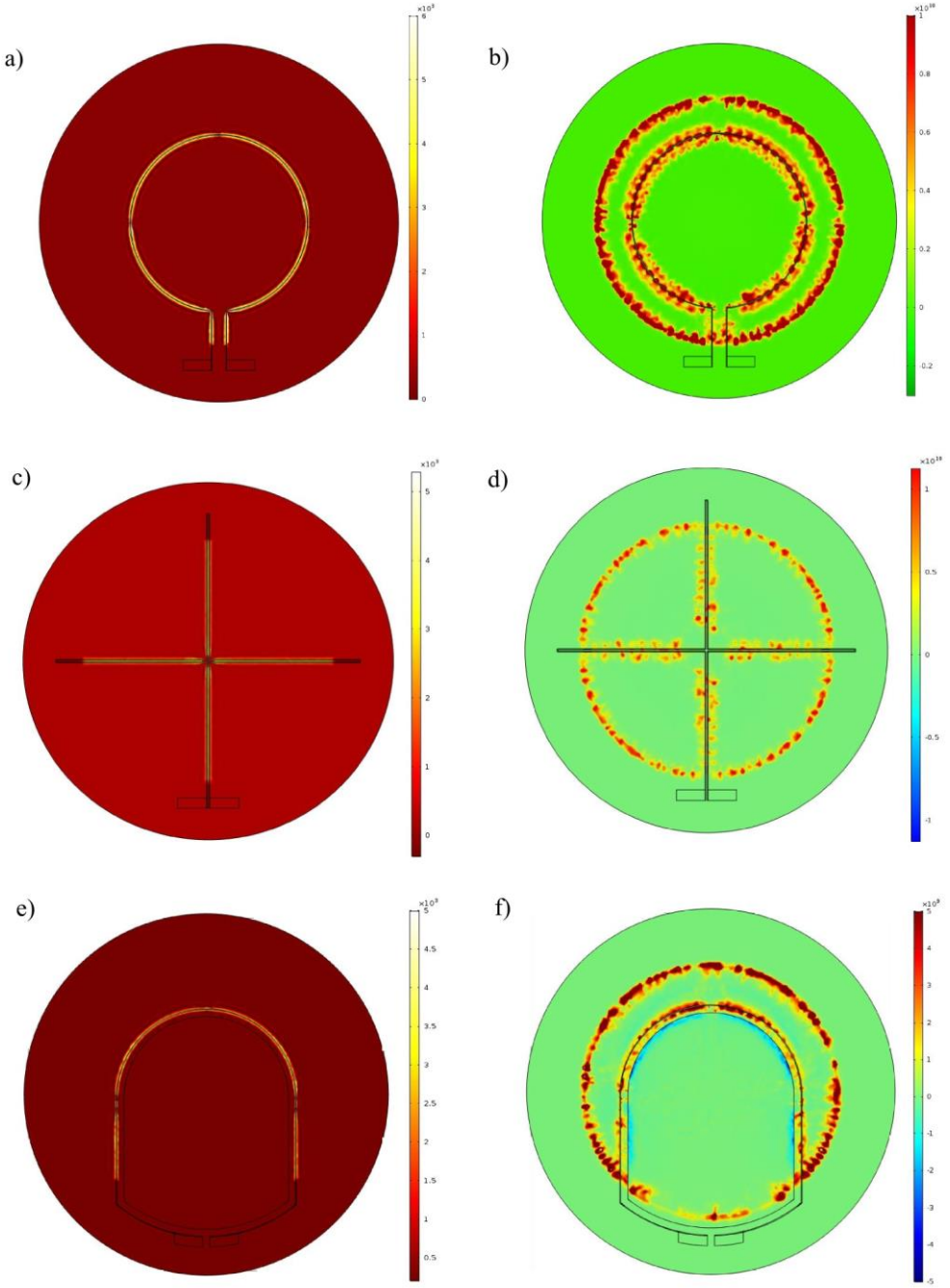

Figure 42: Simulated temperature and thermal stress profiles within the silicon nitride membrane for all the three designs a) and b) circular; c) and d) cross-section; e) and f) parallel-electrode design.

With the obtained temperature profile, the thermal stresses (first principle stresses) within the membrane are simulated and are shown in Fig. 42. The stress profile indicates that there exists two different regions within the membrane where the thermal stresses could reach its maximum value. The first region is around the electrode, where the temperature is highest. Because of the temperature gradient happening between electrode region and the membrane, maximum stresses are built up at this region. The second region is at the outer periphery of the membrane, where the membrane is in connect with the silicon substrate. As the deflection of membrane is constrained at this location stresses built up at this location are maximum. So the possible rupture location is either at the electrode or at the outer periphery of the membrane.

From the simulations, current required to break the designed membrane is determined. This current is termed as breakup current. So, breakup current is the value of applied current, where the thermal stresses developed within the membrane reach the value of fracture strength (2-5 GPa). As different electrode designs have different resistances the breakup current and time required for bursting the membrane are different and are indicated in Table 2.

The schematic circuitry and the experimental setup implemented to investigate the bursting behavior of the silicon nitride membrane are shown in Fig. 43 and Fig. 44. The membrane is connected to a DC-DC converter which provides the required current pulse for the membrane. The time required to burst the membrane is determined using the schematic shown in Fig. 43a. An oscilloscope (Infiniivision, Agilent Technologies) is connected across a 220 Ω resistor to monitor the current pulse duration. Fig. 43b shows the current pulse duration, where the current across the resistor drops to zero as soon as the membrane bursts (creating an open circuit).

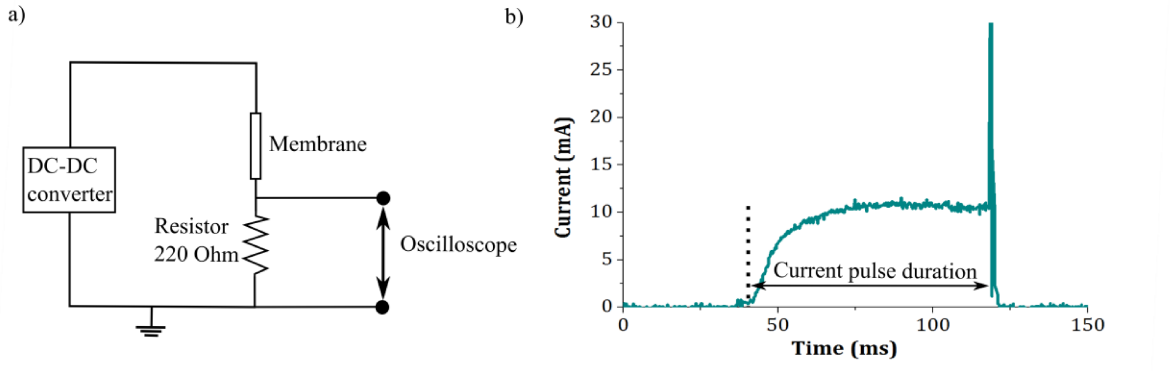

Figure 43: Schematic representation of circuit for measuring the bursting time b) current pulse measured when the membrane bursts (membrane with cross-electrode design).

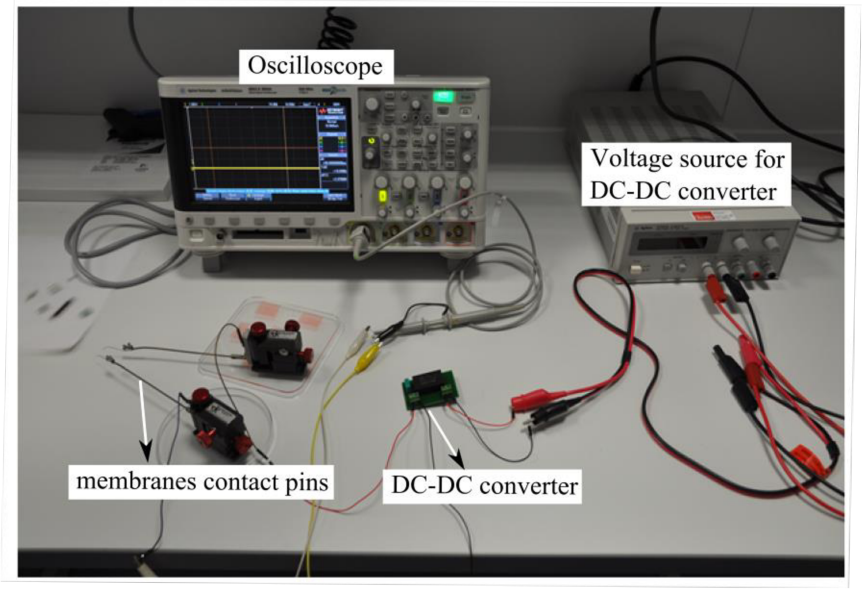

Figure 44: Experimental setup for determining the membrane bursting parameters.

Experimentally determined bursting parameters for three different electrode designs are indicated in Table 2.

Table 2. Bursting parameters of all the three membrane designs obtained from simulations and experiments

Parameter	**Cross-Electrode Design**	**Circular-Electrode Design**	**Parallel-Electrode Design**
Electrode width (μm)	22	22	22
Resistance (kΩ)	9±0.3	5±0.2	16±0.1
Breakup current measured (mA)	12±4	16±3	8±2
Breakup current simulated (mA)	18	26	13
Bursting time measured (msec)	80±12	53±14	174±29

As indicated in the Table 2, 22 μm cross-electrode design with a resistance of 9±0.3 kΩ requires a current of 12±4 mA for bursting the membrane. Each membrane design has been tested 7 times and the error bars indicate the standard deviation calculated from 7 measurements. The time required to burst the membrane is 80±12 msec. The simulated value of break up current is 18 mA. The circular-electrode design has an electrode resistance of 5±0.2 kΩ and its break up current and times are

16±3 mA and 53±14 msec, respectively. The breakup current predicted from the simulation is 26 mA. Similarly for the parallel-electrode design having a resistance of 16±0.1 kΩ, has a breakup current and time of 8±2 mA and 174±29 msec, respectively. Its simulated breakup current is 13 mA. The deviation in the measured and the simulated break up current values could be because of the variations in the internal stress of the silicon nitride, which might be varied during fabrication of the membrane.

All three membrane designs burst reliably with the above mentioned specifications. However, the parallel-electrode design is preferred as it creates a larger opening area (as shown in Fig. 45c). The membrane in this case bursts into tiny pieces because of the internal stresses induced into the membrane by sputtering additional metal layer on the top of membrane. The circular and cross-electrode designs have lower opening area because once the membrane bursts there is a part of the membrane hanging. Though this membrane can be used for sealing the bioreactor, the part of membrane which remains hanging could inhibit the spores from reaching the culture medium.

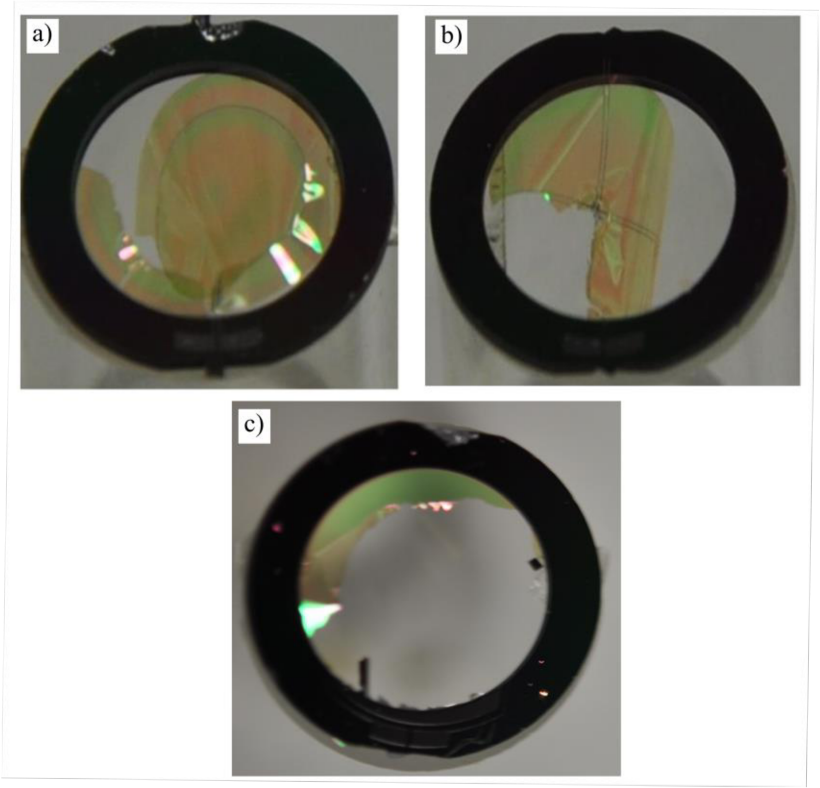

Figure 45: Optical images of bursted silicon nitride membranes a) circular-electrode design b) cross-electrode design c) parallel-electrode design.

5.5 Mold spore detection with membrane sealed bioreactor

The membrane-sealed bioreactor has been tested to check if it is possible to detect mold spores from air sample at a defined time. Also tests were performed to prove if the used membrane (after sealing the bioreactor) hampers the spores to reach the culture medium. The experimental setup for testing single membrane-sealed bioreactor is shown in Fig. 46 [92]. The setup comprises of a single membrane-sealed bioreactor enclosed in a 3D printed housing. The housing has an air inlet (connected to an air pump) and a color sensor is located beneath the bioreactor. The setup also consists of a power module to burst the membrane at a desired time and the impedance module to measure the impedance changes as the mold grows.

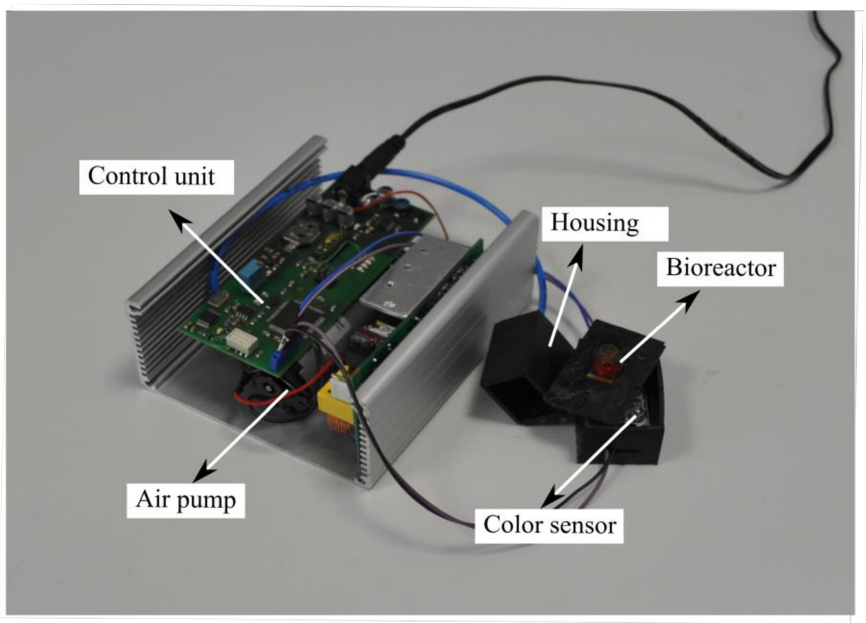

Figure 46: Picture of experimental setup implemented for detection of mold spores from air sampling using single membrane-sealed bioreactor.

For generating spores within the air sample, *Aspergillus penicilliodes* species is grown in a petri dish for 8 weeks in an incubator at 25 °C (8 weeks is enough for this mold species to produce spores). The inlet tube of the air pump is placed on the top of petri dish and the outlet tube is connected to the housing. When the air pump is on, the spores from the petri dish are sucked via the inlet tube and are pumped into the housing which has the membrane-sealed bioreactor enclosed in it. Two different sets of experiments were performed. In the first case, the bioreactor is exposed to spore with its membrane closed. In the second case, the membrane is opened (via current pulse). This will expose the culture medium to the mold spores present in the air sample.

Results indicate that if the bioreactor is not activated (i.e., the silicon nitride membrane of the bioreactor is not opened) the mold spores from the air sample cannot reach the culture medium. Thus no growth of mold observed inside the bioreactor as indicated in Fig. 47a. Also the measured impedance of the culture medium shows no significant change (Fig. 47c). When the bioreactor is activated (i.e., the silicon nitride membrane is opened with a current pulse), the mold spores present in the air sample get captured in the culture medium and start to germinate. Fig. 47b shows the growth of mold after 24 hours within the bioreactor and the culture medium being turned to yellow because of increase in the mediums pH. Fig. 47c shows the impedance growth curve of the mold spores measured at 10 kHz for 120 hours. As described in Chapter 5.3, the impedance of the culture medium increases linearly at the initial stage which is called growth phase. Impedance reaches a saturation point as the growth of mold stops, thus the measured impedance remains constant or decreases slightly because of other metabolites released during this phase.

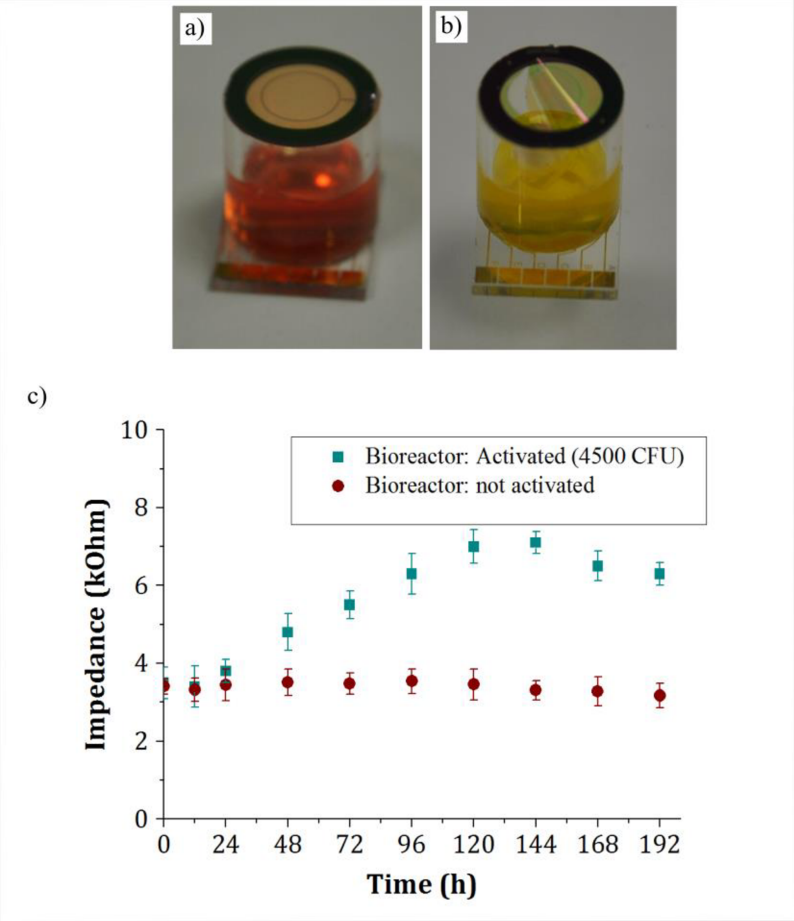

Figure 47: Bioreactor with silicon nitride membrane a) Bioreactor not activated: no growth of mold observed after air sampling b) Bioreactor activated: growth of mold observed once the membrane is opened and the culture medium is exposed to mold spores c) impedance growth curve of *Aspergillus* mold species measured using the sensor system.

These experiments prove that the thin silicon nitride membrane glued onto the bioreactors prevent the spores from reaching the culture medium. The culture medium remains sterile until the membrane is opened at a defined time interval. After thermal opening of the membrane, the bioreactor is able to detect the mold spores present in the air. These experiments provide proof of principle for detection of the mold spores from air sample. This concept is further developed into an array of sensors to realize a sensor system for detection of mold spores, which is described in next sections.

5.6 Bioreactor cartridge for monitoring spore contamination

After successfully testing the membrane-sealed bioreactor, an array of bioreactors is used for the detection of mold spores. As explained, the bioreactor cartridge comprises of sixteen membrane sealed bioreactors arranged in 4 X 4 format. For sampling air into individual bioreactors an air sampling unit is designed. In the following sections, characterization of air sampling unit is illustrated and is followed by the detection of mold in laboratory test environment has been explained.

5.6.1 Airflow and particle distribution

Air sampling unit

Comsol multyphysics is used to simulate the airflow distribution inside the air sampling unit. Fig. 48 shows the simulation result of airflow velocity distribution profile inside the air sampling unit represented in 3D format. At the inlet of the air sampling unit the airflow has a maximum velocity of 5 m/s. The inflow velocity for inner four compartments is found to be 1.5 m/s, whereas for the rest of the compartments the simulated flow rate is 1 m/s.

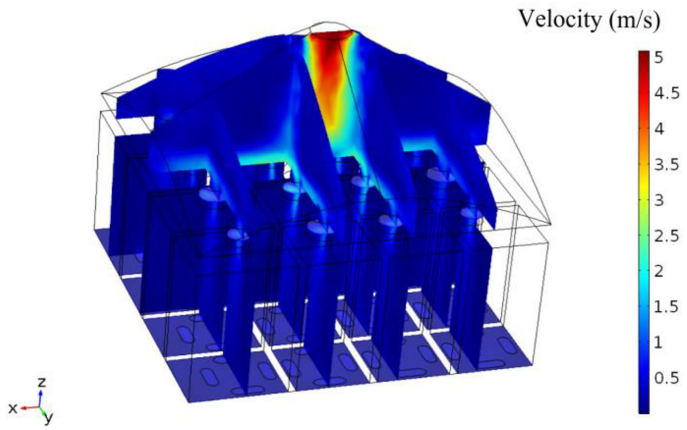

Figure 48: Simulated air flow velocity profile within the non-focused air sampling unit

By using inflow velocities at the inlets (of each compartment) the time required to pump the desired volume of air is calculated. For example, to pump 30 liters of air into the inner four compartments, 12 mins is required whereas for the outer compartments 18 min is necessary. To measure the air flow velocities within the air sampling unit, a PCE-423 air flow sensor is used. The air flow sensor is placed at the exit of each compartment and the flow rate is measured. The measured air flow velocities which are presented in Fig. 49 shows a similar behavior to the simulated air flow profile. From the simulation the air flow velocities within the compartments are in the range from 0.3 – 1.0 m/s, whereas the experimental values fall in the range from 0.2-0.5 m/s. The measured flow rates are higher at the inner four compartments when compared to the outer compartments as predicted from the simulation.

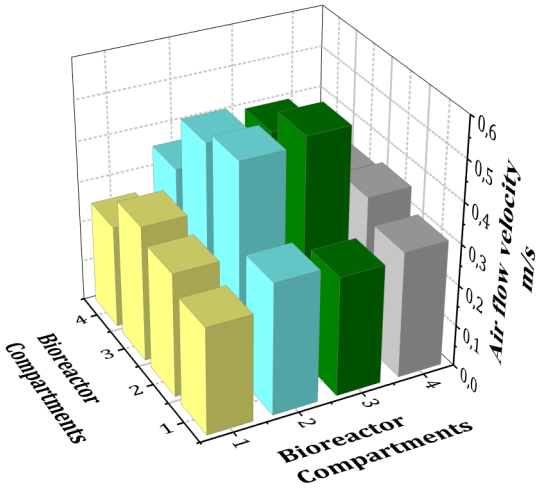

Figure 49: Air flow velocities measured at the end of each compartment inside the 3D printed non-focused air sampling unit.

Air flow measurements are not enough to determine the performance of the air sampling unit. As the target of air sampling unit is to distribute incoming spores uniformly among all the bioreactors enclosed within the compartment, it is necessary to investigate the distribution profile of the mold spores. Uniform distribution of the incoming spores is required for accurate quantification of mold spores.

To measure the spore particles reaching the bioreactors, a polyethersulfone (PES) filter of 0.22 µm pore size is placed within the reaction cavity of the bioreactor (on the top of culture medium). The 0.22 µm PES filters have a diameter of 90 mm and are obtained from Merck Millipore Ltd. These filters are cut into smaller size (7 mm diameter) in order to make them fit inside the reaction cavities. Bioreactors with PES filters placed inside the reaction cavity are shown in Fig. 50. The cartridge is attached to the air sampling unit and is exposed to different spore concentrations. The spores which enter the air sampling unit get distributed and reach the reaction cavity. The

spores entering the bioreactor get stuck within the filter (placed on the top of culture medium). After air sampling the filters are taken out of the reaction cavities and are suspended to count the colony forming units.

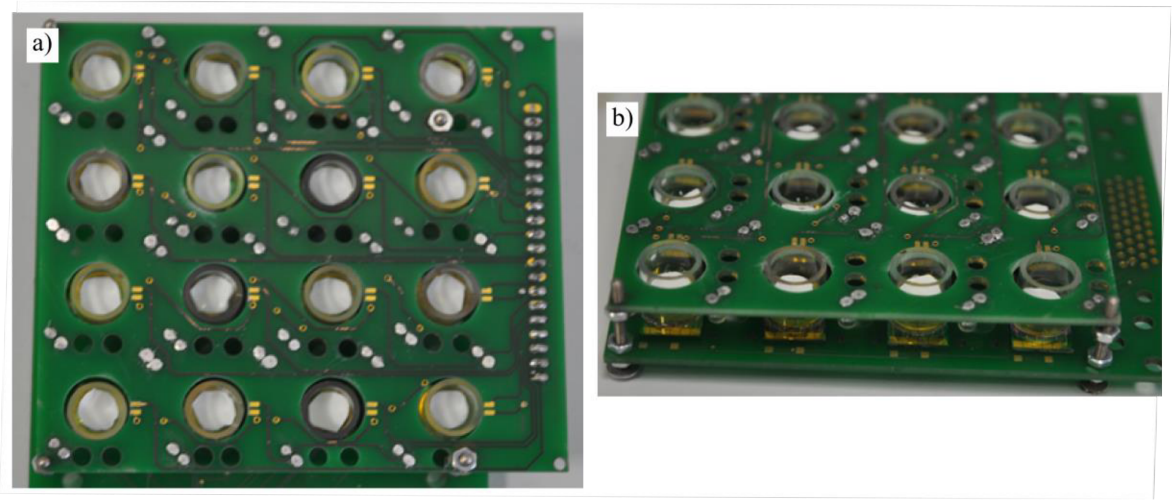

Figure 50: Bioreactor cartridge with PES filters inside each of the reaction cavities, for measuring the spore particles reaching the bioreactor a) top vie b) side view of the cartridge with filters.

To measure the concentration of spores present in each of the PES filter a spore suspension protocol is implemented. First the filter is taken out of the bioreactor using a sterile tweezer and is transferred into a sterile falcon tube consisting of 10 ml sodium chloride and tween solution. This tube is incubated at 35-40 °C for 15 min and is vortexed for 4 min. This solution is diluted with a buffer by a factor of 1:10 or 1:100. 100 µl of each dilution mixture is platted on a PDA agarose and is distributed over the plate using a spatula. The PDA agarose petri dish is incubated in an incubator at 25 °C and the colonies formed are counted after 24 hours. Eq. 21 shows the formula used to calculate the CFU per filter (as only 100 µl is platted from 10 ml sample, Eq. 21 has a multiplication factor of 100). Fig. 51 shows the growth of mold spores in colonies.

$$CFU\ per\ Filter = (\ colonies\ counted) * (dilution\ factor) * 100 \qquad \text{Eq. 21}$$

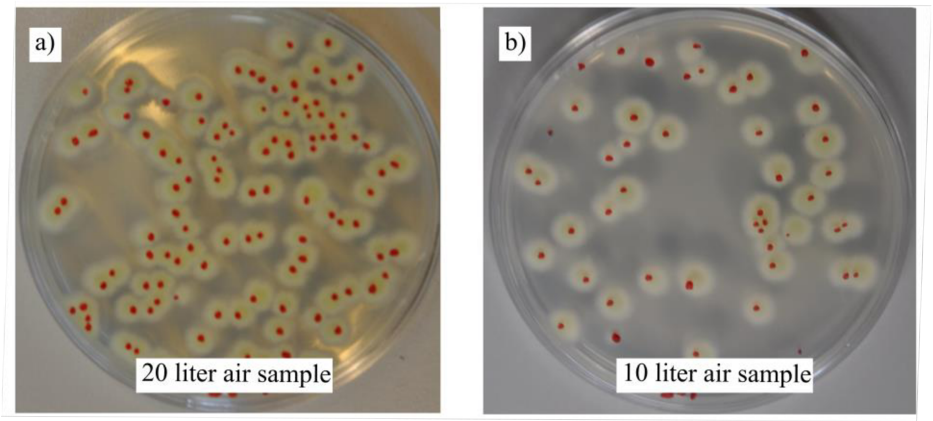

Figure 51: Spores from the filter are suspended and plated on the petri dishes. Mold colonies growing on PDA agarose which are counted in terms of colony forming units a) mold spores in 20 liter air sample b) spores in 10 liter air sample.

Fig. 52 shows the measured spore concentration within a bioreactor cartridge in terms of colony forming units. The results show that the spore distribution within the air sampling unit doesn't follow the air flow profile (see Fig. 49). Even though the air flow profile is uniform, the spores are distributed randomly across all the bioreactors. Experiments were repeated for 4 times and each time different distribution profile of spores is obtained. The measured spore concentration within the bioreactor cartridge shows a factor of 10 difference between the bioreactors.

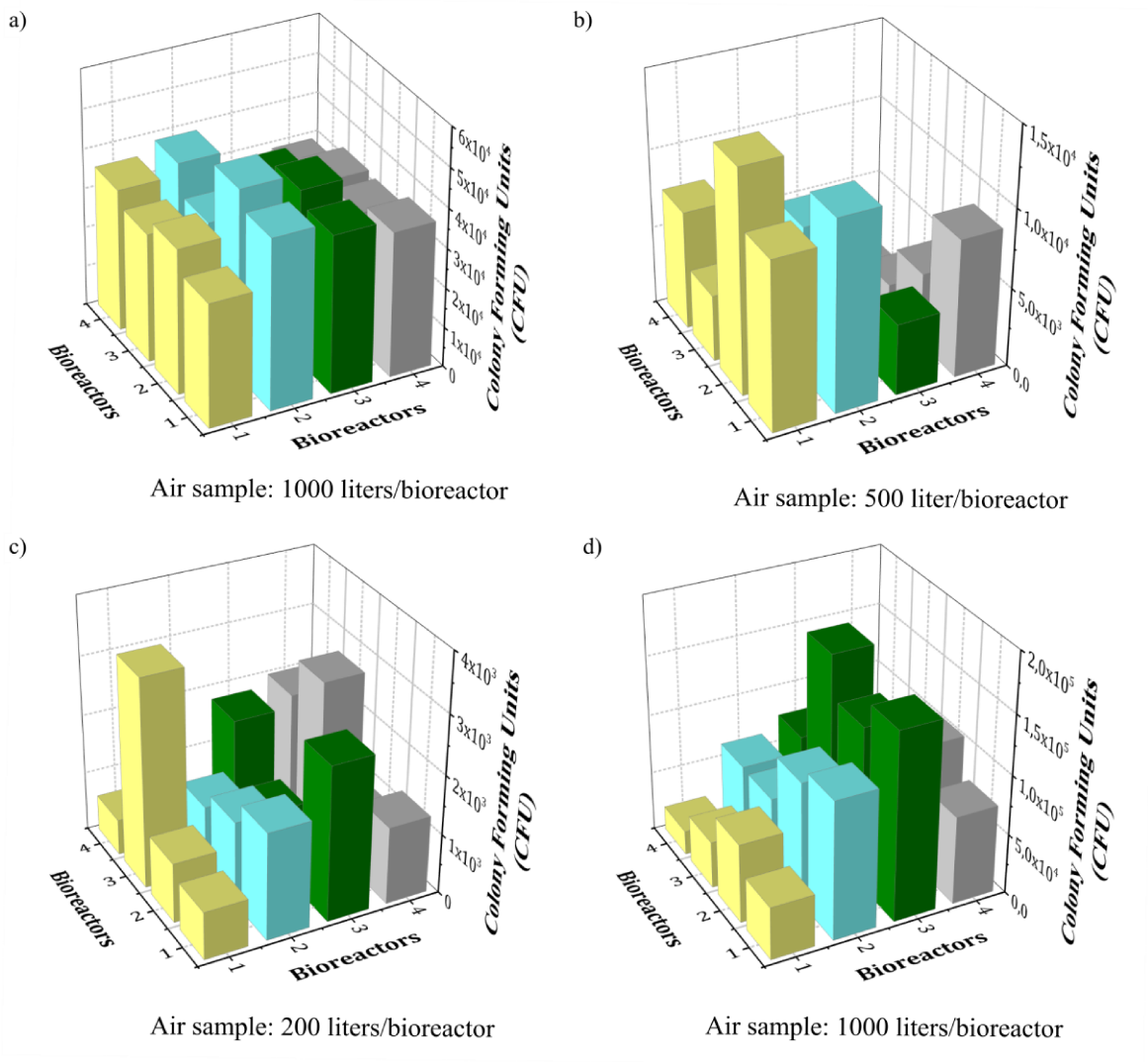

Figure 52: Spore particle distribution measured in terms of colony forming units for different air sample volumes per bioreactor a) 1000 liters b) 500 liters c) 200 liters d) 1000 liters.

To check if this non-uniformity does not occur because of handling errors during filter suspension, the bioreactors are directly exposed to mold spores without filters inside their reaction cavity. The impedance measurements were recorded for a constant time of 24 hours and are represented in Fig. 53. Also in this case, the impedance rate is not uniform, indicating that the spores are not evenly distributed. This non-uniformity is due to the design of non-focused air sampling unit. Within the air sampling unit there is a first chamber which is used for distributing air to all the sixteen compartments. Most of spores are trapped within the first chamber and are not divided into equal amounts.

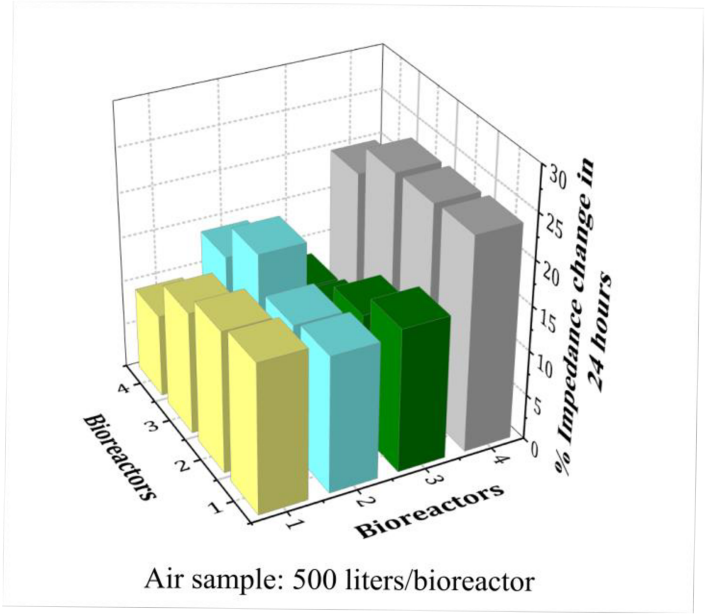

Figure 53: Spore particle distribution measured in terms of percentage impedance change for a time duration of 24 hours.

Another important factor to be considered for the design of air sampling unit is the catching efficiency. Catching efficiency determines the amount of spores captured within the bioreactors. As indicated in Eq. 22, catching efficiency is the ratio of the spores caught inside the bioreactor to the total amount of spores present in the air sample.

$$Catching\ efficiency = \frac{Captured\ spores\ in\ bioreactors}{Total\ amount\ of\ spores} \qquad \text{Eq. 22}$$

The experimental setup for determining the catching efficiency of the air sampling unit is as shown in Fig. 54. Eight week old mold species (which contain spores) are placed in a box. For generating spores within the air sample, a ventilator is used to blow air over these spore samples. Desired volume of air is then pumped into the air sampling unit consisting of bioreactor cartridge. For measuring the captured spores, filters are placed inside all the bioreactors. As it is not possible to determine the absolute value of spores which are pumped into the air sampling unit, a filter is placed at the exit or outlet of the sampling unit such that the entire air exiting the system passes through the outlet filter. After collecting the spores on the filters, they are counted by making suspensions. The catching efficiencies for the non-focused air sampling unit obtained from four measurements is in the range of 42-55 %, as indicated in Table 3.

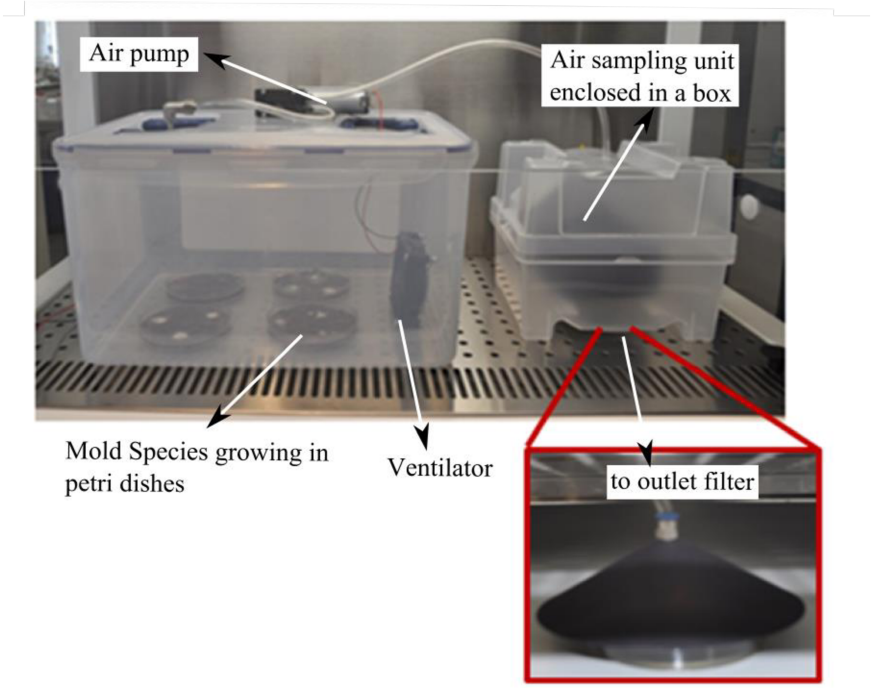

Figure 54: Setup implemented to determine the catching efficiency of the air sampling unit.

Table 3. Catching efficiencies obtained from the air sampling unit

	Test 1	**Test 2**	**Test 3**	**Test 4**
Spores captured in 16 bioreactors (CFU)	576 K	95 K	22 K	1365 K
Spores captured at outlet filter (CFU)	460 K	106 K	31 K	1460 K
Catching efficiency (%)	55	47	42	48

Focused air sampling unit

To improve the spore distribution profile and also to have a higher catching efficiency a second version of air sampling unit has been designed. In this version, the air is focused onto each bioreactor using a funnel shaped outlet. The designed air sampling unit has four outlets which can be scaled up depending on the application. Each funnel shaped outlet is placed at a distance of 3 mm from the bioreactors reaction cavity. This allows the entire air coming out from the outlet to get focused onto the culture medium. The outlet of the air pump is connected to the air sampling unit via multiplexed connector tubes as shown in Fig. 55a. The focused air sampling unit is glued onto the bioreactor cartridge using double sided glue (see Fig. 55b). Air flow measurements are done by placing a PCE-423 air flow sensor at the outlets of the sampling unit. The measurement result shows a uniform flow rate distribution among all the four outlets and is between 10 - 12 m/s.

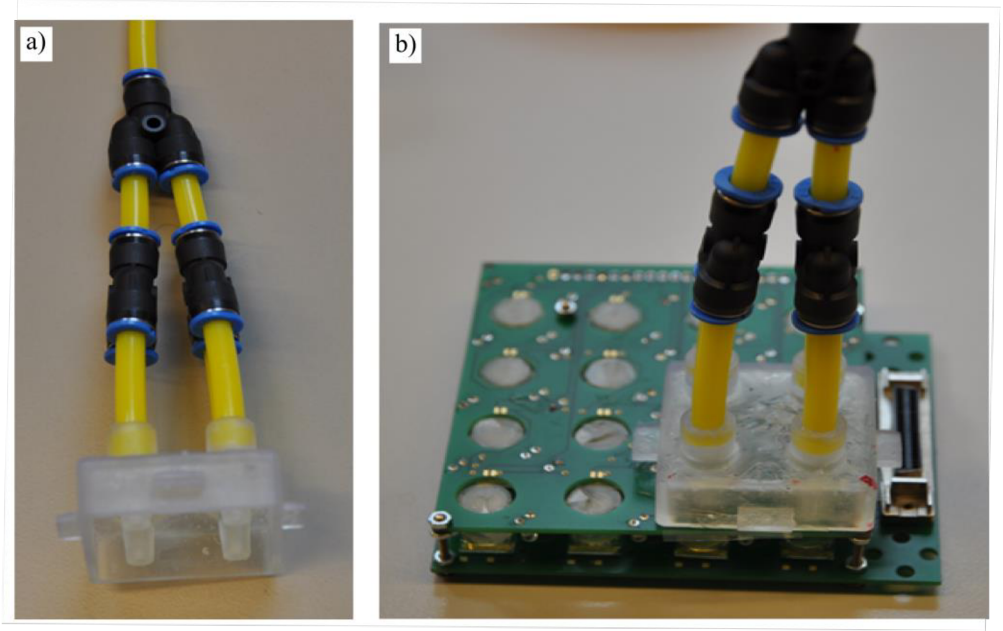

Figure 55: a) Focused air sampling unit with four individual outlets b) focused version of air sampling unit glued on the bioreactor cartridge.

For measuring spore particle distribution, 0.22 µm pore size PES filters are placed inside the reaction cavities of the bioreactor. After air sampling the spores are suspended and they are quantified in terms of colony forming units as described in above section. Fig. 56 represents the results from four different tests (with different spore concentration in the air sample). Results show a better spore distribution profile when compared to the air sampling unit without focused outlets. The difference in the amount of spores between the bioreactors is less than a factor of 2.

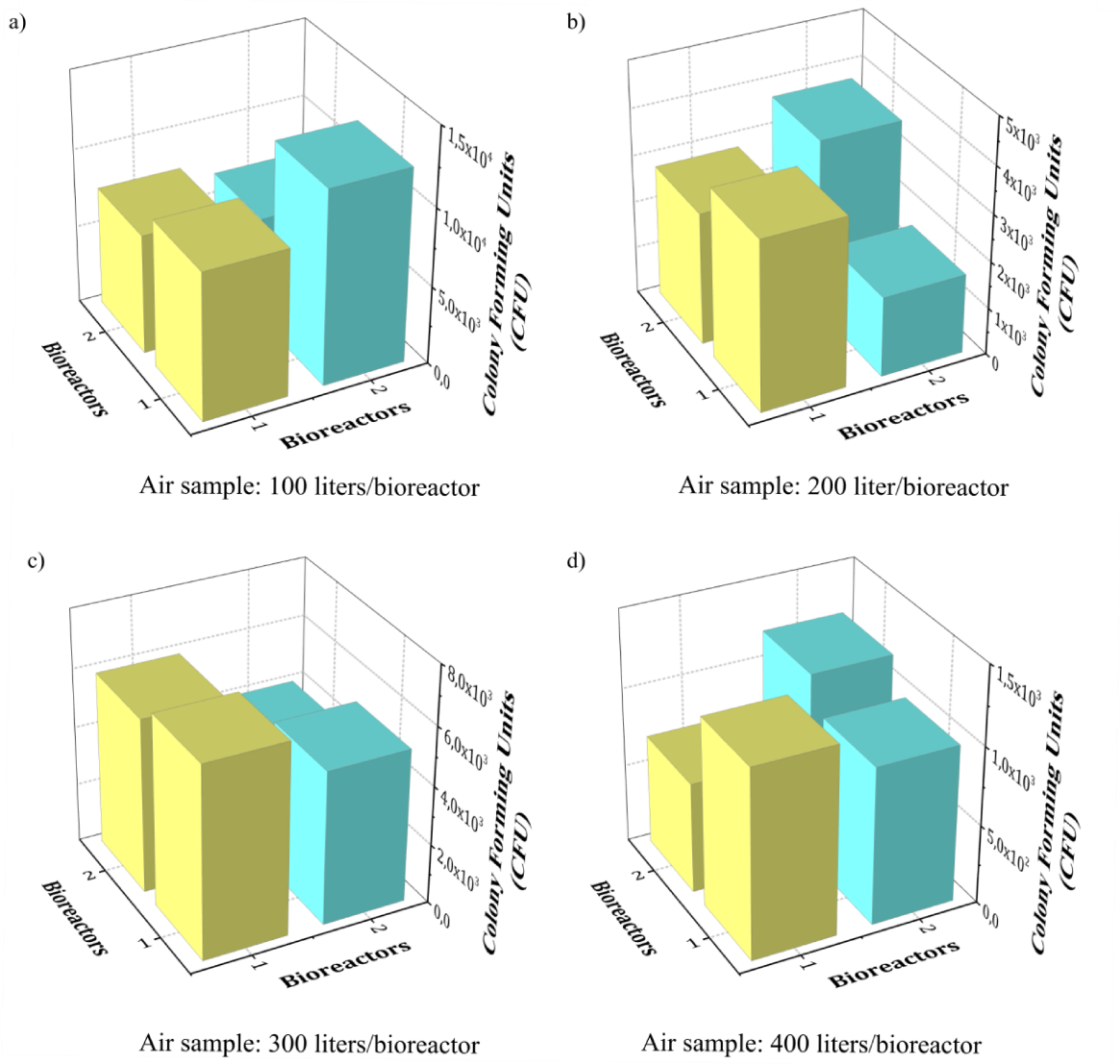

Figure 56: Spore particle distribution measured in terms of colony forming units for different air sample volumes a) 100 liters/bioreactor b) 200 liters/bioreactor c) 300 liters/bioreactor d) 400 liters/bioreactor.

Spore particle distribution is also measured in terms of impedance change for constant time duration of 24 hours. The bioreactor loaded with culture medium is exposed to different spore concentration using the focused version air sampling unit and the impedance growth is measured. The percentage impedance change profile shown in Fig. 57 shows a similar behavior where it also has a difference factor of less than 2. The results indicate that second version of the air sampling unit with focused outlets is efficient in distributing the spores uniformly when compared to the first version of air sampling unit.

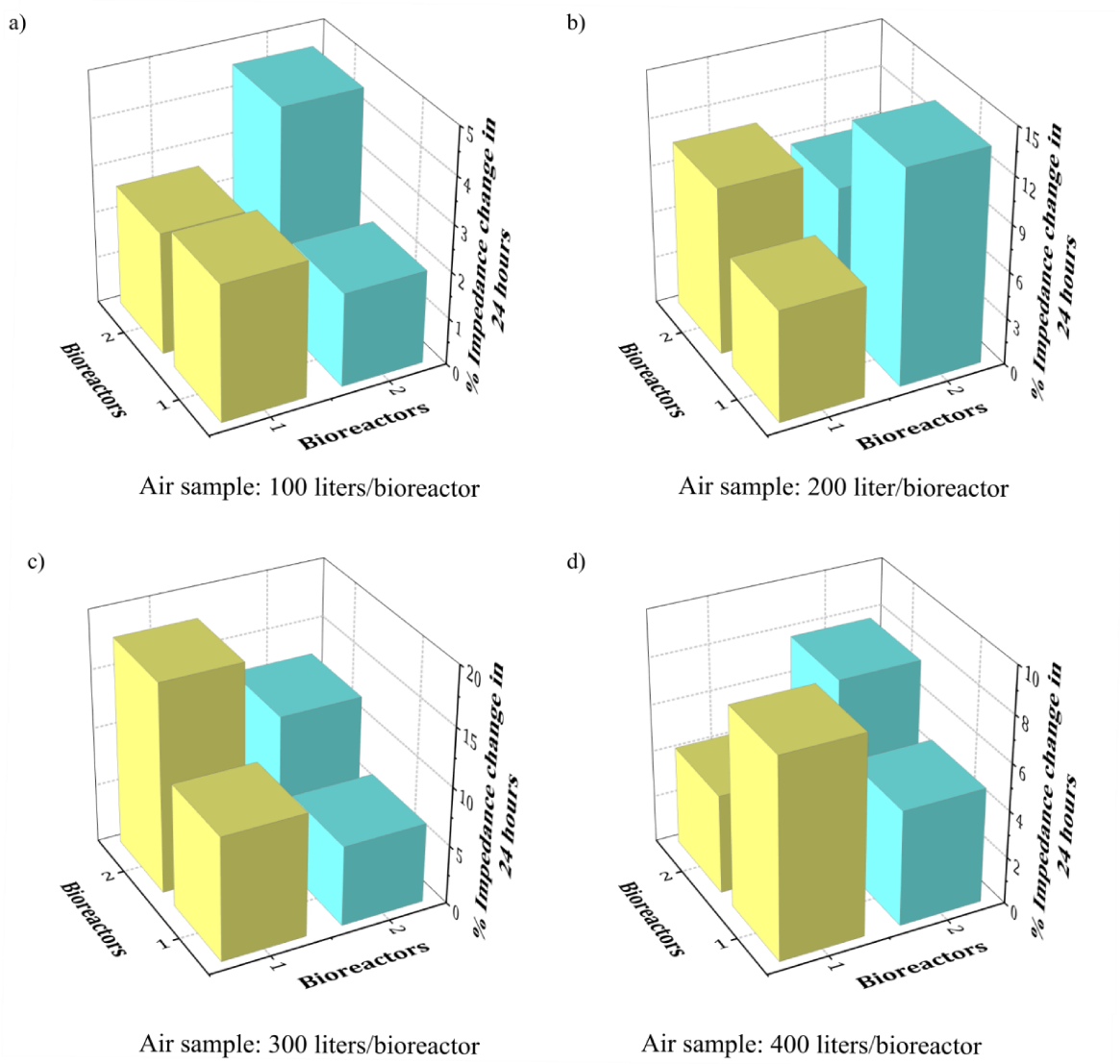

Figure 57: Percentage impedance change measured for a constant time duration of 24 hours for different air sample volumes a) 100 liters/bioreactor b) 200 liters/bioreactor c) 300 liters/bioreactor d) 400 liters/bioreactor.

The experimental setup to determine the catching efficiency of the focused air sampling unit is shown in Fig. 58. The sampling unit is placed in a box, and the spores coming out are collected on an outlet filter. Catching efficiencies are calculated using Eq. 22 and the results are presented in Table 4. The catching efficiency of the focused air sampling unit is in the range from 62-73 %, which is 20 % higher than the catching efficiency of the first version air sampling unit. Hence if a focused air sampling unit is used then the possibility for the spores to get captured and detected using the bioreactor is higher compared to the first version. Using the focused air sampling unit the measured CFU's per bioreactor have differed by a factor 2. This difference might

have occurred due to the dilution plating method employed for counting spores. As extraction of spores from filter is not very reproducible it will contribute to some uncertainty in plating.

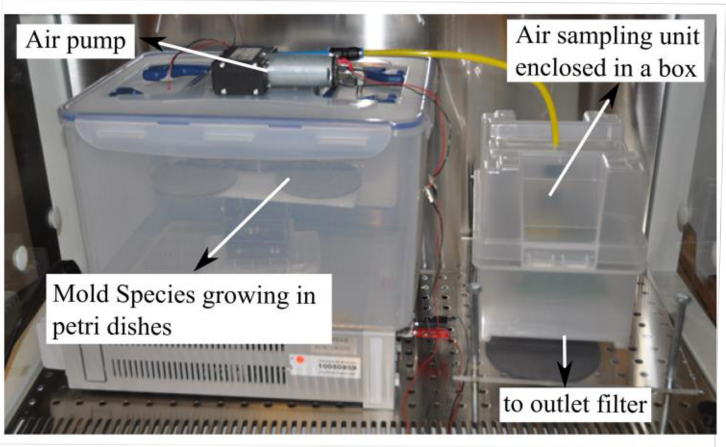

Figure 58: Setup used to determine the catching efficiency of the focused air sampling unit.

Table 4. Catching efficiencies obtained from the focused air sampling unit

	Test 1	Test 2	Test 3	Test 4
Spores captured in 4 bioreactors (CFU)	36 K	11 K	21 K	4 K
Spores captured at outlet filter (CFU)	22 K	7 K	8 K	2 K
Catching efficiency (%)	62	62	72	67

5.6.2 Mold detection and quantification in laboratory

Focused air sampling unit is used for detection and quantification of mold spores. To determine the absolute amount of spores, filters are placed within the bioreactors. By using focused air sampling unit, mold spores can be distributed simultaneously to four bioreactors at the same time. Among these four bioreactors, two of them have filters inside the reaction cavity and the other two are without filters. As the spore distribution within the four bioreactor cavities is less than a factor of 2 (as discussed in section 5.6.1), the impedance measured can be correlated to the amount of spores captured by the filters. Fig. 59a shows four bioreactors which are active. Two of the bioreactors have 0.22 µm PES filters inside them. Focused air sampling unit with four outlets is glued using a double side tape onto the bioreactor cartridge as shown in Fig. 59b. The experimental setup for detecting spores from air sample is shown in Fig. 58. The amount of air that can be sampled into the bioreactor depends on several factors like the volume of the culture medium inside the reaction cavities, tempera-

ture and the humidity of the air. For the experiments performed within this work, a 200 µl of culture medium is used. For this volume of culture medium, a maximum of 250 liters of air can be pumped (using the focused sampler) into the reaction cavities at a temperature of 23 (± 1) °C and with relative humidity of 50-55 %. Pumping more than 250 liters of air will start to make the culture medium dry, which could inhibit the growth of mold so it is not recommended. Depending on the application, the air sampling volume can be scaled up or down. For example if the sampling is done at a relative humidity of 80-85 % then 500 liters of air sampling volume can be used. If more volume of air is desired then higher amount of culture medium is loaded into the reaction cavities.

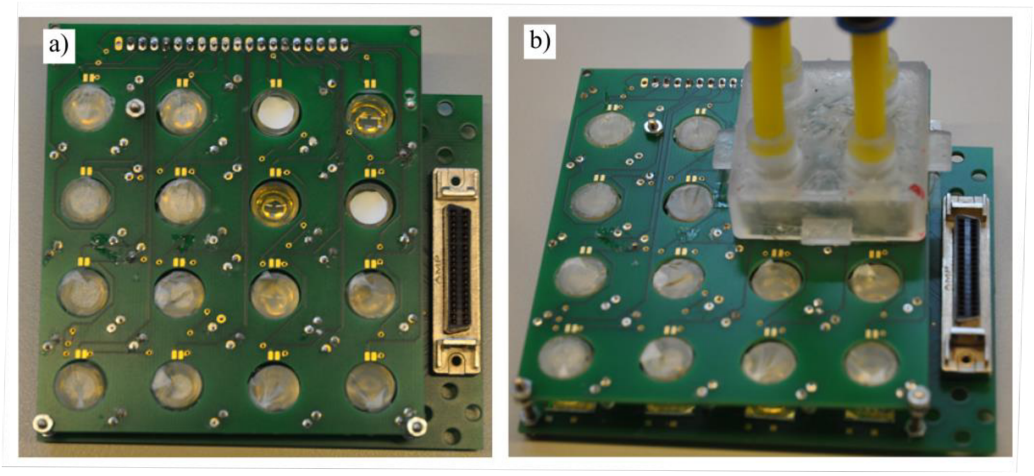

Figure 59: a) Bioreactor cartridge with filters placed in two of the bioreactors for determining spore concentrations and two without filters for measuring impedance b) Air sampling unit glued onto the bioreactor cartridge.

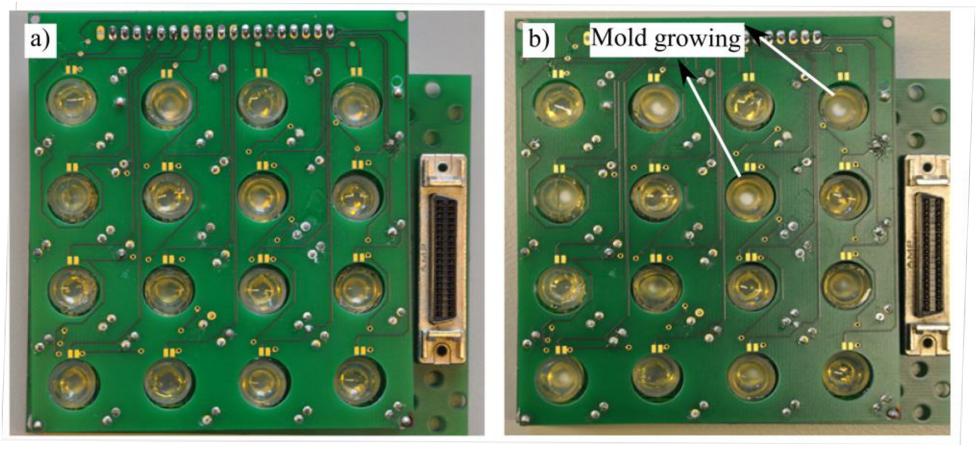

Figure 60: a) 12 hours after air sampling: mold spores starts to produce visible hyphae b) 24 hours after air sampling: mold growing in bioreactors. As the air sampling unit focuses the mold spores into a spot, the mold growth is concentrated at the center of the reaction cavity and later spreads throughout the surface.

Four different experiments have been performed with 40, 80, 400, 800 liters of sampling volumes. As this incoming air is divided among four bioreactors, the amount of air per bioreactor will be 10, 20, 100, 200 liters respectively. The growth of mold after air sampling is shown in Fig 60. From the pictures it is clear that by using focused air sampling unit, most of the spores are focused at the center, which can be observed in Fig. 60b where the mold growth starts from the center and then gradually spreads.

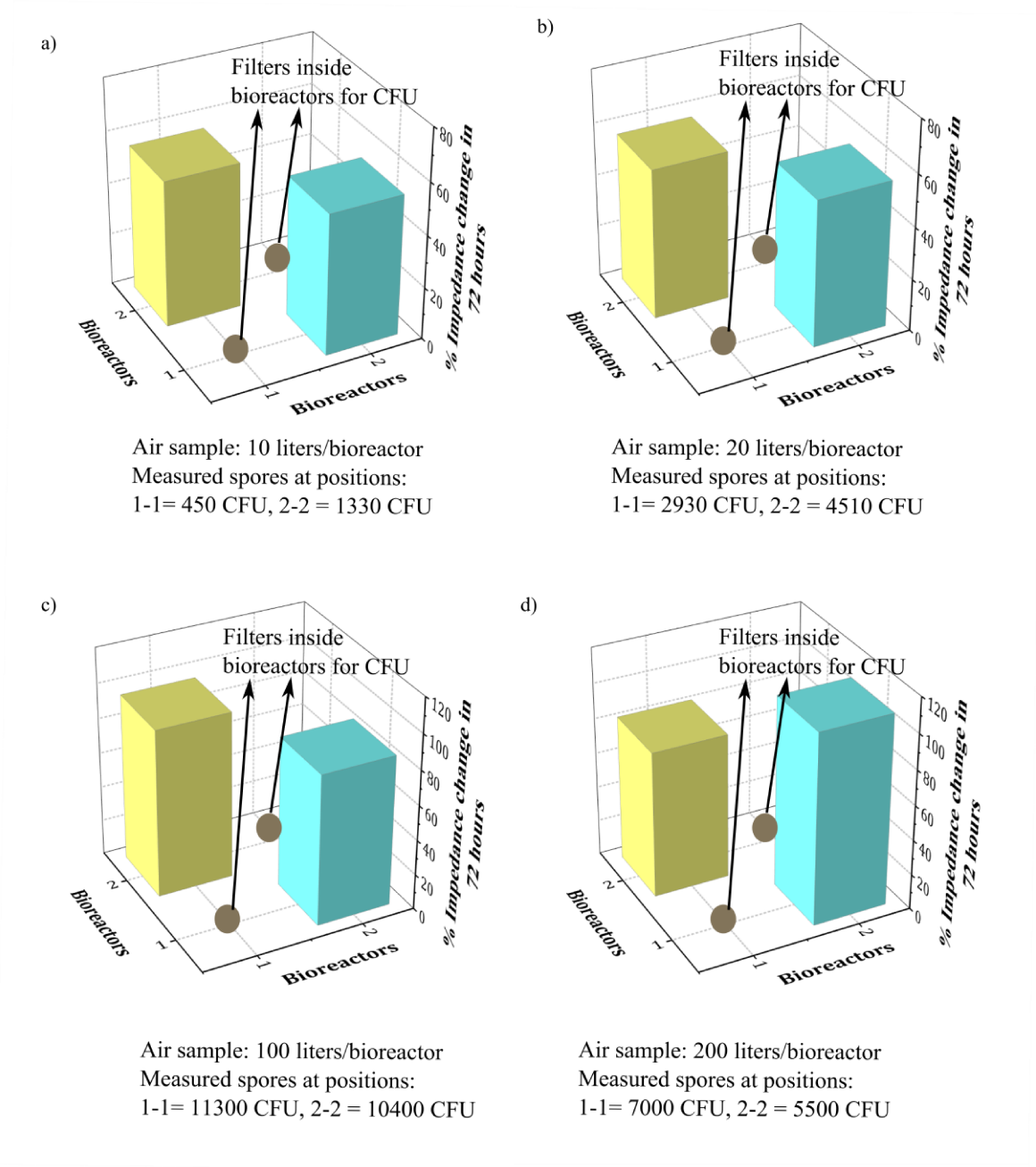

Figure 61: Impedance change measured for a constant detection time of 72 hours with the respective the spore concentrations determined using the filters for different air sampling volumes a) 10 liters b) 20 liters c) 100 liters d) 200 liters.

The amount of spores captured within the filter is determined in terms of colony forming units and the impedance change is measured at 10 kHz. The measurement results obtained are indicated in Fig. 61. As the rate of impedance change depends on the initial spore concentrations, the percentage impedance change measured for a constant time period varies based on the initial spore concentration. Results indicated in Fig. 61 show that percentage of impedance change is higher with higher amount of spores. If the amount of spores is in the range from 400 -500 CFU then there is 50 - 55 % impedance change in 72 hours (Fig. 61a). For the initial spore concentration of 2930 - 7000 CFU, there is 58 - 61 % impedance change within 72 hours (Fig 61b and 61d). The impedance change for 72 hours will be 98 % if the initial spore concentration is in the range of 10400 - 11300 CFU.

Measuring the spore concentrations at the outlet filter provides a good indicator to the amount of spores captured within the bioreactors. Considering a catching efficiency of 62 %, by knowing the amount of spores it is possible to determine the amount of spores captured in all the bioreactors. For example consider test 1 (see Fig. 61a) where the amount of spores captured at the outlet filter are 800 CFU/40 liters. For a catching efficiency of 62 %, the total amount of spores in the air sample can be calculated, which is 2105/40 liters. As 62 % of total spores are being captured in the bioreactors, the calculated amount of spores per reactor will be in the range from 326 CFU/ bioreactor per 10 liters. Table 5 shows the calculated CFU using the spores measured at the outlet filter and their corresponding percentage impedance change in 24 and 72 hours. So knowing the amount of spores at the outlet is an indirect indicator to the amount of captured spores.

Table 5. Calculated CFU's per bioreactor using the measured spore concentrations at the outlet filter

Measured spores at outlet filter (CFU)	Calculated CFU/ bioreactor	Percentage impedance change in 24 hours (for 62 % catching efficiency)	Percentage impedance change in 72 hours (for 62 % catching efficiency)
70-150	29-62	+ 1-2 %	+ 18-37 %
800-1200	326-490	+ 3-4 %	+ 46-54 %
7000-13600	2855-5540	+ 10-18 %	+ 61-95 %

5.7 Detection of mold spores in archives

The sensor system has been implemented in an archive for measuring the spore concentrations present within the indoor air. Experiments have been performed with the biological project partners BMA labor GmbH at an archive located in Bochum, Germany. Fig. 62a shows the picture of the contaminated archive where the measurements were carried out. Fig. 62d shows the spore concentrations measured by BMA Labor GmbH within the contaminated and uncontaminated archives. Spore concentrations are measured in two scenarios. In the first scenario, measurements are done without disturbing the indoor air. In the second case, the indoor air within the archive is disturbed using a ventilator. This will allow the spores settled within the archive to move and thus increasing the spore concentration. Spore concentrations are measured every month (1 year) by BMA labor GmbH and are indicated in Fig. 62d [115].

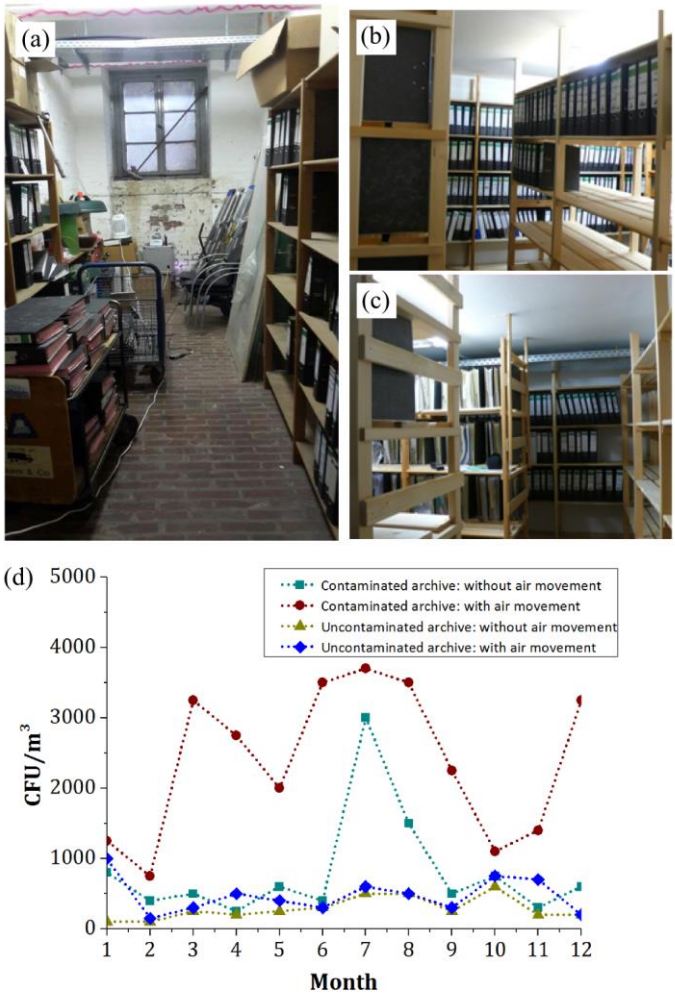

Figure 62: a), b), c) pictures of contaminated and uncontaminated archives (Bochum city, Germany) d) Monthly spore concentrations measured within the archives by our project partners (data obtained from BMA Labor GmbH).

From the measurement results it is clear that, in an uncontaminated archive the measured spore concentrations remain the same in both scenarios, i.e., when measured with air movement or when measured without air movement. The spore concentration of an uncontaminated archive is in the range of 100 – 1000 CFU/m^3. In the case of contaminated archives, the spore concentration measured without disturbing the indoor air is in between 250 – 800 CFU/m^3. If the indoor air within the contaminated archive is disturbed then the measured spore concentration is in the range of 1000 – 3700 CFU/m^3. This indicates that there is an increase in the spore concentrations by a factor of 4 within a contaminated archive (see Fig 62d). This difference between the measured spore concentrations (with air movement and without air movement) is used as trigger event for monitoring archive environment.

The designed sensor system is placed inside the contaminated archive at two different locations as shown in Fig. 63. In both locations, 1000 liters of air volume is pumped into the air sampling unit, resulting in 250 liters/bioreactor. Two sets of measurements were performed at each location one without disturbing and the other with disturbing the indoor air. For determining the amount of spores captured within the bioreactors, two bioreactors are covered with filters and two of them are without filter. As a reference, 250 liters of air is collected into petri dish (consisting of PDA agarose) for counting the spores in terms of colony forming units.

Figure 63: Different locations inside the contaminated archive where spore concentrations are measured.

Results obtained from the sensor system are represented in Fig. 64. Percentage impedance change measured for a constant duration of 72 hours is shown in Fig. 64a and the corresponding CFU's measured is represented in Fig. 64b. The measured spores without air movement using the filters are in the range from 150-370 CFU and the corresponding percentage impedance change within 72 hours is 9 – 26 %. For reference, the spore concentration is also determined using the traditional culturing technique and is 368 CFU (indicated as a red dotted line in Fig. 64b). When the air is disturbed in the archive and the measurement is repeated at the same position, the detected spores are in the range of 1060-1210 CFU, which produces 49 - 55 % impedance change in 72 hours. The amount of spores determined using reference measurement is 772 CFU. As the concentration of measured spores at same position are different when measured with and without disturbing the air the archive is contaminated. Same results were obtained from the reference measurements using cultivation technique. This shows that the sensor system provides reliable results and is in comparison to the standard cultivation technique.

Measurements were repeated at a different position within the same contaminated archive and similar results were obtained. At position 2, the measured spore concentration without disturbing the air is in the range of 260 CFU. This produces an impedance change of 35 % within 72 hours. Whereas, if the air is disturbed then the measured spores are in the range of 1080 CFU and it produces an impedance change of 55 % in 72 hours. The reference measurement also indicates an increase in the spore concentration from 154 CFU to 910 CFU, when measured without and with disturbing air, respectively.

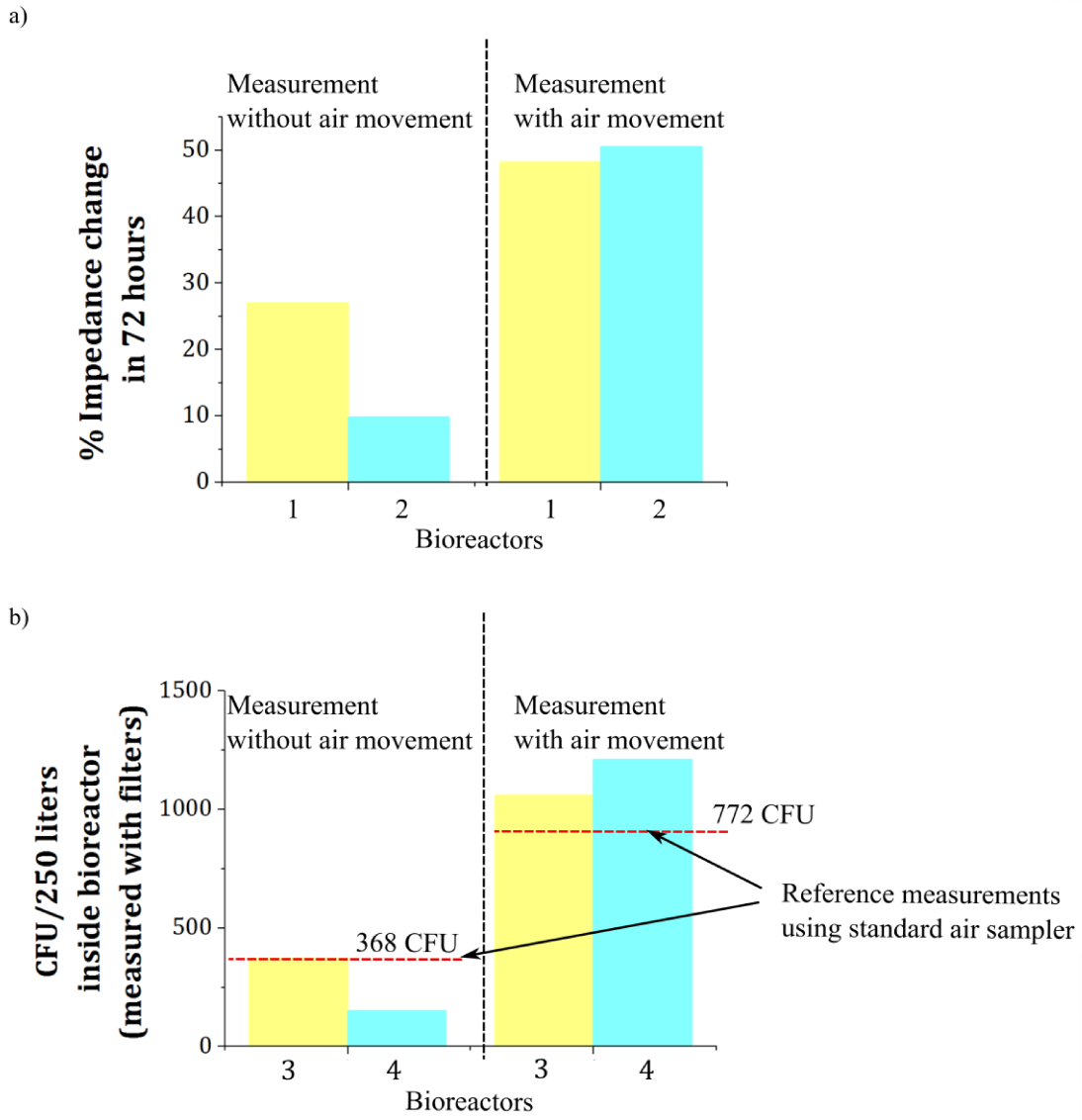

Figure 64: Spore concentrations measured in a contaminated archive a) impedance change measured using the bioreactors, air sampling done with and without disturbing the indoor air b) corresponding colony forming units measured using the filters, placed inside the bioreactors. Red dotted line indicates the reference measurement obtained from standard air sampler.

The impedance growth curves obtained from the sensor is plotted in Fig. 65. From the measured growth curves it is clear that, if there is no air movement then there are fewer spores inside the bioreactor thus producing low impedance change. Fig. 65 shows that with air movement there are 772 CFU measured and its impedance change is higher compared to the 368 CFU measured without air movement.

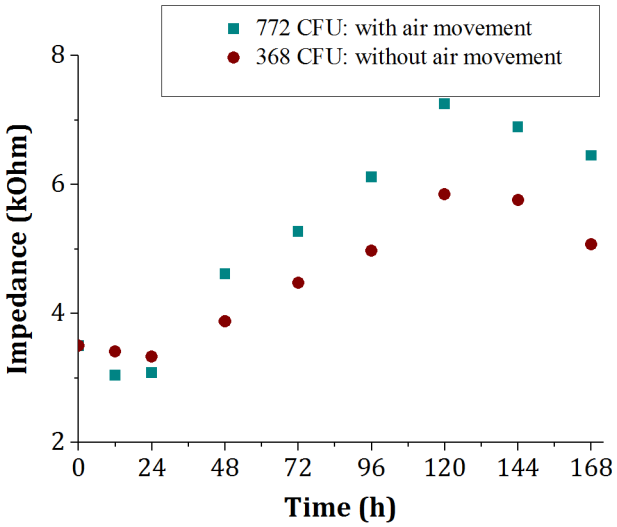

Figure 65: Impedance growth curves measured inside the contaminated archive with air movement and without air movement.

More measurements have been done inside the contaminated archives to further validate the sensor system. Two tests were done on simultaneous days and for each test one complete cartridge comprising of 16 bioreactors has been used. For each test, out of 16 bioreactors, 8 were covered with filters to measure the amount of spores in terms of CFU and the other 8 were without filters with which the impedance measurements are recorded. A standard culturing technique is used using traditional sampler (MBASS30) for obtaining reference values. Results from the measurements are indicated in Table 6 and 7.

Table 6: Test 1 mold detection using the bioreactors inside the contaminated archives using the sensor system for 250 liters of air sample (day 1)

Bioreactors (without filters)	+ % Impedance change in 72 hours	Bioreactor (with filters inside)	CFU/bioreactor
1	44	9	940
2	36	10	1400
3	29	11	380
4	48	12	640
5	49	13	1540
6	38	14	707
7	38	15	500
8	42	16	300

Reference CFU/250 liters obtained from standard culturing technique: 575 CFU - 816 CFU

Table 7: Test 2 mold detection using the bioreactors inside the contaminated archives using the sensor system for 250 liters of air sample (day 2)

Bioreactors (without filters)	+ % Impedance change in 72 hours	Bioreactor (with filters inside)	CFU/bioreactor
1	32	9	330
2	28	10	950
3	35	11	740
4	30	12	120
5	32	13	470
6	30	14	250
7	34	15	350
8	42	16	700

Reference CFU/250 liters obtained from standard culturing technique: 235 CFU - 565 CFU

Results indicated that the sensor system is able to determine the spore concentrations inside the contaminated archives. Test results on day 1 (Table 6) show, the reference value (per CFU/250 liters obtained from standard culturing technique) are in the range from 575 – 816 CFU. By using the sensor system, the measured spores with filters inside the bioreactors is in the range from 300 – 1540 CFU and the corresponding percentage impedance change within 72 hours is 29 – 49 %.

Results on day 2 (Table 7) of the measurement also show that there is contamination within the archives. From the sensor system, the measured spores are in the range from 120 – 950 CFU and the corresponding percentage impedance change within 72 hours is in the range from 28 – 42 %. The reference values on day 2 are 235 – 565 CFU. These measurements prove that the sensor system is reliable and has been successfully implemented to determine the contamination within archive.

6 Auto-fluorescence based mold spore detection

In addition to the designed mold sensor system, which is based on the detection of mold spore concentrations based on their growth, a second sensor system has been designed based on the optical properties of the mold spores. This optical sensor system has been fully automated (from sampling to detection) to detect and differentiate the mold spores [116–118]. In this sensor system, the air sample is collected onto an adhesive tape using an air pump. After sample collection, the tape is moved under the microscope objective. The optical images of the spores are taken with white light and analyzed using an image processing software to identify and determine the amount spores. This sensor system has the advantage of rapid spore detection, as it does not require the spores to germinate or grow.

It is known that biological species show auto-fluorescence behavior. Also spores exhibit auto-fluorescence. When the spores are excited with a light source of specific wavelength, they emit light at different wavelengths. This auto-fluorescence property is an interesting contribution to the optical sensor system that has been designed in other project [117]. Investigations on the auto-fluorescence properties of archive mold spores are described in the following sections.

6.1 Introduction

Auto-fluorescence is the process of emission of light by the biological molecules when they are excited by a specific wavelength of light. Auto-fluorescence is also called as the intrinsic fluorescence because it involves natural light emission without addition of external markers (the light emission is due to the intrinsic molecules present within the biological organism). The biomolecules that have auto-fluorescence properties are called fluorophores.

Typical fluorophores present in the biological organisms that are responsible for light emission are, Tryptophane and Tyrosine amino acids, some coenzymes like Nicotinamide adenine dinucleotide (NADH), Nicotinamide Adenine Dinucleotide Phosphate (NADPH), Flavins like riboflavin, Flavin adenine dinucleotide (FAD), Mononucleotide Flavin (FMN), etc [119,120]. The presence of these molecules within the biological

organism or an airborne spore will result in auto-fluorescence. The excitation and emission spectrum for different biological molecules is presented in [119,120]. Depending on the type of biomolecule present in the organism, the excitation wavelength can be varied from 200 - 600 nm and the emission intensity (from 280 – 700 nm) is measured either to detect or to quantify the bio-organism.

In this thesis, auto-fluorescence properties of mold species responsible for archive contamination have been investigated. The spores produced by the mold species could have different shapes (ellipsoid, circular, etc.) and sizes. Typically airborne mold spores are in the range of 2- 20 µm [121–123]. Amino acids (Tryptophan and Tyrosine) and enzymes (NADH, NADPH, Flavin's) are the major Fluorophores that are present within the airborne mold spores. Because of these fluorophores mold spores exhibit auto-fluorescence property. In general, two different sets of excitation wavelengths can be used for the detection of mold spores i.e., 260 - 280 nm and 340 - 380 nm. For exiting amino acids the wavelength of 260 - 280 nm is applied, whereas the emission fluorescence of enzymes is investigated by applying a light source with the wavelength of 340 - 380 nm [119,124,125]. Based on these excitation wavelengths, there exists a sensor system for detection of pollens and spores [34,126].

The auto-fluorescence from the airborne mold spores is mostly due to the presence of Flavin's, Ergosterol and Chitins [119]. Ergosterol is a specific sterol compound found only in cell membranes of the mold. As it is present in very small amounts the fluorescence emission due to Ergosterol is very weak. Chitin is the most commonly found cell wall component in molds. When excited with a wavelength of 370 nm it emits light at 450 nm wavelength. An excitation wavelength of 260 - 280 nm can be used to activate proteins like Tyrosine, Tryptophan and Phenylalanine (mostly amino acids) present within mold spores [127–130]. A major disadvantage of using short UV range from 260 – 280 nm is that the organic pollutants present in the air will also absorb this wavelength and emit light in visible spectrum. Thus exciting the sample at 260 – 280 nm makes it hard to differentiate the mold spores from dust particles. Hence in this work, emission spectrum of enzymes has been used to detect mold spores. Thus a light source with an excitation wavelength of 365 nm is employed. At this wavelength only Flavins, NADH, NADPH enzymes will absorb the light and re-emits the light at a wavelength of 400 - 560 nm [119]. When excited with 365 nm the dust particles from the environment will not emit light. Thus with 365 nm source, it is possible to discriminate the archive mold spores with non-biological dust.

6.2 Spore detection method

This section describes the construction of an auto-fluorescence setup for the detection of mold spores. The measurement setup comprises of a UV LED light source, an Excitation filter, a beam splitter, an Emission filter, biconvex lenses, optical lens tubes

and a CMOS image camera. The schematic diagram showing the construction of the auto-fluorescence setup is shown in Fig. 66a. The CMOS image camera can be replaced with a spectrometer for determining the wavelength peaks emitted by the mold spores of different species.

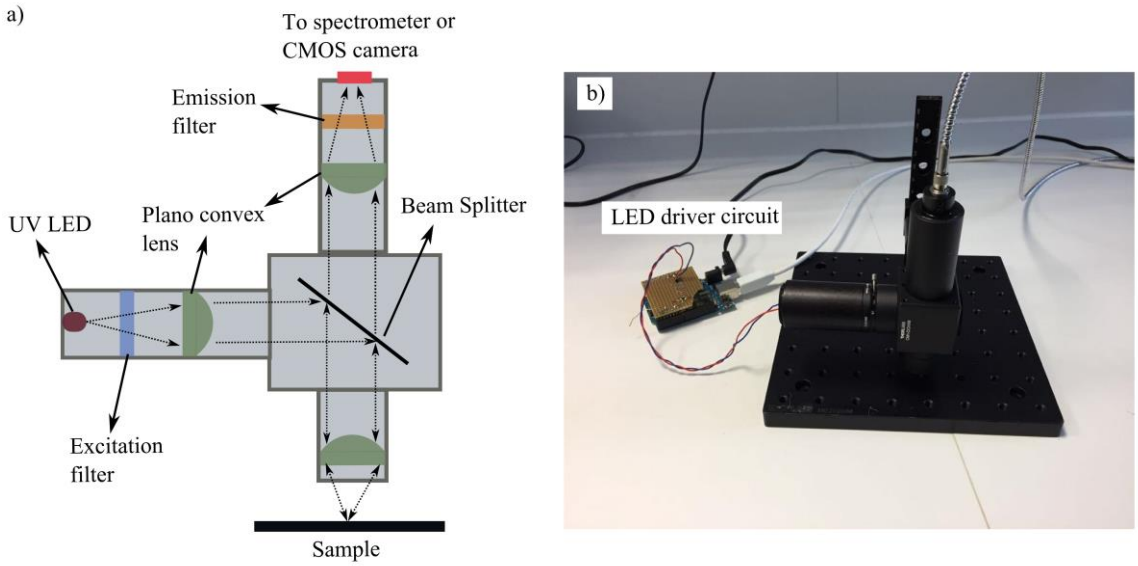

Figure 66: a) Schematic view of the optical setup for measuring auto-fluorescence properties of the spores b) picture of the auto-fluorescence setup.

An UV LED (LZ1-00UV00, from LED Engin) which has an emission peak of 365 nm wavelength and is mounted on a metal-core printed circuit board is used as an excitation source. Though the emission peak of this LED is located around 365 nm, it also emits light in visible region. To suppress other wavelength emitted by the UV LED an excitation filter is coupled to the source. In this work, a band pass filter (AHF F39-370 from AHF analysentechnik AG) is used as an excitation filter. This filter has 90-95 % transmission in the wavelengths from 350-390 nm and has 0 % transmission in the visible region. Using excitation filter ensures that the excitation wavelength of the light is as close as possible to the fluorophore molecules absorption profile. The light from the source is then collimated using plano-convex lens (LA1951-A, Thorlabs GmbH). A beam splitter (DMLP425R, Thorlabs GmbH) is used to reflect this UV light onto the sample. The beam splitter is selected such that it has 80 – 90 % reflectance in the UV region (at 365 nm) and has 80 - 90 % transmission in the visible region. The reflected light from the beam splitter is focused onto the sample using a plano-convex lens. Once the sample is exited with the 365 nm UV light, the fluorophores present in the mold spores absorb the UV light and emit the visible light. This allows in detection of spores using a CMOS camera or by using a spectrometer. The auto-fluorescence setup to be integrated in the optical sensor system is shown in Fig. 66b.

6.3 Results and discussion

Optical images obtained from the auto-fluorescence system are presented in Fig. 67. Fig. 67a shows the white light image of the air sample. In this picture one can observe the spore particles and also dust. The presence of dust particles could make it hard for the image processing tools to detect the spores. Fig. 67b shows the auto-fluorescence picture of the same sample. As the dust particles do not contain fluorophores they do not emit light. The spores observed in this picture are from *Eurotium Amstelodami* species and have an emission peak at 546 nm. At this emission wavelength they are green in color. Fig. 67c shows the Eurotium species, when excited with 365 nm UV light.

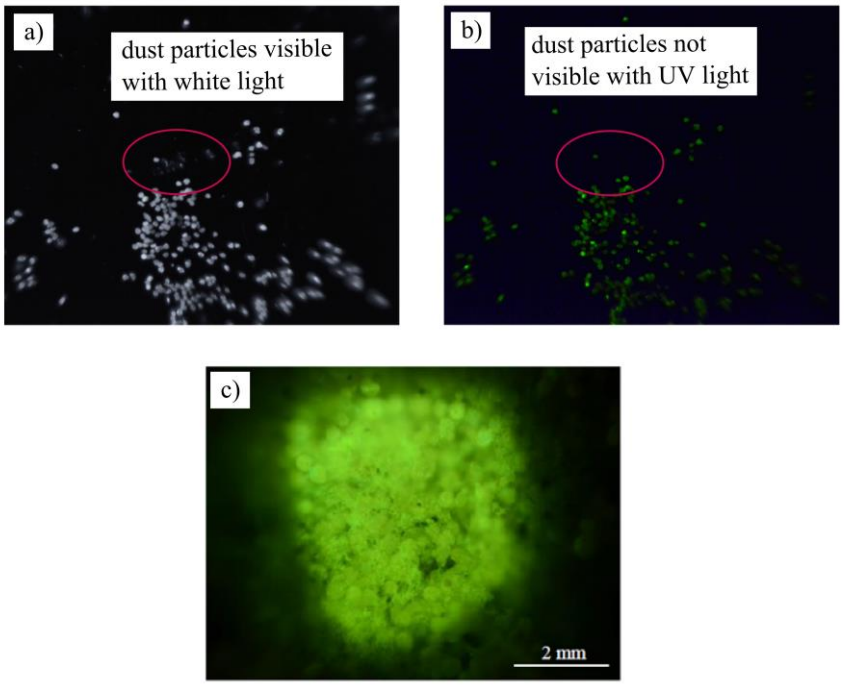

Figure 67: Microscopic pictures of aerosol sample a) illumination under white light shows both dust and *Eurotium* spores b) under UV excitation only *Eurotium* spores are visible and they have an emission peak at 540 nm c) *Eurotium* sample showing auto-fluorescence behavior under UV light.

Air samples collected from the contaminated archives (Bochum, Germany) illuminated with white light and UV light are shown in Fig. 68. If white light is used (see Fig. 68a) it will be difficult to count the amount of spores as the spore contour is not clearly distinguishable from other particles (like dust, polymer particles etc.) Fig. 68b shows the same air sample under UV excitation. With spores exhibiting auto-fluorescence property under UV light, they can be clearly distinguished from other

dust particles (blue color particles are small polymer or plastic dust). By applying image processing tools it is possible to count the number of spores.

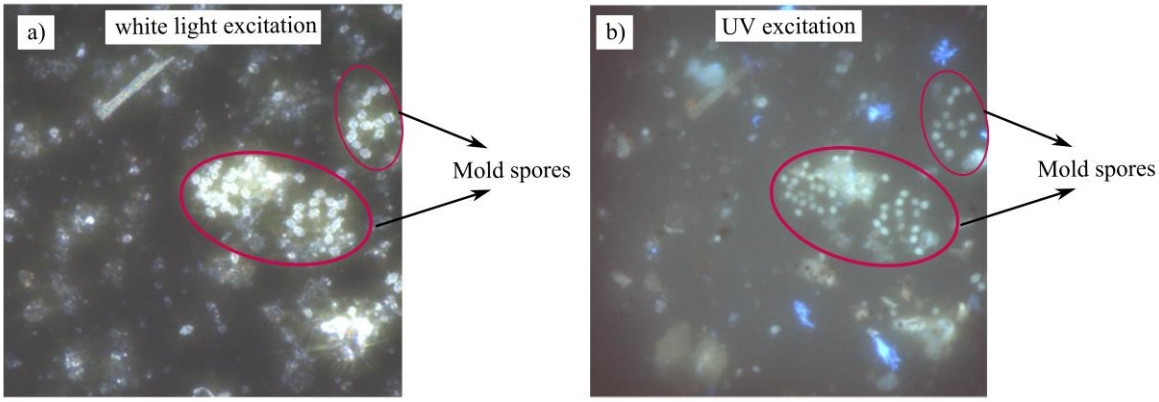

Figure 68: Air sample collected from contaminated archive a) under white light it is hard to differentiate the spores from the dust samples b) when excited with UV light, spores can be easily distinguished from dust and other fluorescent particles. Spores are indicated within red circles.

Emission peaks for different mold species involved in archive contamination has been investigated and is represented in Table 8. *Eurotium Amstelodami* which is a major mold species involved in contamination of books has an emission peak of 540 nm (green color in visible region) when excited with 365 nm. Whereas other mold spores from *Aspergillus* species are blue in color as they have emission peaks in the wavelength of 470-480 nm. Emission pictures of different mold spores under white and UV lights are shown in Fig. 69. Having different emission spectrum in visible region allows in differentiating the mold spores. The auto-fluorescence concept has been successfully implemented in the autonomous optical sensor system for detection and differentiation of indoor mold spore contamination.

Table 8: emission peaks of different mold species when excited with 365 nm UV light

	Eurotium Amstelodami	***Aspergillus Penicilloides***	***Aspergillus Restrictus***
Emission peak (nm)	540	470	480

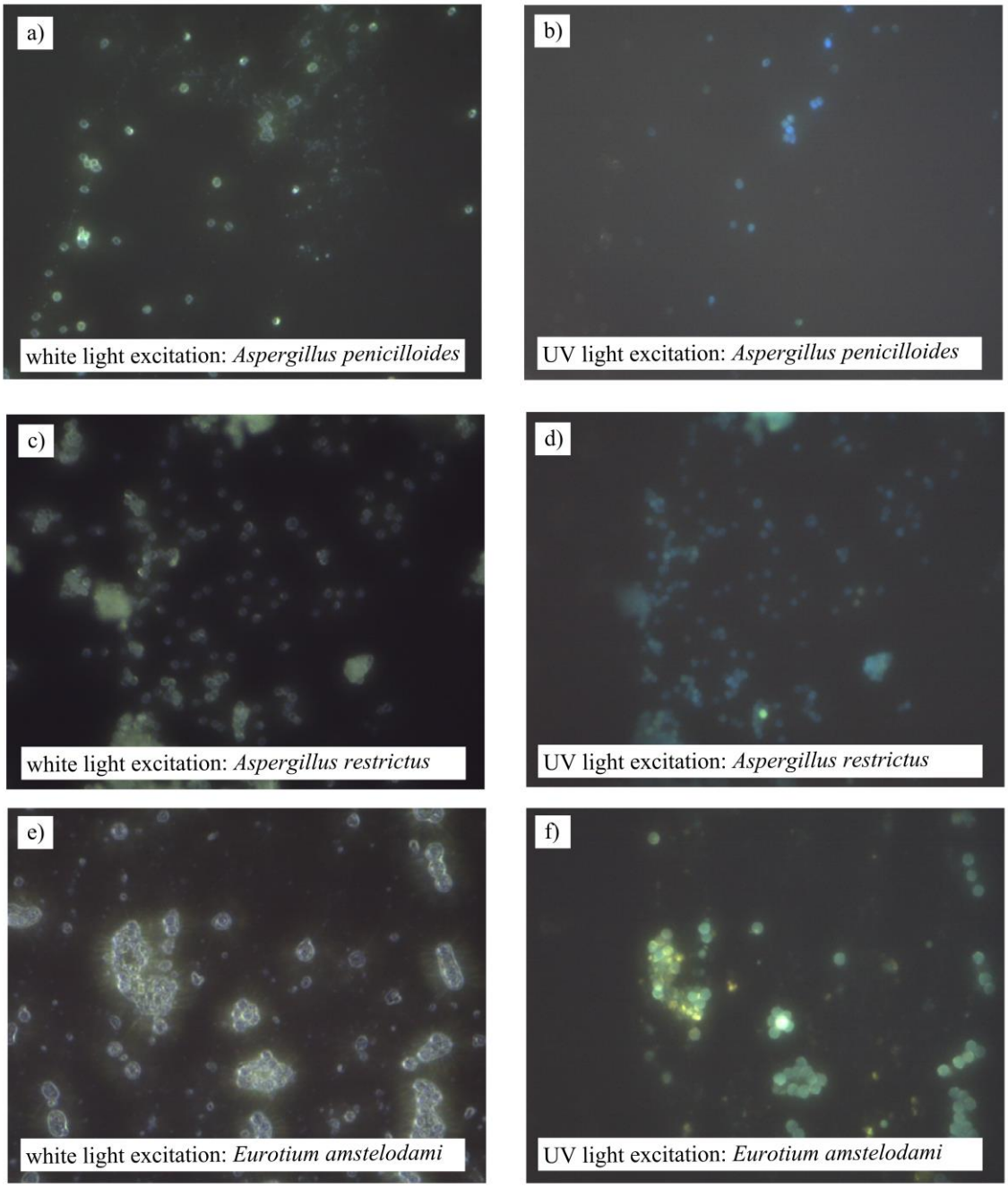

Figure 69: Pictures of mold spores under white light and with UV excitation a) *Aspergillus penicilloides* under white light b) *Aspergillus penicilloides* under UV light c) *Aspergillus restrictus* under white light d) *Aspergillus restrictus* under UV light e) *Eurotium amstelodami* under white light f) *Eurotium amstelodami* under UV light.

7 Sensor sticker for detection of mold contamination on bananas

7.1 Introduction

Bananas are one of the world's largest produced and consumed fruit. According to the statistics from the United Nations food and agricultural organization, more than 100 million tonnes of bananas are produced yearly. Major portion of these bananas are being produced by Asian and Latin American countries. Approximately 17 million tonnes of produced bananas are being exported every year worldwide [131,132]. As European climatic conditions are not suitable for banana plantation, among the exported bananas, 25 % of the bananas are being imported by Europe [133].

One of the major challenges in importing bananas is to preserve their quality during transportation [134]. Logistic companies should ensure that the bananas being imported arrive at the destination without damage and also should not be ripened. They are generally transported from Latin American countries to Europe. As a first step, the bananas are processed at a station, where they are cleaned and are loaded into boxes. These boxes are arranged in the form of pallets and moved into a transport container (which has climate control) and are shipped. After about 21 days of transport, the bananas arrive at the destination. Based on the demand and requirement, the bananas are ripened and distributed to different consumer markets.

Mold contamination of bananas is one of the major factors involved in the loss of bananas during transportation [135,136]. In addition to the loss of food, mold growth on bananas incurs huge transport losses to the logistic companies. Mold spores generally get attached to the bananas surface during their growth or during pre- or post-harvesting process at the banana field. Once attached to the banana, there is high chance that these spores remain on their surface even after processing. After processing, the bananas are packed and transported in the containers. The humidity within the plastic foil (where bananas are packed) can reach up to 80 % RH during transportation (due to condensation) even though the foil contains holes [135]. Because of high humidity, there is a possibility that the spores (on the banana) start to germinate by utilizing the nutrients present on the banana. As the mold starts to grow, it could spread and contaminate the entire container.

In addition to the financial and food loss, the growth of mold produces mycotoxins and mobile volatile organic compounds as they grow. These secondary compounds when consumed or inhaled are proven to be dangerous to human and animal health [3]. Considering this risk, it is necessary to investigate the influence of spores on the development of mold on bananas. Till date, there exists no sensor to detect the presence of mold spores on bananas. Hence, a sensor sticker has been designed, which can be put on the banana surface to determine mold spore concentrations. The detection principle is based on culture medium, which has been explained in Chapter 3. In the presented approach, a culture medium is placed on a capacitive sensor, which is fabricated on a polyimide foil. As the spores germinate, they change the culture medium to acidic or basic, which changes the dielectric properties of the medium. This is measured by the capacitive sensor [137].

7.2 Materials and methods

A capacitive sensor is used consisting of Tantalum electrodes on a polyimide foil. The electrodes have a thickness of about 400 nm and the polyimide foil is 5 µm thick. For the description of the sensors please refer to [138]. Culture medium with integrated air cavities is made using 3D printed mould. Later, the culture medium is placed on top of the capacitive sensor with the mediums air cavities facing upwards. For testing, mold spores of desired concentration is deposited on the surface of banana and the capacitive sensor is put on the banana with culture medium in direct contact the spores. The spores use the culture medium and start to germinate. The mold spore germination is determined by measuring the capacitance changes. Design and fabrication steps involved in manufacturing of the capacitive sensor are shown in Fig. 70.

The sensor foil has dimensions of 10 mm x 3 mm. It has 428 fingers for measuring capacitance of the culture medium. Each electrode is 7 µm wide and is 3 mm long. Distance between electrodes is 7 µm. The fabrication of the flexible capacitive sensor starts with spin coating of polyimide (U-Varnish S) on a silicon wafer, which is followed by a curing step. As an adhesive layer 30 nm of titanium is sputtered onto the polyimide. Tantalum oxide (50 nm) and tantalum (300 nm) are sputtered and acts as metal electrodes. The metal electrodes are patterned using reactive ion etching. As a final step polyimide is etched in oxygen and CF_4 plasma to form individual sensors. To form a passivation layer (tantalum oxide), anodic oxidation is performed, resulting in a tantalum oxide layer on the electrodes [138].

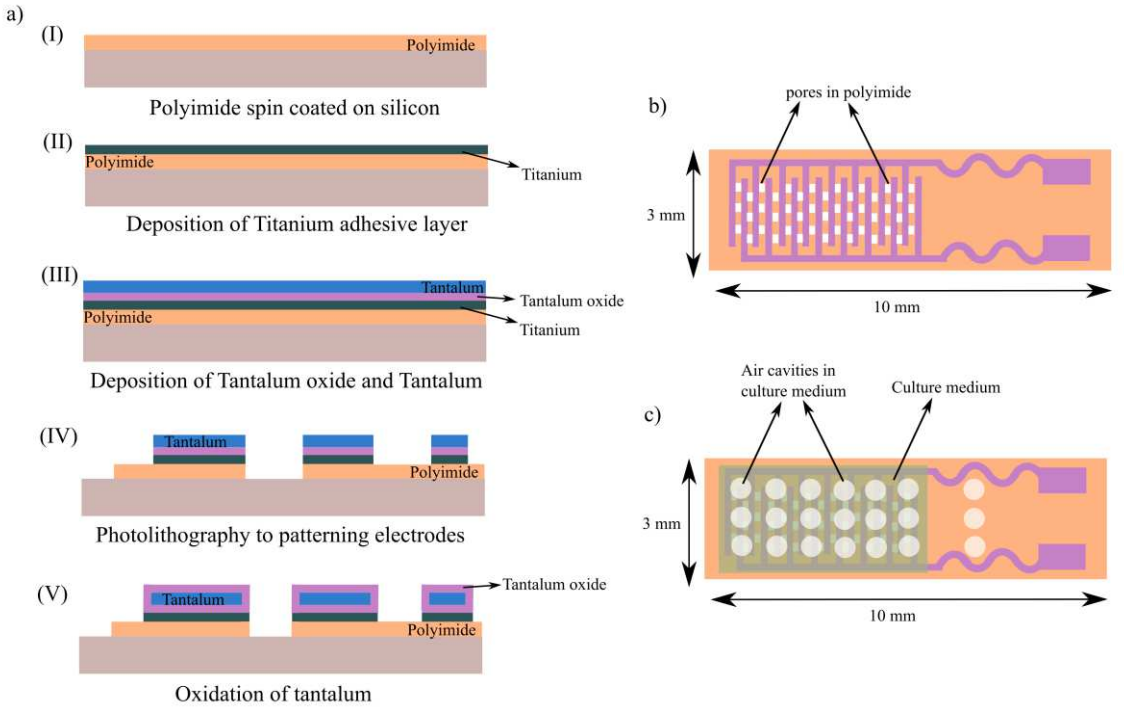

Figure 70: a) schematic view of the fabrication steps involved in manufacturing the capacitive sensor b) design of the capacitive sensor c) schematic of the culture medium with air cavities placed on the capacitive sensor [138].

As the sensor sticker is put on the banana using an adhesive tesa film, air cavities (oxygen) are integrated within the culture medium to provide the necessary amount of air for the fungi to grow. The sticker also prevents proliferation of mold (once the spores germinate). For preparing the culture medium, PDA agarose powder is suspended in deionized water and the mixture is autoclaved at 121 °C for 15 min. After autoclaving, the culture medium is transferred onto a 3D printed mould as shown in Fig. 71.

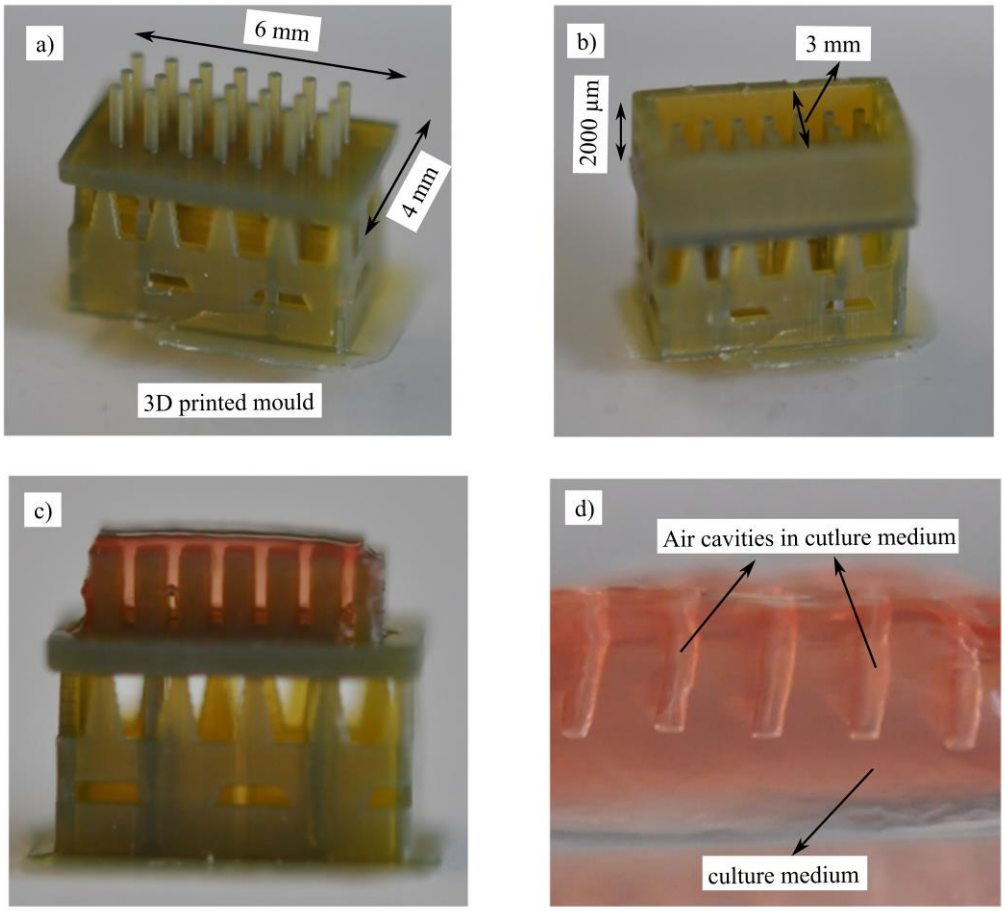

Figure 71: a) and b) 3D printed mould with pillars c) culture medium turned into gel in the mould d) culture medium pealed off from the mould.

When the culture medium is pipetted into the 3D printed moulds, it is still in liquid form (at 45 °C). Once the culture medium cools down to room temperature it turns into a gel, which is later pealed out of the mould using a tweezer and is placed on the capacitive sensor. The thickness of the culture medium depends on the mould cavity and is 2000 µm. For good visualization (in Fig. 71), the culture medium is prepared with Methyl red indicator dye. Fig. 71d shows the pealed out culture medium from the mould with integrated air cavities.

For assembling the sensor sticker, firstly the capacitive sensor is glued onto a transparent adhesive tape (TESA film) such that the sticky side of the film is in contact with the backside of the sensor. Later the culture medium with integrated air cavities is pealed out of mould and is transferred onto the sensor as shown in Fig. 72a and 72b. As a final step, the sensor is put onto the surface of banana with the culture medium facing the banana surface (Fig. 72c). The adhesive film ensures that the culture medium and the capacitive sensor do not slide over to another location on banana. The banana with the sensor sticker is placed inside a standard plastic bag (which is nor-

mally used for banana transportation within containers). As the spores (which are in contact with the culture medium) starts to germinate they change the dielectric constant of the culture medium, resulting in capacitance change. The capacitance measurements are done using an IVIUM spectrum analyzer.

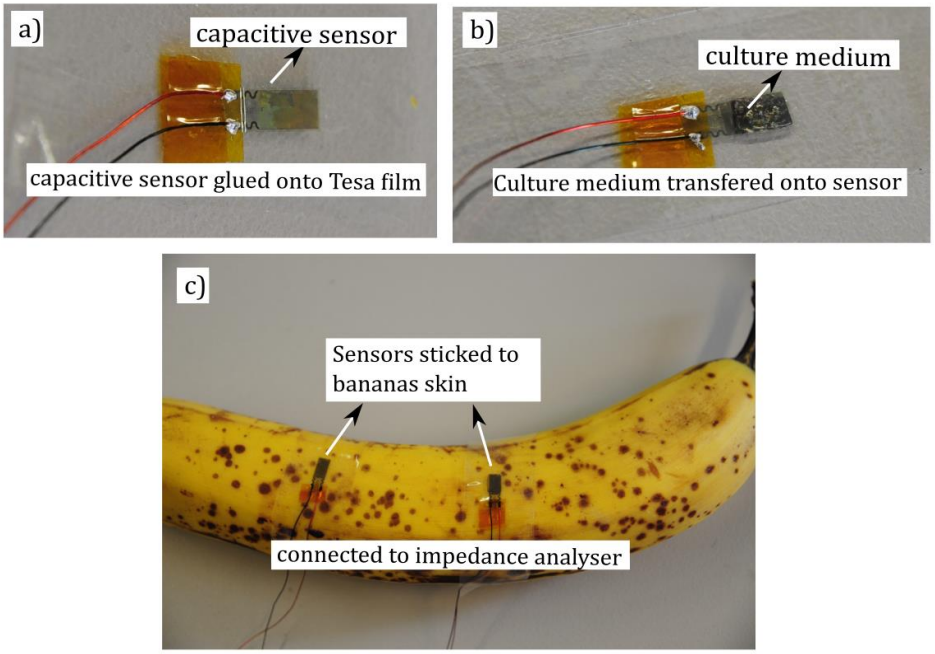

Figure 72: a) capacitive sensor glued onto the adhesive TESA film b) culture medium placed on the top of the capacitive sensor c) the sensor put onto the banana surface for detection of spores.

7.3 Results and discussion

The sensor performance has been tested by detecting *Fusarium Oxysporum* spores. *Fusarium Oxysporum* is one of the major mold species responsible for banana contamination. For testing the sensor, two different spore concentrations of *Fusarium* (10^3 CFU/ml and 10^4 CFU/ml) have been transferred onto the skin of banana using a pipette. The banana is then placed in a flow box for 6-8 hours. This allows the liquid to evaporate and the spores get settled or deposited on the surface of banana. Now, the sticker is placed on the surface where the spores are located. The spores start to germinate by utilizing the culture medium. As the spores grow they release acidic or basic byproducts. Production of acid increases the number of polar molecules within the culture medium, thus enhancing the dielectric permittivity. With acid production, the measured capacitance increases with time. Similarly with the production of basic byproducts the dielectric permittivity of the culture medium decreases. This decreases the value of measured capacitance with time. As Fusarium Oxysproum starts to germinate it produces basic byproducts (amino group byproducts), as a result the measured capacitance decreases.

The capacitance change measured with the sensor as the mold spores germinate is represented in Fig. 73 [137]. The measurement results are for a spore concentration of 10^4 CFU/ml (approximately 555 CFU/mm^2). Capacitance measurements are recorded for time duration of 18 hours. Results indicate that within 6 hours there is 5 % change in the capacitance. Measurements were performed 3 times, which showed similar results.

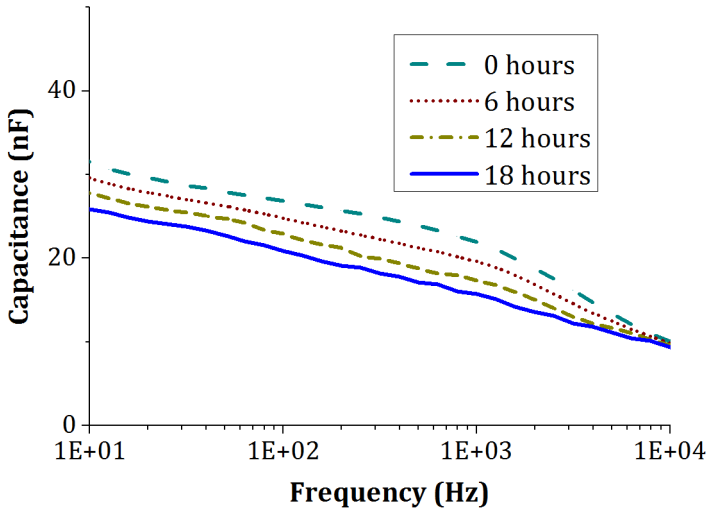

Figure 73: Capacitance measured with the sensor at different times during the growth of *Fusarium Oxysporum* spores with an initial concentration of 10^4 CFU/ml.

The sensor performance has been tested by detecting different concentrations of *Fusarium oxysporum* spores. For a spore concentration of 10^3 CFU/ml, the capacitance of the culture medium changes by 5 % in 9 hours. Whereas for a concentration of 10^4 CFU/ml it takes 6 hours. All the measurements are done at 1 kHz. Results indicate that if the initial spore concentration is high then it takes less time to change the capacitance of the medium. The results demonstrate the working principle of a novel sensor sticker that can be put on the surface of banana to detect the spore concentrations. By integrating wireless readout and communication electronics, the designed sensor sticker could be used to monitor the amount of spores on the bananas.

8 Conclusion

This chapter discusses major conclusions and the future possibilities of this research work. The aim of the research is to investigate different possibilities for detection of mold growth, and to design an autonomous sensor system for monitoring mold spore contaminations in indoor environment (particularly in archives). The presented mold sensor system with a replaceable bioreactor cartridge provides the possibility for autonomous long-term monitoring. Furthermore, this concept can be implemented for the detection of spores in other indoor environments.

In this research, different mold spore detection methods and their possibilities to be integrated into an autonomous sensor system have been investigated. Various mold detection methods like PCR, molecular methods, MVOC's, FTIR and ATP-bioluminescence are not suitable for designing a cost effective out-of-lab sensor system. These methods are complex to be integrated into an autonomous sensor system as they require several sample preparation steps. Also the reagents employed in these methods are costly and not stable for longer durations. Hence in this thesis, methods are investigated for making a standalone sensor system suitable for mold detection.

The mold detection is done by employing a impedance microbiology principle, which is based on the measurement of electrical properties of the culture medium as the mold spores germinate. Main advantage of designing a sensor using the culturing method is that it specifically detects the viable mold spores. The viable spores are active spores (i.e., can germinate), which are responsible for spreading the mold contamination within the archives. For automating the culturing technique a membrane sealed bioreactor has been designed and fabricated. The bioreactor consists of an impedance sensor to measure the electrical properties of the culture medium (as the mold grows), a reaction cavity in which the culture medium is stored, and a sacrificial silicon nitride membrane to prevent the culture medium from contamination.

For the detection of the mold growth, a novel approach has been developed by integrating impedance and colorimetric principles. As the mold spores germinate, the impedance of the culture medium changes (due to the pH change). This change in impedance is monitored using a symmetrical two-electrode configuration. A major drawback of the impedance measurements is that it does not have a reference measurement within the sensor. Though without the reference measurement, the pH

changes can be monitored by utilizing the electrodes (by measuring the impedance), it is not possible to determine the absolute pH value of the culture medium. To determine the absolute pH value, a calibration step is required before the impedance measurements. To avoid this calibration step, a colorimetric reference has been integrated within the sensor.

Using this colorimetric principle the absolute pH value of culture medium and the sensitivity of the sensor per unit pH change are determined directly on-chip. By using the integrated approach, detection of the mold growth has been successfully demonstrated. Major mold species responsible for contamination in the archives like, *Eurotium amstelodami*, *Aspergillus penicilloides*, *Aspergillus restrictus* and *Cladosporium cladosporiodes* have been successfully detected on-chip. This method is highly reproducible and could be used to determine the spore concentration as low as 100 CFU/ml.

As the designed sensor system is aimed to monitor the archive mold spores at desired time intervals, the concept of sealing the bioreactor with a sacrificial membrane has been investigated. To realize autonomous functionality, it is necessary to prevent the culture medium (stored within the bioreactors) from contamination. To do so, the bioreactor is sealed with a thin sacrificial membrane. Sealing the bioreactor with the membrane prevents the mold spores from reaching the culture medium and it allows activating the bioreactor at defined time intervals. The sacrificial membranes can be activated using a current pulse and is made of silicon nitride. Three different electrode designs have been investigated to determine the bursting behavior of the membrane. The parallel electrode design has proven to give the best performance because it opens up the maximum surface area. Also, the break up current for this design is 8±2 mA and has a bursting time of 174±29 msec.

The membrane sealed bioreactor has been tested successfully to detect mold spores from the air sample. The results demonstrate that the mold spores do not reach the culture medium if the membrane is not activated, thus maintaining the sterile condition of the culture medium. Once the membrane is activated (bursts open) the spores from the air sample settle in the culture medium and start to grow which is later detected using integrated approach.

For long-term monitoring of the mold spores within archives a bioreactor cartridge has been designed. The bioreactor cartridge comprises of an array of membrane sealed bioreactors connected in a 4x4 format. The designed autonomous sensor system comprises of an air sampling unit, an air pump, a replaceable bioreactor cartridge and a control unit. The air sampling unit distributes the indoor air uniformly among all the bioreactors and has a catching efficiency of 62-72 %. The control unit activates individual bioreactors at a defined time and initiates the detection process. Laboratory experiments demonstrate that by using the sensor system it is possible to detect

and quantify the mold spores present in the air sample. The sensor system has been successfully implemented in an archive for measuring spores concentrations in real-life environment. The measurements obtained from the field tests indicate a contamination in the archive, which show good clear agreement with the reference measurements. In conclusion, a novel mold sensor system has been designed, realized, and characterized for the detection of mold growth in archives. Using the replaceable bioreactor array provides the possibility for long-term monitoring of archives. Improvements in the air sampling unit to increase the catching efficiency and the distribution profile will further increase the performance of the sensor system.

In addition to the designed sensor system based on the mold growth, an optical sensor system has been designed in another project. In this research, the auto-fluorescence properties of specific mold spores (which are responsible for archive contamination) have been investigated. This study has showed that by using an excitation source of 365 nm the spore particles exhibit auto-fluorescence behavior and could be clearly distinguished from the dust particles, thus increasing the performance of the optical sensor system. Also mold spores responsible for archive contamination have different emission spectrums. *Eurotium Amstelodami* mold species has an emission peak of 540 nm. *Aspergillus Penicilloides* and *Aspergillus Restrictus* have peaks at 470 and 480 nm respectively. This investigation has provided an interesting contribution in designing an optical sensor system, where the auto-fluorescence concept has been successfully implemented for detection of mold spores.

In this research, a novel concept of using a sensor sticker for monitoring the mold spore concentration on fruits during transportation has been presented. The sensor sticker has been successfully applied on banana to detect different spore concentrations of *Fusarium Oxysporum,* which is a major mold species responsible for banana contamination. By integrating readout electronics the designed sticker can be an optimum solution to monitor growth of mold on fruits during transportation.

Acknowledgements

During my doctoral period at the University of Bremen, there has been immense support from many people both from within the university, as well from outside, whom I would like to thank.

First of all, I would like to thank my parents, Vijayasekhara Reddy and Jyotheeswari, for their everlasting love and support. I am blessed to have them, who encouraged me through out my academic education and paved the path to pursue PhD. I would also thank my family, friends for their encouragement. Heartful thanks goes to my sister Sharmila and my brother-in-law Abhishek for their everlasting love and support.

I would like to express my deepest gratitude to my supervisor Prof. Dr. Michael Vellekoop for providing me the opportunity to work at the institute for microsensors, -actuators and –systems (IMSAS). I will always remember the time spent with him having critical discussions, which immensely contributed to my scientific work. His experience and guidance has been useful for my personal development. Thank you Michiel.

I am thankful to Prof. Dr. Bernhard Jakoby from Johannes Kepler University Linz, Austria who has accepted to be my second reviewer. Thank you Prof. Bernhard Jakoby for spending time and reviewing my thesis.

I express my sincere thanks to Prof. Walter Lang for his constant support and guidance through out the project. His valuable remarks on my journal and conference papers increased the quality of my work.

This research is a part of BMBF project “MaUS: Mikroreaktorensystem zur autonomen Untersuchung von Schimmelpilzbelastungen” which is supported by the Federal Ministry of Education and Research, Germany, under reference number 031A257A-D. I acknowledge the financial support from the BMBF. This work would not have been possible without the support from the project partners, BMA Labor GmbH, Dole GmbH, microFAB GmbH and VEW GmbH.

My special thanks goes to Mathias Frodl from microFAB GmbH for fabricating the impedance sensors and the silicon nitride membranes. His experience in MEMS foundry

helped to achieve the milestones within prescribed timeframe. Special thanks goes to Ute Stephan and Bianca from BMA Labor GmbH, who helped in biological analysis and for their support during field tests at Bochum. I should also thank responsible persons at the Stadt Archives, Bochum for giving us permission whenever it is necessary to do measurements inside archives.

Special thanks to Dr. Sander van den Driesche, who invested his valuable time helping me in designing experiments and guiding me to develop the idea of integrating impedance sensor with an optical reference.

Heart full thanks to my friend Roland Blank, who provided his valuable suggestions in designing electronic circuitry. It was great experience working with Roland and Tahir in the MaUS project. I also thank Tahir for providing nice suggestions during hardware implementation. I will never forget fun times we had during our field tests.

Furthermore, I wish to thank my fellow Ph.D colleagues for their cooperation during my stay at IMSAS. It was great time I shared with Reza Ebrahimifard, Mahmuda Akhtar and Valeria Fioravanti. Special thanks to my office mates Chanaka Lloyd, Steffen Janßen, Martin Oellers and Frank Bunge who are always enthusiastic in sharing thoughts and discussions. Frieder Lucklum for his support in stereo lithography. I thank Lisa Reichel and the administrative staff of IMSAS for all their support. Also, I would like to thank students who I supervised: Bilal Ahmad, Chun-Fan Dai, Abhishek Chakroborty, Rahar Amin and Syed Zaidi for their work in the project. I would like to thank all the IMSAS technicians for their constant help, which allowed me to finish this thesis successfully. Specially, I should thank Ingrid Michels for her help in wire-bonding the sensors. Also, heartful thanks to Ibrahim Ersöz, Andre Bödecker and Christian Habben for their valuable support in technology issues. As a part of clean room practical's I received great help from Melanie Kirsch, Eva-Maria Meyer and Eileen Ritter, thank you for your support. Special thanks goes to Meike Mehrtens for helping me with the financial documents for project MaUS.

Special thanks to Martin Oellers, for being a good friend and helping me personally in some difficult situations. Also, I thank him for printing my thesis and submitting it to the examination department.

Finally, but foremost, I would like to express my heart full thanks to my lovely wife Lavanya for her unconditional love and support. She has been my backbone who built my confidence and helped me to stay optimistic through out my PhD thesis. Thank you for your continuous motivation during this thesis my Love.

List of publications

Journal papers

Papireddy Vinayaka, P.; van den Driesche, S.; Blank, R.; Tahir, M. W.; Frodl, M.; Lang, W.; Vellekoop, M. J., *An Impedance-Based Mold Sensor with on-Chip Optical Reference*. Sensors 2016 16, (10), p 1603, 2016 DOI 10.3390/s16101603.

Blank, R.; Papireddy Vinayaka, P.; Tahir, M. W.; Yong, J.; Vellekoop, M. J.; Lang, W., *Comparison of Several Optical Methods for an Automated Fungal Spore Sensor System Concept*. Ieee Sens J 16, (14), pp 5596-5602, 2016 DOI 10.1109/JSEN.2016.2567538

Tahir, M. W.; Zaidi, N. A.; Blanke, M.; Papireddy Vinayaka, P.; Vellekoop, M. J.; Lang, W., *Fungus Detection Through Optical Sensor System Using Two Different Kinds of Feature Vectors for the Classification*. lEEE Sensors Journal 17, (16), pp 5341-1748, 2017 DOI 10.1109/JSEN.2017.2723052.

International conferences

Papireddy Vinayaka, P., S. Van Den Driesche, S. Janssen, M. Frodl, R. Blank, F. Cipriani, W. Lang, M.J. Vellekoop, On-Chip monitoring of pH change in agar-gels during fungi growth by integrating impedance and colorimetric principles, in: Procedia Eng., 2014: pp. 373–376. doi:10.1016/j.proeng.2014.11.739.

Papireddy Vinayaka, P.; Driesche van den, S.; Janssen, S.; Frodl, M.; Blank, R.; Cipriani, F.; Lang, W.; Vellekoop, M. J. Impedance spectroscopy for detection of mold in archives with an integrated reference measurement. Proc. SPIE Microtechnologies, Vol. 9518, 95180T, Barcelona, Spanien, pp 1-6, 2015 DOI 10.1117/12.2178510.

Papireddy Vinayaka, P.; van den Driesche, S.; Blank, R.; Chakraborty, A.; Amin, R.; Tahir, M. W.; Zaidi, N. A.; Frodl, M.; Lang, W.; Vellekoop, M. J. *Membrane-sealed bioreactor for on-site autonomous detection of fungi spore contamination in archives.* Proc. Eurosensors 2016, Budapest, Ungarn, Procedia Engineering 168, pp 529-532, 2016 DOI 10.1016/j.proeng.2016.11.515.

Papireddy Vinayaka, P.; Kahali Moghaddam, M.; van den Driesche, S.; Blank, R.; Vellekoop, M. J. *Sensor Sticker for Detection of Fungi Spore Contamination on Bananas* Proc. CIMTEC 2016 11th International Conference "Medical Applications of Novel Biomaterials and Nanotechnology", Perugia, Italien, pp Vol.100, 130-133, 2016 DOI 10.4028/www.scientific.net/AST.100.130.

Papireddy Vinayaka, P.; Blanke, M.; Frodl, M.; Tahir, W.; Zaidi, N. A.; Oellers, M.; Driesche van den, S.; Lang, W.; Vellekoop, M. J. *A replaceable bioreactor array for monitoring mold spore contamination in archives.* Proc. MikroSystemTechnik Kongress 2017, München, Deutschland, pp 641-644, 2017.

Blank, R.; Papireddy Vinayaka, P.; Tahir, M. W.; Vellekoop, M. J.; Lang, W. Optical Sensor System for the Detection of Mold. Concept for a fully automated sensor system for the detection of airborne fungal spores. Proc. IEEE Sensors, Busan, Südkorea, pp 677-682, 2015.

Blank, R.; Papireddy Vinayaka, P.; Tahir, M. W.; Yong, J.; Vellekoop, M. J.; Lang, W. *Development of a Fungal Risk Monitor for the Next Generation of Intelligent Containersaper.* Proc. IEEE Sensors, Orlando, Florida, USA, pp 677-682, 2016.

Tahir, M. W.; Zaidi, N. A.; Papireddy Vinayaka, P.; Vellekoop, M. J.; Lang, W. *Detection of Fungus through an Optical Sensor System using the Histogram of Oriented Gradients.* Proc. IEEE Sensors, Orlanda, Florida, USA, pp 418-420, 2016 DOI 10.1109/ICSENS.2016.7808537.

Tahir, M. W.; Zaidi, N. A.; Papireddy Vinayaka, P.; Lang, W. *Fungus Detection System.* Proc. 2016 IEEE International Conference on Autonomic Computing (ICAC), Würzburg, Dutschland, pp 227-228, 2016 DOI 10.1109/ICAC.2016.50.

Tahir, M. W.; Zaidi, N. A.; Blank, R.; Papireddy Vinayaka, P.; Vellekoop, M. J.; Lang, W. Comparison of Pre-processing on Different Kind of Images Produced by Optical Sensor System. Proc. 2nd International Conference on Sensors Engineering and Electronics Instrumental Advances (SEIA' 2016), Barcelona, Spanien, pp 41-43, 2016.

Tahir, M. W.; Zaidi, N. A.; Blank, R.; Papireddy Vinayaka, P.; Vellekoop, M. J.; Lang, W. *An Efficient and Simple Embedded System of Fungus Detection System.* Proc. INMIC 2017, Lahore, Pakistan, 2017.

Other publications

Zaidi, N. A.; Tahir, M. W.; Papireddy Vinayaka, P.; Lucklum, F.; Vellekoop, M. J.; Lang, W. *Detection of Ethylene using Gas Chromatographic System.* Proc. Eurosensors 2016, Budapest, Ungarn, Procedia Engineering 168, pp 380-383, 2016 DOI dx.doi.org/10.1016/j.proeng.2016.11.140.

Oellers, M.; Bunge, F.; Lucklum, F.; Papireddy Vinayaka, P.; Habben, C.; Kirsch, M.; van den Driesche, S.; Vellekoop, M. J. *Microfluidic swap structure to enhance on-chip liquid mixing.* Proc. IEEE SENSORS 2017, Glasgow, Scotland, pp 1706-1708, 2017.

Oellers, M.; Bunge, F.; Papireddy Vinayaka, P.; Driesche, S. v. d.; Vellekoop, M. J. *Flow-Ratio Monitoring in a Microchannel by Liquid-Liquid Interface Interferometry.* Proc. Eurosensors Paris, Frankreich, p 498, 2017 DOI 10.3390/proceedings1040498.

Bibliography

[1] T.H.E.F. Ungi, M. Species, Meredith Blackwell 2, 98 (2011) 426–438. doi:10.3732/ajb.1000298.

[2] R.K. Bush, J.M. Portnoy, A. Saxon, A.I. Terr, R.A. Wood, The medical effects of mold exposure., J. Allergy Clin. Immunol. 117 (2006) 326–33. http://www.ncbi.nlm.nih.gov/pubmed/16514772.

[3] J.F. Grernmels, I.I. Will, Mycotoxins : Their implications for human and animal health MYCOTOXINS : THEIR IMPLICATIONS FOR HUMAN AND ANIMAL HEALTH, 2176 (2017). doi:10.1080/01652176.1999.9695005.

[4] A.E. Statement, Council on Scientific Affairs Adverse Human Health Effects Associated with, (n.d.) 470–478.

[5] I. Air, B.M. No, I. Air, Meta-analyses of the associations of respiratory health effects with dampness and mold in homes, (2007) 284–296. doi:10.1111/j.1600-0668.2007.00475.x.

[6] M.J. Mendell, A.G. Mirer, K. Cheung, M. Tong, J. Douwes, Respiratory and Allergic Health Effects of Dampness , Mold , and Dampness ‐ Related Agents : A Review of the Epidemiologic Evidence, 748 (2011) 748–756. doi:10.1289/ehp.1002410.

[7] H.G. Schlegel, General Microbiology, Seventh, 2003.

[8] J. Webster, R. Weber, Introduction to Fungi, Third, 2007.

[9] C.-G. Bornehag, G. Blomquist, F. Gyntelberg, B.J. Rvholm, P. Malmberg, L. Nordvall, A. Nielsen, G. Pershagen, A.J. Sundell, INDOOR AIR Dampness in Buildings and Health Nordic Interdisciplinary Review of the Scientific Evidence on Associations between Exposure to Dampness'' in Buildings and Health Effects (NORDDAMP), Indoor Air. 11 (2001) 72–86. doi:10.1034/j.1600-0668.2001.110202.x.

[10] C.G. Tischer, J. Heinrich, Exposure assessment of residential mould, Fungi and microbial components in relation to children's health: Achievements and challenges, Int. J. Hyg. Environ. Health. 216 (2013) 109–114. doi:10.1016/j.ijheh.2012.05.002.

[11] W.E. Horner, A. Helbling, J.E. Salvaggio, S.B. Lehrer, Fungal allergens., Clin. Microbiol. Rev. 8 (1995) 161–79. http://www.ncbi.nlm.nih.gov/pubmed/7621398 (accessed September 25, 2017).

[12] a P. Verhoeff, H. a Burge, Health risk assessment of fungi in home

environments., Ann. Allergy. Asthma Immunol. 78 (1997) 544-54–6. doi:10.1016/S1081-1206(10)63214-0.

[13] R. Sharpe, C.R. Thornton, N.J. Osborne, Modifiable factors governing indoor fungal diversity and risk of asthma, Clin. Exp. Allergy. 44 (2014) 631–641. doi:10.1111/cea.12281.

[14] J.W. Bennett, M. Klich, M. Mycotoxins, Mycotoxins, Society. 16 (2003) 497–516. doi:10.1128/CMR.16.3.497.

[15] C.A. Robbins, L.J. Swenson, M.L. Nealley, R.E. Gots, B.J. Kelman, Health effects of mycotoxins in indoor air: A critical review, Appl. Occup. Environ. Hyg. 15 (2000) 773–784. doi:10.1080/10473220050129419.

[16] F. Fung, R.F. Clark, Health Effects of Mycotoxins: A Toxicological Overview, J. Toxicol. Clin. Toxicol. 42 (2004) 217–234. doi:10.1081/CLT-120030947.

[17] A. Korpi, J. Järnberg, A.-L. Pasanen, Microbial Volatile Organic Compounds, Crit. Rev. Toxicol. 39 (2009) 139–193. doi:10.1080/10408440802291497.

[18] R. Persoons, S. Parat, M. Stoklov, A. Perdrix, A. Maitre, Critical working tasks and determinants of exposure to bioaerosols and MVOC at composting facilities, Int. J. Hyg. Environ. Health. 213 (2010) 338–347. doi:10.1016/j.ijheh.2010.06.001.

[19] S. DAGNAS, J.-M. MEMBRÉ, Predicting and Preventing Mold Spoilage of Food Products, J. Food Prot. 76 (2013) 538–551. doi:10.4315/0362-028X.JFP-12-349.

[20] H.J. Moon, G. Augenbroe, Assessing mold risks in buildings under uncertainty, Coll. Archit. Doctor of (2005) 245.

[21] H. Brandl, Bioaerosols in Indoor Environment - A Review with Special Reference to Residential and Occupational Locations, Open Environ. Biol. Monit. J. 4 (2011) 83–96. doi:10.2174/1875040001104010083.

[22] B. Ghosh, H. Lal, A. Srivastava, Review of bioaerosols in indoor environment with special reference to sampling, analysis and control mechanisms, Environ. Int. 85 (2015) 254–272. doi:10.1016/j.envint.2015.09.018.

[23] J.H. Vincent, Sampling for Bioaerosols, 2007. doi:10.1002/9780470060230.ch19.

[24] C. Urz, F. De Leo, Sampling with adhesive tape strips: An easy and rapid method to monitor microbial colonization on monument surfaces, J. Microbiol. Methods. 44 (2001) 1–11. doi:10.1016/S0167-7012(00)00227-X.

[25] J.B. Hart, M.L. French, H.E. Eitzen, M. a Ritter, Rodac plate-holding device for sampling surfaces during surgery., Appl. Microbiol. 26 (1973) 417–8. http://www.pubmedcentral.nih.gov/articlerender.fcgi?artid=379803&tool=pmcentrez&rendertype=abstract.

[26] E. De Boer, R.R. Beumer, Methodology for detection and typing of foodborne microorganisms, Int. J. Food Microbiol. 50 (1999) 119–130. doi:10.1016/S0168-1605(99)00081-1.

[27] A.A.V.I. Gouveia, M.A. Nicoletti, Influence of the sampling technique on microorganism detection in the monitoring of flat surfaces, Lat. Am. J. Pharm.

34 (2015).

[28] A. Mouilleseaux, Sampling methods for bioaerosols, Aerobiologia (Bologna). 6 (1990) 32–35. doi:10.1007/BF02539039.

[29] W.D. Griffiths, I.W. Stewart, S.J. Futter, S.L. Upton, D. Mark, The development of sampling methods for the assessment of indoor bioaerosols, J. Aerosol Sci. 28 (1997) 437–457. doi:10.1016/S0021-8502(96)00446-6.

[30] M. Yao, G. Mainelis, Analysis of portable impactor performance for enumeration of viable bioaerosols, J. Occup. Environ. Hyg. 4 (2007) 514–524. doi:10.1080/15459620701407388.

[31] M. Yao, G. Mainelis, Effect of physical and biological parameters on enumeration of bioaerosols by portable microbial impactors, J. Aerosol Sci. 37 (2006) 1467–1483. doi:10.1016/j.jaerosci.2006.06.005.

[32] P. Xu, L. Jigang, Computer assistance image processing spores counting, in: Proc. - 2009 Int. Asia Conf. Informatics Control. Autom. Robot. CAR 2009, 2009: pp. 203–206. doi:10.1109/CAR.2009.10.

[33] J. Wagner, J. MacHer, Automated spore measurements using microscopy, image analysis, and peak recognition of near-monodisperse aerosols, Aerosol Sci. Technol. 46 (2012) 862–873. doi:10.1080/02786826.2012.674232.

[34] K. Schmitt, G. Sulz, T. Klockenbring, B. Seidel, A. Holl??nder, Gel-based biochip for the detection of airborne contaminants, in: Microsyst. Technol., 2010: pp. 717–722. doi:10.1007/s00542-009-0987-y.

[35] M. Almaguer, M.J. Aira, F.J. Rodríguez-Rajo, T.I. Rojas, Study of airborne fungus spores by viable and non-viable methods in Havana, Cuba, Grana. 52 (2013) 289–298. doi:10.1080/00173134.2013.829869.

[36] S. Sieuwerts, F.A.M. De Bok, E. Mols, W.M. De Vos, J.E.T. Van Hylckama Vlieg, A simple and fast method for determining colony forming units, Lett. Appl. Microbiol. 47 (2008) 275–278. doi:10.1111/j.1472-765X.2008.02417.x.

[37] C. Calderon, E. Ward, J. Freeman, A. McCartney, Detection of airborne fungal spores sampled by rotating-arm and Hirst-type spore traps using polymerase chain reaction assays, J. Aerosol Sci. 33 (2002) 283–296. doi:10.1016/S0021-8502(01)00179-3.

[38] R.H. Williams, E. Ward, H.A. Mccartney, Methods for Integrated Air Sampling and DNA Analysis for Detection of Airborne Fungal Spores Methods for Integrated Air Sampling and DNA Analysis for Detection of Airborne Fungal Spores, Appl. Environ. Microbiol. 67 (2001) 2453–2459. doi:10.1128/AEM.67.6.2453.

[39] Z. Wu, G. Blomquist, S.-O. Westermark, X.-R. Wang, Application of PCR and probe hybridization techniques in detection of airborne fungal spores in environmental samples., J. Environ. Monit. 4 (2002) 673–678. doi:10.1039/b203048a.

[40] S. Li, R.R. Marquardt, D. Abramson, Immunochemical detection of molds: A review, J. Food Prot. 63 (2000) 281–291.

[41] T. Han, M. Wren, K. DuBois, J. Therkorn, G. Mainelis, Application of ATP-based

bioluminescence for bioaerosol quantification: Effect of sampling method, J. Aerosol Sci. 90 (2015) 114–123. doi:10.1016/j.jaerosci.2015.08.003.

[42] J.W. Park, C.W. Park, S.H. Lee, J. Hwang, Fast monitoring of indoor bioaerosol concentrations with ATP bioluminescence assay using an electrostatic rod-type sampler, PLoS One. 10 (2015). doi:10.1371/journal.pone.0125251.

[43] I.Y. Goryacheva, S. de Saeger, S.A. Eremin, C. van Peteghem, Immunochemical methods for rapid mycotoxin detection: Evolution from single to multiple analyte screening: A review, in: Food Addit. Contam., 2007: pp. 1169–1183. doi:10.1080/02652030701557179.

[44] A. Salman, L. Tsror, A. Pomerantz, R. Moreh, S. Mordechai, M. Huleihel, FTIR spectroscopy for detection and identification of fungal phytopathogenes, Spectroscopy. 24 (2010) 261–267. doi:10.3233/SPE-2010-0448.

[45] K. Sogawa, M. Watanabe, K. Sato, S. Segawa, C. Ishii, A. Miyabe, S. Murata, T. Saito, F. Nomura, Use of the MALDI BioTyper system with MALDI-TOF mass spectrometry for rapid identification of microorganisms, Anal. Bioanal. Chem. 400 (2011) 1905–1911. doi:10.1007/s00216-011-4877-7.

[46] T. Larsen, J. Axelsen, H.W. Ravn, Simplified and rapid method for extraction of ergosterol from natural samples and detection with quantitative and semi-quantitative methods using thin-layer chromatography, J. Chromatogr. A. 1026 (2004) 301–304. doi:10.1016/j.chroma.2003.10.128.

[47] A.L. Pasanen, K. Yli-Pietilä, P. Pasanen, P. Kalliokoski, J. Tarhanen, Ergosterol content in various fungal species and biocontaminated building materials, Appl. Environ. Microbiol. 65 (1999) 138–142. doi: .

[48] R.F. LeBouf, S.A. Schuckers, A. Rossner, Preliminary assessment of a model to predict mold contamination based on microbial volatile organic compound profiles, Sci. Total Environ. 408 (2010) 3648–3653. doi:10.1016/j.scitotenv.2010.04.054.

[49] H. Schleibinger, D. Laussmann, C.G. Bornehag, D. Eis, H. Rueden, Microbial volatile organic compounds in the air of moldy and mold-free indoor environments, in: Indoor Air, 2008: pp. 113–124. doi:10.1111/j.1600-0668.2007.00513.x.

[50] R. Chollet, M. Kukuczka, N. Halter, M. Romieux, F. Marc, H. Meder, V. Beguin, S. Ribault, Rapid detection and enumeration of contaminants by ATP bioluminescence using the milliflex?? rapid microbiology detection and enumeration system, J. Rapid Methods Autom. Microbiol. 16 (2008) 256–272. doi:10.1111/j.1745-4581.2008.00132.x.

[51] L. Bourassa, S.M. Butler-Wu, MALDI-TOF mass spectrometry for microorganism identification, in: Methods Microbiol., 2015: pp. 37–85. doi:10.1016/bs.mim.2015.07.003.

[52] P. Mehrotra, Biosensors and their applications - A review, J. Oral Biol. Craniofacial Res. 6 (2016) 153–159. doi:10.1016/j.jobcr.2015.12.002.

[53] L. Su, W. Jia, C. Hou, Y. Lei, Microbial biosensors: A review, Biosens. Bioelectron. 26 (2011) 1788–1799. doi:10.1016/j.bios.2010.09.005.

[54] N.J. Ronkainen, H.B. Halsall, W.R. Heineman, Electrochemical biosensors, Chem.

Soc. Rev. 39 (2010) 1747. doi:10.1039/b714449k.

[55] D. Grieshaber, R. MacKenzie, J. Vörös, E. Reimhult, Electrochemical Biosensors - Sensor Principles and Architectures, Sensors. 8 (2008) 1400–1458. doi:10.3390/s8031400.

[56] M. Pohanka, C. Republic, Electrochemical biosensors – principles and applications, Methods. 6 (2008) 57–64. http://www.zsf.jcu.cz/jab/6_2/pohanka.pdf.

[57] D.W. Kimmel, G. Leblanc, M.E. Meschievitz, D.E. Cliffel, Electrochemical sensors and biosensors, Anal. Chem. 84 (2012) 685–707. doi:10.1021/ac202878q.

[58] C. Apetrei, M.L. Rodríguez-Méndez, V. Parra, F. Gutierrez, J.A. De Saja, Array of voltammetric sensors for the discrimination of bitter solutions, in: Sensors Actuators, B Chem., 2004: pp. 145–152. doi:10.1016/j.snb.2004.04.047.

[59] A. Walcarius, C. Gondran, S. Cosnier, Amperometric Sensors, in: Chem. Biol. Microsens. Appl. Liq. Media, 2013: pp. 115–171. doi:10.1002/9781118603871.ch5.

[60] J. Wang, Electrochemical glucose biosensors, in: Electrochem. Sensors, Biosens. Their Biomed. Appl., 2008: pp. 57–69. doi:10.1016/B978-012373738-0.50005-2.

[61] E. Boubour, R.B. Lennox, Insulating properties of self-assembled monolayers monitored by impedance spectroscopy, Langmuir. 16 (2000) 4222–4228. doi:10.1021/la991328c.

[62] M. Schienle, C. Paulus, A. Frey, F. Hofmann, B. Holzapfl, P. Schindler-Bauer, R. Thewes, A fully electronic DNA sensor with 128 positions and in-pixel A/D conversion, in: IEEE J. Solid-State Circuits, 2004: pp. 2438–2445. doi:10.1109/JSSC.2004.837084.

[63] A.J. Bard, L.R. Faulkner, N. York, C. @bullet, W. Brisbane, S.E. Toronto, ELECTROCHEMICAL METHODS Fundamentals and Applications, 1944. doi:10.1016/B978-0-12-381373-2.00056-9.

[64] M.J. Milgrew, M.O. Riehle, A fully-integrated cmos microsensor array for imaging the hydrogen ion activity of living cells, Sensors And Actuators. (2008) 1117–1119.

[65] P. Bergveld, Thirty years of ISFETOLOGY: What happened in the past 30 years and what may happen in the next 30 years, Sensors Actuators, B Chem. 88 (2003) 1–20. doi:10.1016/S0925-4005(02)00301-5.

[66] V.F. Lvovich, Impedance Spectroscopy: Applications to Electrochemical and Dielectric Phenomena, 2012. doi:10.1002/9781118164075.

[67] M.E. Orazem, B. Tribollet, Electrochemical Impedance Spectroscopy, 2008. doi:10.1002/9780470381588.

[68] P. Electrochemistry, C. Elements, C. Equivalent, C. Models, C.I. Values, Basics of Electrochemical Impedance Spectroscopy, Appl. Note AC. 286 (2004) 1–6. doi:10.1152/ajpregu.00432.2003.

[69] K.R. Rogers, Principles of Affinity-Based Biosensors, Mol. Biotechnol. 14 (2000) 109–130. doi:10.1385/MB:14:2:109.

[70] R. Schweiss, C. Werner, W. Knoll, Impedance spectroscopy studies of interfacial acid-base reactions of self-assembled monolayers, J. Electroanal. Chem. 540 (2003) 145–151. doi:10.1016/S0022-0728(02)01303-7.

[71] M.I. Prodromidis, Impedimetric immunosensors-A review, Electrochim. Acta. 55 (2010) 4227–4233. doi:10.1016/j.electacta.2009.01.081.

[72] J.S. Daniels, N. Pourmand, Label-free impedance biosensors: Opportunities and challenges, Electroanalysis. 19 (2007) 1239–1257. doi:10.1002/elan.200603855.

[73] K. Gunnarsson, Affinity-Based Biosensors for Biomolecular Interaction Analysis, Curr. Protoc. Immunol. Chapter 18 (2001) Unit 18.6. doi:10.1002/0471142735.im1806s33.

[74] L. Yang, R. Bashir, Electrical/electrochemical impedance for rapid detection of foodborne pathogenic bacteria, Biotechnol. Adv. 26 (2008) 135–150. doi:10.1016/j.biotechadv.2007.10.003.

[75] X. Zhang, F. Li, A.N. Nordin, J. Tarbell, I. Voiculescu, Toxicity studies using mammalian cells and impedance spectroscopy method, Sens. Bio-Sensing Res. 3 (2015) 112–121. doi:10.1016/j.sbsr.2015.01.002.

[76] D.A. Boehm, P.A. Gottlieb, S.Z. Hua, On-chip microfluidic biosensor for bacterial detection and identification, Sensors Actuators, B Chem. 126 (2007) 508–514. doi:10.1016/j.snb.2007.03.043.

[77] R. Gómez-Sjöberg, D.T. Morisette, R. Bashir, Impedance microbiology-on-a-chip: Microfluidic bioprocessor for rapid detection of bacterial metabolism, J. Microelectromechanical Syst. 14 (2005) 829–838. doi:10.1109/JMEMS.2005.845444.

[78] R. Gomez, R. Bashir, A. Sarikaya, Microfluidic biochip for impedance spectroscopy of biological species, Biomed. Microdevices. 3 (2001) 201–209. doi:10.1023/A:1011403112850.

[79] J.K. Magnuson, L.L. Lasure, Organic Acid Production by Filamentous Fungi, in: Adv. Fungal Biotechnol. Ind. Agric. Med., 2004: pp. 307–340. doi:10.1007/978-1-4419-8859-1_12.

[80] K. Ludwig, Archives Conservators Discussion Group 2001: mold remediation in archives, B. & Pap. Gr. Annu. 20 (2001) 41.

[81] P.P. Vinayaka, R. Blank, M. Frodl, M.W. Tahir, N.A. Zaidi, M. Oellers, S. Van Den Driesche, W. Lang, M.J. Vellekoop, A replaceable bioreactor array for monitoring mold spore contamination in archives, in: MST Kongress, 2017.

[82] P.P. Vinayaka, S. van den Driesche, R. Blank, M.W. Tahir, M. Frodl, W. Lang, M.J. Vellekoop, An impedance-based mold sensor with on-chip optical reference, Sensors (Switzerland). 16 (2016). doi:10.3390/s16101603.

[83] P. Papireddy Vinayaka, S. Van Den Driesche, S. Janssen, M. Frodl, R. Blank, F. Cipriani, W. Lang, M.J. Vellekoop, Impedance spectroscopy for detection of mold in archives with an integrated reference measurement, Proc. {SPIE}, Bio-MEMS Med. Microdevices II. 9518 (2015) 95180T. doi:10.1117/12.2178510.

[84] P.P. Vinayaka, S. Van Den Driesche, S. Janssen, M. Frodl, R. Blank, F. Cipriani, W.

Lang, M.J. Vellekoop, On-Chip monitoring of pH change in agar-gels during fungi growth by integrating impedance and colorimetric principles, in: Procedia Eng., 2014: pp. 373–376. doi:10.1016/j.proeng.2014.11.739.

[85] W. Mansfield Clark, H.A. Lubs, the Colorimetric Determination of Hydro- Gen Ion Concentration and Its Applica- Tions in Bacteriology Part Iii, (1916) 191–236. http://jb.asm.org/.

[86] Emerson Process Management, The Theory of pH Measurement, Rosemount Anal. Inc. (2010) 1–8.

[87] G.B. Kauffman, The Bronsted-Lowry acid base concept, J. Chem. Educ. 65 (1988) 28. doi:10.1021/ed065p28.

[88] R.F. Michael Clugston, Advanced Chemistry, Oxford university press, 2000.

[89] O.J.T. Frederick A. Bettelheim, William H. Brown, Mary K. Campbell, Shawn O. Farrell, Introduction to General, Organic and biochemistry, 11th ed., Cengage learning, 2016.

[90] R. W. Sabnis, Handbook of Acid-Base Indicators, CRC Press, 2007.

[91] a K. Covington, C. Red, E. Orange, E. Violet, Acid-Base Indicators, CRC Handb. Chem. Phys. (2003) 15–17.

[92] P.P. Vinayaka, S. Van Den Driesche, R. Blank, A. Chakraborty, R. Amin, M.W. Tahir, N.A. Zaidi, M. Frodl, W. Lang, M.J. Vellekoop, Membrane-sealed Bioreactor for On-site Autonomous Detection of Fungi Spore Contamination in Archives, in: Procedia Eng., 2016: pp. 529–532. doi:10.1016/j.proeng.2016.11.515.

[93] M. Roth, S. Vogel, U. Schaber, H.-E. Endres, Electrically removable, micromachined encapsulation for sensitive materials, Sensors Actuators A Phys. 62 (1997) 633–635. doi:10.1016/S0924-4247(97)01482-9.

[94] M. Allain, J. Berthier, S. Basrour, P. Pouteau, Electrically actuated sacrificial membranes for valving in microsystems, J. Micromechanics Microengineering. 20 (2010) 35006. doi:10.1088/0960-1317/20/3/035006.

[95] M. Allain, J. Berthier, S. Basrour, P. Pouteau, Sacrificial membranes for serial valving in microsystems, in: Tech. Proc. 2009 NSTI Nanotechnol. Conf. Expo, NSTI-Nanotech 2009, 2009.

[96] W.J. Arora, A.J. Nichol, H.I. Smith, G. Barbastathis, Membrane folding to achieve three-dimensional nanostructures: Nanopatterned silicon nitride folded with stressed chromium hinges, Appl. Phys. Lett. 88 (2006) 1–3. doi:10.1063/1.2168516.

[97] A.M. Cardenas-Valencia, J. Dlutowski, J. Bumgarner, C. Munoz, W. Wang, R. Popuri, L. Langebrake, Development of various designs of low-power, MEMS valves for fluidic applications, Sensors Actuators, A Phys. 136 (2007) 374–384. doi:10.1016/j.sna.2006.12.016.

[98] J.P. Raskin, F. Iker, N. André, B. Olbrechts, T. Pardoen, D. Flandre, Bulk and surface micromachined MEMS in thin film SOI technology, Electrochim. Acta. 52 (2007) 2850–2861. doi:10.1016/j.electacta.2006.09.021.

[99] J.P. Laconte, J., Flandre, D. et Raskin, Chapter 2 Thin dielectric films stress extraction, in: Micromachined Thin-Film Sensors for Soi-Cmos Co-Integration,

2006: pp. 47–103. doi:10.1007/0-387-28843-0_3.

[100] M.L. Cardenas, A.M. Cardenas-Valencia, J. Dlutowski, J. Bumgarner, L. Langebrake, A finite element method modeling approach for the development of metal/silicon nitride MEMS single-use valve arrays, J. Micromechanics Microengineering. 17 (2007) 1671–1679. doi:10.1088/0960-1317/17/8/034.

[101] F. Biró, Z. Hajnal, A.E. Pap, I. Barsony, Multiphysics modelling of the fabrication and operation of a micro-pellistor device, in: 2014 15th Int. Conf. Therm. Mech. Multi-Physics Simul. Exp. Microelectron. Microsystems, EuroSimE 2014, 2014. doi:10.1109/EuroSimE.2014.6813867.

[102] COMSOL Multiphysics, Introduction to COMSOL Multiphysics, Manual. (2009) 168. http://cdn.comsol.com/documentation/5.1.0.145/IntroductionToCOMSOLMultiphysics.pdf.

[103] L. Jiang, N.S. Korivi, Microfluidics: technologies and applications, Springer, 2014. doi:10.1533/9780857098757.424.

[104] J.C.J. H. S. Carslaw, Conduction of Heat in Solids, , Oxford, second, Oxford Science publicaitons, 1959.

[105] B. Merle, M. Göken, Fracture toughness of silicon nitride thin films of different thicknesses as measured by bulge tests, Acta Mater. 59 (2011) 1772–1779. doi:10.1016/j.actamat.2010.11.043.

[106] R.L. Edwards, G. Coles, W.N. Sharpe, Comparison of Tensile and Bulge Tests for Thin-Film Silicon Nitride, Exp. Mech. 44 (2004) 49–54. doi:10.1177/0014485104039749.

[107] D.R. Ciarlo, Silicon nitride thin windows for biomedical microdevices, Biomed. Microdevices. 4 (2002) 63–68. doi:10.1023/A:1014275913962.

[108] B.S. Ian Gibson, David Rosen, Additive manufacturing technologies: 3D printing, rapid prototyping and direct digital manufacturing, second, Springer, n.d.

[109] K. Chabowski, T. Piasecki, A. Dzierka, K. Nitsch, Simple wide frequency range impedance meter based on AD5933 integrated circuit, Metrol. Meas. Syst. 22 (2015) 13–24. doi:10.1515/mms-2015-0006.

[110] J. Ferreira, F. Seoane, A. Ansede, R. Bragos, AD5933-based spectrometer for electrical bioimpedance applications, J. Phys. Conf. Ser. 224 (2010) 12011. doi:10.1088/1742-6596/224/1/012011.

[111] J. Toro, C. Daza, F. Vega, L. Diaz, C. Torres, Portable equipment for determining ripeness in hass avocado using a low cost color sensor, in: Speckle 2015 Vi Int. Conf. Speckle Metrol., 2015. doi:10.1117/12.2196752.

[112] S. Sharma, S. Pathak, K.P. Sharma, Toxicity of the azo dye methyl red to the organisms in microcosms, with special reference to the Guppy (Poecilia reticulata Peters), Bull. Environ. Contam. Toxicol. 70 (2003) 753–760. doi:10.1007/s00128-003-0047-8.

[113] S.C. DeVito, Predicting Azo Dye Toxicity, Crit. Rev. Environ. Sci. Technol. 23 (1993) 249–324. doi:10.1080/10643389309388453.

[114] F.P. Van Der Zee, S. Villaverde, Combined anaerobic-aerobic treatment of azo

dyes - A short review of bioreactor studies, Water Res. 39 (2005) 1425–1440. doi:10.1016/j.watres.2005.03.007.

[115] U. Stephan, B. Schröer, S. Thomas, M. Axel, B. Roland, K. Christoph, P. Papireddy Vinayaka, 7. Zwischenbericht Gesamtbericht des Konsortiums, 2017.

[116] R. Blank, P. Papireddy Vinayaka, M.W. Tahir, J. Yong, M.J. Vellekoop, W. Lang, Comparison of Several Optical Methods for an Automated Fungal Spore Sensor System Concept, IEEE Sens. J. 16 (2016) 5596–5602. doi:10.1109/JSEN.2016.2567538.

[117] R. Blank, P.P. Vinayaka, M.W. Tahir, M.J. Vellekoop, W. Lang, Optical sensor system for the detection of mold: Concept for a fully automated sensor system for the detection of airborne fungal spores, in: 2015 IEEE SENSORS - Proc., 2015. doi:10.1109/ICSENS.2015.7370346.

[118] M.W. Tahir, N.A. Zaidi, R. Blank, P.P. Vinayaka, W. Lang, Fungus detection system, in: Proc. - 2016 IEEE Int. Conf. Auton. Comput. ICAC 2016, 2016: pp. 227–228. doi:10.1109/ICAC.2016.50.

[119] C. Pöhlker, J.A. Huffman, U. Pöschl, Autofluorescence of atmospheric bioaerosols - Fluorescent biomolecules and potential interferences, Atmos. Meas. Tech. 5 (2012) 37–71. doi:10.5194/amt-5-37-2012.

[120] C. Pöhlker, J.A. Huffman, U. Pöschl, Autofluorescence of atmospheric bioaerosols: Spectral fingerprints and taxonomic trends of pollen, Atmos. Meas. Tech. 6 (2013) 3369–3392. doi:10.5194/amt-6-3369-2013.

[121] T. Reponen, S.A. Grinshpun, K.L. Conwell, J. Wiest, M. Anderson, Aerodynamic versus physical size of spores: Measurement and implication for respiratory deposition, Grana. 40 (2001) 119–125. doi:10.1080/00173130152625851.

[122] T. Reponen, K. Willeke, V. Ulevicius, A. Reponen, S.A. Grinshpun, Effect of relative humidity on the aerodynamic diameter and respiratory deposition of fungal spores, Atmos. Environ. 30 (1996) 3967–3974. doi:10.1016/1352-2310(96)00128-8.

[123] T.M. Madelin, H.E. Johnson, Fungal and actinomycete spore aerosols measured at different humidities with an aerodynamic particle sizer, J. Appl. Bacteriol. 72 (1992) 400–409. doi:10.1111/j.1365-2672.1992.tb01853.x.

[124] R.L. Day, L.C. Lee, Optical emission from photoexcitation of aerosol particles produced by reaction of ozone with 1,3-butadiene, Appl. Opt. 22 (1983) 2546–2550. doi:10.1364/AO.22.002546.

[125] J. Ho, Future of biological aerosol detection, Anal. Chim. Acta. 457 (2002) 125–148. doi:10.1016/S0003-2670(01)01592-6.

[126] H. Kanaani, M. Hargreaves, Z. Ristovski, L. Morawska, Performance assessment of UVAPS: Influence of fungal spore age and air exposure, J. Aerosol Sci. 38 (2007) 83–96. doi:10.1016/j.jaerosci.2006.10.003.

[127] D. Yeloff, C. Hunt, Fluorescence microscopy of pollen and spores: A tool for investigating environmental change, Rev. Palaeobot. Palynol. 133 (2005) 203–219. doi:10.1016/j.revpalbo.2004.10.002.

[128] Y. Le Pan, S.C. Hill, R.G. Pinnick, J.M. House, R.C. Flagan, R.K. Chang, Dual-

excitation-wavelength fluorescence spectra and elastic scattering for differentiation of single airborne pollen and fungal particles, Atmos. Environ. 45 (2011) 1555–1563. doi:10.1016/j.atmosenv.2010.12.042.

[129] S.E. Saari, M.J. Putkiranta, J. Keskinen, Fluorescence spectroscopy of atmospherically relevant bacterial and fungal spores and potential interferences, Atmos. Environ. 71 (2013) 202–209. doi:10.1016/j.atmosenv.2013.02.023.

[130] D.J. O'Connor, D. Iacopino, D.A. Healy, D. O'Sullivan, J.R. Sodeau, The intrinsic fluorescence spectra of selected pollen and fungal spores, Atmos. Environ. 45 (2011) 6451–6458. doi:10.1016/j.atmosenv.2011.07.044.

[131] H. and T. (RAMHOT) Food and Agriculture Organization of the United Nations (FAO) Market and Policy Analyses of Raw Materials, Intergovernmental group on bananas and tropical fruits, Banan. Mark. Rev. Bbnana Stat. 2012-2013. (2014) 1–6.

[132] FAO, Banana market 2013-2014, Cirad. 218 (2014) 1–8.

[133] L.T. Raynolds, The Global Banana Trade, in: Banan. Wars - Power, Prod. Hist. Am., 2003: pp. 23–47.

[134] R. Jedermann, U. Praeger, M. Geyer, W. Lang, Remote quality monitoring in the banana chain, Philos. Trans. R. Soc. A Math. Phys. Eng. Sci. 372 (2014) 20130303–20130303. doi:10.1098/rsta.2013.0303.

[135] S. Janssen, I. Pankoke, K. Klus, K. Schmitt, U. Stephan, J. Wollenstein, Two underestimated threats in food transportation: mould and acceleration, Philos. Trans. R. Soc. A Math. Phys. Eng. Sci. 372 (2014) 20130312–20130312. doi:10.1098/rsta.2013.0312.

[136] M. Soltani, R. Alimardani, M. Omid, Prediction of banana quality during ripening stage using capacitance sensing system, Aust. J. Crop Sci. 4 (2010) 443–447.

[137] P. Papireddy Vinayaka, M. Kahali Moghaddam, S. van den Driesche, R. Blank, W. Lang, M.J. Vellekoop, Sensor Sticker for Detection of Fungi Spore Contamination on Bananas, Adv. Sci. Technol. 100 (2016) 130–133. doi:10.4028/www.scientific.net/AST.100.130.

[138] M. Kahali Moghaddam, A. Breede, A. Chaloupka, A. Bödecker, C. Habben, E.M. Meyer, C. Brauner, W. Lang, Design, fabrication and embedding of microscale interdigital sensors for real-time cure monitoring during composite manufacturing, Sensors Actuators, A Phys. 243 (2016) 123–133. doi:10.1016/j.sna.2016.03.017.